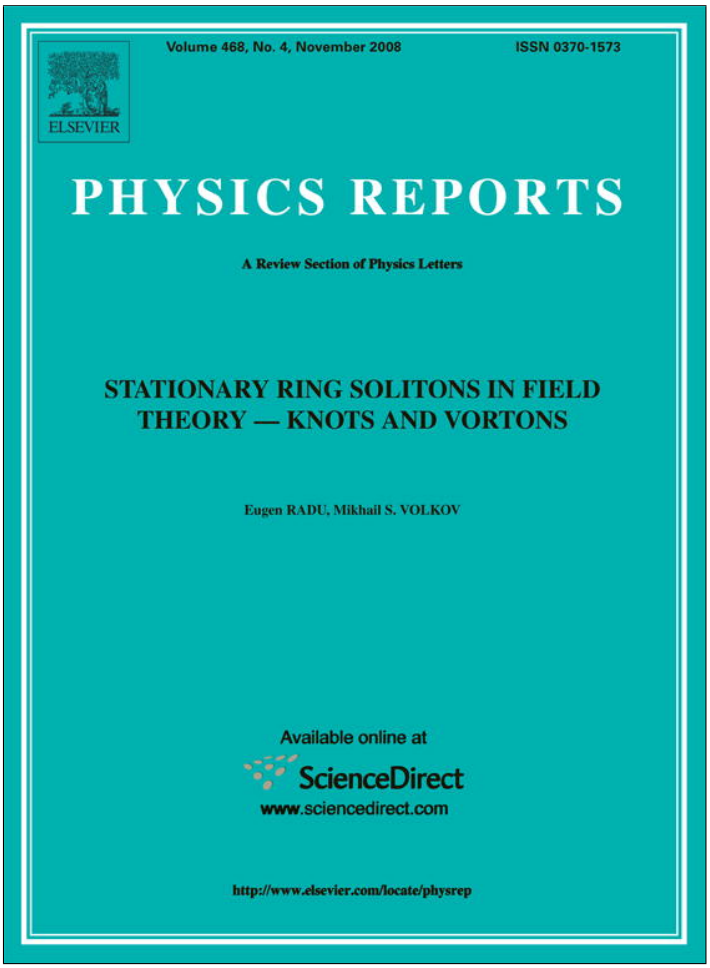

Physics Reports 468 (2008) 101–151

Contents lists available at ScienceDirect

Physics Reports

journal homepage: www.elsevier.com/locate/physrep

Stationary ring solitons in field theory — Knots and vortons

Eugen Radu, Mikhail S. Volkov *

Laboratoire de Mathématiques et Physique Théorique CNRS-UMR 6083, Université de Tours, Parc de Grandmont, 37200 Tours, France

ARTICLE INFO

Article history:
Accepted 24 July 2008
Available online 20 August 2008
editor: A. Schwimmer

PACS:
11.10.Lm
11.27.+d
98.80.Cq

Keywords:
Classical field theory
Gauge fields
Solitons
Vortices

ABSTRACT

We review the current status of the problem of constructing classical field theory solutions describing stationary vortex rings in Minkowski space in $3+1$ dimensions. We describe the known up to date solutions of this type, such as the static knot solitons stabilized by the topological Hopf charge, the attempts to gauge them, the anomalous solitons stabilized by the Chern–Simons number, as well as the non-Abelian monopole and sphaleron rings. Passing to the rotating solutions, we first discuss the conditions ensuring that they do not radiate, and then describe the spinning Q-balls, their twisted and gauged generalizations reported here for the first time, spinning skyrmions, and rotating monopole–antimonopole pairs. We then present the first explicit construction of global vortons as solutions of the elliptic boundary value problem, which demonstrates their non-radiating character. Finally, we describe the analogs of vortons in the Bose–Einstein condensates, analogs of spinning Q-balls in the non-linear optics, and also moving vortex rings in superfluid helium and in ferromagnetics.

Contents

* Corresponding author.
E-mail addresses: Eugen.Radu@lmpt.univ-tours.fr (E. Radu), Michael.Volkov@lmpt.univ-tours.fr (M.S. Volkov).

0370-1573/$ – see front matter © 2008 Elsevier B.V. All rights reserved.
doi:10.1016/j.physrep.2008.07.002

1. Introduction

Stationary vortex loops are often discussed in the literature in various contexts ranging from the models of condensed matter physics [11,12,17,41,124,137,146,147,149], to high energy physics and cosmology [29,45,46,48,165,177]. Such objects could be quite interesting physically and might be responsible for a plenty of important physical phenomena, starting from the structure of quantum superfluids [54] and Bose–Einstein condensed alkali gases [117] to the baryon asymmetry of the Universe, dark matter, and the galaxy formation [165]. These intriguing physical aspects of vortex loops occupy therefore most of the discussions in the literature, while much less attention is usually paid to their mathematical existence. In most considerations the existence of such loops is discussed only qualitatively, using plausibility arguments, and the problem of constructing the corresponding field theory solutions is rarely addressed, such that almost no solutions of this type are explicitly known.

The physical arguments usually invoked to justify the loop existence arise within the effective macroscopic description of vortices [1,129]. Viewed from large distances, their internal structure can be neglected and the vortices can be effectively described as elastic thin ropes or, if they carry currents, as thin wires [32–35,122]. This suggests the following engineering procedure: to 'cut out' a finite piece of the vortex, then 'twist' it several times and finally 'glue' its ends. The resulting loop will be stabilized against contraction by the potential energy of the twist deformation, that is by the positive pressure contributed by the current and stresses [43,42,86,130]. Equally, instead of twisting the rope, one can first 'make' a loop and then 'spin it up' thus giving to it an angular momentum to stabilize it against shrinking [47,48]. Depending on whether they are spinning or not, such loops are often called in the literature vortons and knots (also springs), respectively.

These macroscopic arguments are suggestive. However, they cannot guarantee the existence of loops as stationary field theory objects, since they do not take into account all the field degrees of freedom that could be essential. Speaking more rigorously, one can prepare twisted or spinning loop configurations as the initial data for the fields. However, nothing guarantees that these data will evolve to non-trivial equilibrium field theory objects, since, up to few exceptions, the typical field theory models under consideration do not have a topological energy bound for static loop solitons. For spinning loops the situation can be better, since the angular momentum can provide an additional stabilization of the system. However, nothing excludes the possibility of radiative energy leakages from spinning loops. Since there is typically a current circulating along them, which means an accelerated motion of charges, it seems plausible that spinning loops should radiate, in which case they would not be *stationary* but at best only quasistationary. In fact, loop formation is generically observed in dynamical vortex network simulations (although for currentless vortices), and these loops indeed radiate rapidly away all their energy (see e.g. [26]).

The lack of explicit solutions renders the situation even more controversial. In fact, although there are explicit examples of loop solitons in *global* field theory, which means containing only scalar fields with global internal symmetries, almost

nothing is known about such solutions in *gauge* field theory. Vortons, for example, were initially proposed more than 20 years ago in the context of the local $U(1) \times U(1)$ theory of superconducting cosmic strings of Witten [177]. However, not a single field theory solution of this type has been obtained up to now. Search for static knot solitons in the Ginzburg–Landau-type gauge field theory models has already 30 years of history, the result being always negative. All this casts some doubts on the existence of stationary, non-radiating vortex loops in physically interesting gauge field theory models. However, rigorous no-go arguments are not known either. As a result, the existence of such solutions has been neither confirmed nor disproved.

Interestingly, *exact* solutions describing ring-type objects are known in curved space. These are black rings in the multidimensional generalizations of General Relativity — spinning toroidal black holes (see [58] for a review). It seems therefore that Einstein's field equations, notoriously known for their complexity, are easier to solve than the non-linear equations describing loops made of interacting gauge and scalar fields in Minkowski space.

It should be emphasized that the problem here is not related to the dynamical stability of these loops. In order to be stable or unstable they should first of all exist as stationary field theory solutions. The problem is related to the very existence of such solutions. One should be able to decide whether they exist or not, which is a matter of principle, and this is the main issue that we address in this paper. Therefore, when talking about loops stabilized by some forces, we shall mean the force balance that makes possible their existence, and not the stability of these loops with respect to all dynamical perturbations. If they exist, their dynamical stability should be analyzed separately, but we shall call *solitons* all localized, globally regular, finite energy field theory solutions, irrespectively of their stability properties. It should also be stressed that we insist on the *stationarity* condition for the solitons, which implies the absence of radiation. Quasistationary loops which radiate slowly and live long enough could also be physically interesting, but we are only interested in loops which could live infinitely longtime, at least in classical theory.

Trying to clarify the situation, we review in what follows the known field theory solutions in Minkowski space in $3 + 1$ dimensions describing stationary ring objects. We shall divide them in two groups, depending on whether they do have or do not have an angular momentum. Solutions without angular momentum are typically static, that is they do not depend on time and also do not typically have an electric field. We start by describing the static knot solitons stabilized by the Hopf charge in a global field theory model. Then we review the attempts to generalize these solutions within gauge field theory, with the conclusion that some additional constraints on the gauge field are necessary, since fixing only the Hopf charge does not seem to be sufficient to stabilize the system in this case. We then consider two known examples of static ring solitons in gauge field theory: the anomalous solitons stabilized by the Chern–Simons number, and the non-Abelian monopole and sphaleron rings.

Passing to the rotating solutions, we first of all discuss the issue of how the presence of an angular momentum, associated to some internal motions in the system, can be reconciled with the absence of radiation which is normally generated by these motions. One possibility for this is to consider time-independent solitons in theories with local internal symmetries. They will not radiate, but it can be shown for a number of important field theory models that the angular momentum vanishes in this case. Another possibility arises in systems with global symmetries, where one can consider *non-manifestly* stationary and axisymmetric fields containing spinning phases. Such fields could have a non-zero angular momentum, but the absence of radiation is not automatically guaranteed in this case. The general conclusion is that the existence of non-radiating spinning solitons, although not impossible, seems to be rather restricted. Such solutions seem to exist only in some quite special field theory models, while generic spinning field systems should radiate.

Nevertheless, non-radiating spinning solitons in Minkowski space in $3 + 1$ dimensions exist, and we review below all known examples: these are the spinning Q-balls, their twisted and gauged generalizations, spinning Skyrmions and rotating monopole–antimonopole pairs. In addition, there are also vortons, and below we present for the first time numerical solutions of elliptic equations describing vortons in the global field theory limit. Although global vortons have been studied before by different methods, our construction shows that they indeed exist as stationary, non-radiating field theory objects.

We also discuss stationary ring solitons in non-relativistic physics. Surprisingly, it turns out that the relativistic vortons can be mapped to the 'skyrmion' solutions of the Gross–Pitaevskii equation in the theory of Bose–Einstein condensation. In addition, it turns out that Q-balls can describe light pulses in media with non-linear refraction — 'light bullets'. Finally, for the sake of completeness, we discuss also the moving vortex rings stabilized by the Magnus force in continuous media theories, such as in the superfluid helium and in ferromagnetics.

In our numerical calculations we use an elliptic PDE solver with which we have managed to reproduce most of the solutions we describe, as well as obtain a number of new results presented below for the first time. The latter include the explicit vorton solutions, spinning twisted Q-balls, spinning gauged Q-balls, as well as the 'Saturn', 'hoop' and bi-ring solutions for the interacting Q-balls. We put the main emphasis on describing how the solutions are constructed and not to their physical applications, so that our approach is just the opposite and therefore complementary to the one generally adopted in the existing literature. As a result, we outline the current status of the ring soliton existence problem — within the numerical approach. Giving mathematically rigorous existence proofs is an issue that should be analyzed separately. It seems that our global vorton solutions could be generalized in the context of gauge field theory. The natural problem to attack would then be to obtain vortons in the electroweak sector of Standard Model.

In this text the signature of the Minkowski spacetime metric $g_{\mu\nu}$ is chosen to be $(+, -, -, -)$, the spacetime coordinates are denoted by $x^\mu = (x^0, x^k) \equiv (t, \mathbf{x})$ with $k = 1, 2, 3$. All physical quantities discussed below, including fields, coordinates, coupling constants and conserved quantities are dimensionless.

2. Knot solitons

Let us first consider solutions with zero angular momentum stabilized by their intrinsic deformations. We shall start by discussing the famous example of static knotted solitons in a non-linear sigma model. Since this is the best known and also in some sense canonical example of knot solitons, we shall describe it in some detail. We shall then review the status of gauge field theory generalizations of these solutions.

2.1. Faddeev–Skyrme model

More than 30 years ago Faddeev introduced a field theory consisting of a non-linear O(3) sigma model augmented by adding a Skyrme-type term [61,62]. This theory can also be obtained by a consistent truncation of the O(4) Skyrme model (see Section 5.2.1). Its dynamical variables are three scalar fields $\mathbf{n} \equiv n^a = (n^1, n^2, n^3)$ constraint by the condition

$$\mathbf{n} \cdot \mathbf{n} = \sum_{a=1}^{3} n^a n^a = 1,$$

so that they span a two-sphere S^2. The Lagrangian density of the theory is

$$\mathcal{L}[\mathbf{n}] = \frac{1}{32\pi^2} \left(\partial_\mu \mathbf{n} \cdot \partial^\mu \mathbf{n} - \mathcal{F}_{\mu\nu} \mathcal{F}^{\mu\nu} \right) \tag{2.1}$$

where

$$\mathcal{F}_{\mu\nu} = \frac{1}{2} \epsilon_{abc} n^a \partial_\mu n^b \partial_\nu n^c \equiv \frac{1}{2} \mathbf{n} \cdot (\partial_\mu \mathbf{n} \times \partial_\nu \mathbf{n}). \tag{2.2}$$

The Lagrangian field equations read

$$\partial_\mu \partial^\mu \mathbf{n} + \partial_\mu \mathcal{F}^{\mu\nu} (\mathbf{n} \times \partial_\nu \mathbf{n}) = (\mathbf{n} \cdot \partial_\mu \partial^\mu \mathbf{n})\, \mathbf{n}. \tag{2.3}$$

In the static limit the energy of the system is

$$E[\mathbf{n}] = \frac{1}{32\pi^2} \int_{\mathbb{R}^3} \left((\partial_k \mathbf{n})^2 + (\mathcal{F}_{ik})^2 \right) \mathrm{d}^3\mathbf{x} \equiv E_2 + E_4. \tag{2.4}$$

Under scale transformations, $\mathbf{x} \to \Lambda \mathbf{x}$, one has $E_2 \to \Lambda E_2$ and $E_4 \to E_4/\Lambda$. The energy will therefore be stationary for $\Lambda = 1$ if only the virial relation holds,

$$E_2 = E_4. \tag{2.5}$$

This shows that the four derivative term E_4 is necessary, since otherwise the virial relation would require that $E_2 = 0$, thus ruling out all non-trivial static solutions — in agreement with the Hobart–Derrick theorem [92,52].

Any static field $\mathbf{n}(\mathbf{x})$ defines a map $\mathbb{R}^3 \to S^2$. Since for finite energy configurations $\mathbf{n}$ should approach a constant value for $|\mathbf{x}| \to \infty$, all points at infinity of $\mathbb{R}^3$ map to one point on S^2. Using the global O(3)-symmetry of the theory one can choose this point to be the north pole of the S^2,

$$\lim_{|\mathbf{x}| \to \infty} \mathbf{n}(\mathbf{x}) = \mathbf{n}_\infty = (0, 0, 1). \tag{2.6}$$

Notice that this condition leaves a residual O(2) symmetry of global rotations around the third axis in the internal space,

$$n^1 + \mathrm{i} n^2 \to (n^1 + \mathrm{i} n^2) \mathrm{e}^{\mathrm{i}\alpha}, \quad n^3 \to n^3. \tag{2.7}$$

The position of the field configuration described by $\mathbf{n}(\mathbf{x})$ can now be defined as the set of points where the field is as far as possible from the vacuum value, that is the preimage of the point $-\mathbf{n}_\infty$ antipodal to the vacuum $+\mathbf{n}_\infty$. This preimage forms a closed loop (or collection of loops) called position curve. Solitons in the theory can therefore be viewed as string-like objects, stabilized by their topological charge to be defined below.

At the intuitive level, these solitons can be viewed as closed loops made of twisted vortices. Specifically, the theory admits solutions describing straight vortices that can be parametrized in cylindrical coordinates $\{\rho, z, \varphi\}$ as $n^3 = \cos\Theta(\rho)$, $n^1 + \mathrm{i} n^2 = \sin\Theta(\rho)\, \mathrm{e}^{\mathrm{i}pz + \mathrm{i}n\varphi}$, where $n \in \mathbb{Z}$ is the vortex winding number [111]. The phase $pz + n\varphi$ thus changes both along and around the vortex and the vector $\mathbf{n}$ rotates around the third internal direction as one moves along the vortex, which can be interpreted as *twisting* of the vortex. It seems plausible that a loop made of a piece of length L of such a twisted vortex, where $pL = 2\pi m$, could be stabilized by the potential energy of the twist deformation. For such a twisted loop the phase increases by $2\pi n$ after a revolution around the vortex core and by $2\pi m$ as one travels along the loop, where $m \in \mathbb{Z}$ is the number of twists. If the loop is homeomorphic to a circle, then the product nm gives the value of its topological invariant: the Hopf charge.

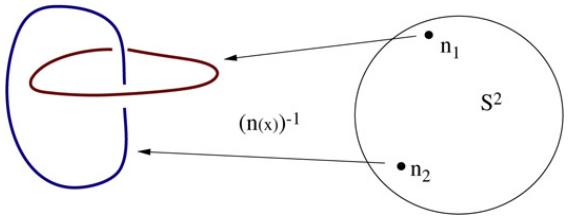

Fig. 1. Preimages of any two points $\mathbf{n}_1$ and $\mathbf{n}_2$ on the target space S^2 are two loops. The number of mutual linking of these two loops is the Hopf charge $N[\mathbf{n}]$ of the map $\mathbf{n}(\mathbf{x})$. Here the case of $N = 1$ is schematically shown.

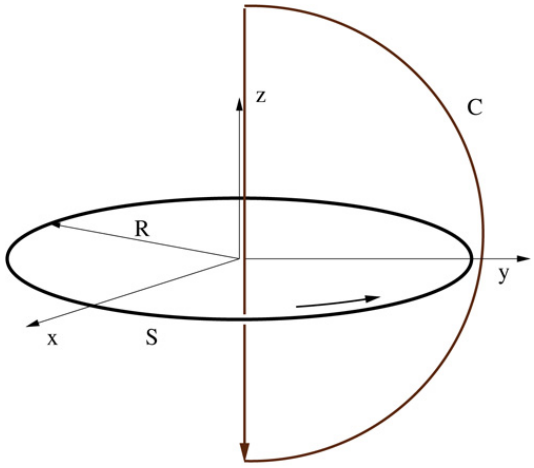

Fig. 2. Knot topology: the complex phase of the field in Eq. (2.10) winds along two orthogonal directions: along S and along the contour C consisting of the z-axis and a semi-circle whose radius expands to infinity. A similar winding of phases is found for other systems to be discussed below: for vortons, skyrmions, and twisted Q-balls.

2.2. Hopf charge

The condition (2.6) allows one to view the infinity of $\mathbb{R}^3$ as one point, thus effectively replacing $\mathbb{R}^3$ by its one-point compactification S^3. Any smooth field configuration can therefore be viewed as a map

$$\mathbf{n}(\mathbf{x}) : S^3 \to S^2. \tag{2.8}$$

Any such map can be characterized by the topological charge $N[\mathbf{n}] \in \pi_3(S^2) = \mathbb{Z}$ known as the Hopf invariant. This invariant has a simple interpretation. The preimage of a generic point on the target S^2 is a closed loop. If a field has Hopf number N then the two loops consisting of preimages of two generic distinct points on S^2 will be linked exactly N times (see Fig. 1).

Although there is no local formula for $N[\mathbf{n}]$ in terms of $\mathbf{n}$, one can give a non-local expression as follows. The 2-form $\mathcal{F} = \frac{1}{2}\mathcal{F}_{ik}\mathrm{d}x^i \wedge \mathrm{d}x^k$ defined by Eq. (2.2) is closed, $\mathrm{d}\mathcal{F} = 0$, and since the second cohomology group of S^3 is trivial, $H(S^3) = 0$, there globally exists a vector potential $\mathcal{A} = \mathcal{A}_k \mathrm{d}x^k$ such that $\mathcal{F} = \mathrm{d}\mathcal{A}$. The Hopf index can then be expressed as

$$N[\mathbf{n}] = \frac{1}{8\pi^2}\int \epsilon_{ijk}\mathcal{A}_i\mathcal{F}_{jk}\,\mathrm{d}^3\mathbf{x}. \tag{2.9}$$

For any smooth, finite energy field configuration $\mathbf{n}(\mathbf{x})$ this integral is integer-valued [119].

It can be shown that the maximal symmetry of $\mathbf{n}(\mathbf{x})$ compatible with a non-vanishing Hopf charge is O(2) [111]. It follows that spherically symmetric fields are topologically trivial. However, axially symmetric fields can have any value of the Hopf charge. Using cylindrical coordinates such fields can be parametrized as [111]

$$n^1 + \mathrm{i}n^2 = \mathrm{e}^{\mathrm{i}(m\varphi - n\psi)}\sin\Theta, \quad n^3 = \cos\Theta \tag{2.10}$$

where $n, m \in \mathbb{Z}$ and Θ, ψ are functions of ρ, z. Since $\mathbf{n} \to \mathbf{n}_\infty$ asymptotically, Θ should vanish for $r = \sqrt{\rho^2 + z^2} \to \infty$. The regularity at the z-axis requires for $m \neq 0$ that Θ should vanish also there. As a result, one has $\mathbf{n} = \mathbf{n}_\infty$ both at the z-axis and at infinity, that is at the contour C shown in Fig. 2. Next, one assumes that $\mathbf{n} = -\mathbf{n}_\infty$ on a circle S around the z-axis which is linked to C as shown in Fig. 2 (more generally, one can have $\mathbf{n} = -\mathbf{n}_\infty$ on several circles around the z-axis). The phase function ψ is supposed to increase by 2π after one revolution along C. Since $\cos\Theta$ interpolates between -1 and 1 on every trajectory from S to C, it follows that surfaces of constant Θ are homeomorphic to tori.

The preimage of the point $-\mathbf{n}_\infty$ consists of m copies of the circle S. The preimage of $\mathbf{n}_\infty$ consists of n copies of the contour C. These two preimages are therefore linked mn times.

One can also compute $\mathcal{F} = \mathrm{d}\mathcal{A}$ according to (2.2), from where one finds

$$\mathcal{A} = n\cos^2\frac{\Theta}{2}\,\mathrm{d}\psi + m\sin^2\frac{\Theta}{2}\,\mathrm{d}\varphi \tag{2.11}$$

so that $\mathcal{A}\wedge\mathcal{F} = nm\cos^2\frac{\Theta}{2}\sin\Theta\,\mathrm{d}\psi\wedge\mathrm{d}\Theta\wedge\mathrm{d}\varphi$. Inserting this to (2.9) gives the Hopf charge

$$N[\mathbf{n}] = mn. \tag{2.12}$$

Following Ref. [158], we shall call the fields given by the ansatz (2.10) $\mathbf{A}_{mn}$.

Let us consider two explicit examples of the $\mathbf{A}_{mn}$ field. Let us introduce toroidal coordinates $\{u, v, \varphi\}$ such that

$$\rho = (R/\tau)\,\sinh u, \quad z = (R/\tau)\,\sin v, \tag{2.13}$$

where $\tau = \cosh u - \cos v$ with $u \in [0, \infty)$, $v = [0, 2\pi)$. The correct boundary conditions for the field will then be achieved by choosing in the ansatz (2.10)

$$\Theta = \Theta(u), \quad \psi = v, \tag{2.14}$$

where $\Theta(0) = 0$, $\Theta(\infty) = \pi$.

Another useful parametrization is achieved by expressing n^a in terms of its complex stereographic projection coordinate

$$W = \frac{n^1 + \mathrm{i}n^2}{1 + n^3}. \tag{2.15}$$

The values $W = 0, \infty$ correspond to the vacuum and to the position curve of the soliton, respectively. Passing to spherical coordinates $\{r, \vartheta, \varphi\}$ one introduces

$$\phi = \cos\chi(r) + \mathrm{i}\sin\chi(r)\cos\vartheta, \quad \sigma = \sin\chi(r)\sin\vartheta\,\mathrm{e}^{\mathrm{i}\varphi}, \tag{2.16}$$

such that $|\phi|^2 + |\chi|^2 = 1$, where $\chi(0) = \pi$, $\chi(\infty) = 0$. A particular case of the field (2.10) is then obtained by setting

$$W = \frac{(\sigma)^m}{(\phi)^n}. \tag{2.17}$$

2.3. Topological bound and the $N = 1, 2$ hopfions

The following inequality for the energy (2.4) and Hopf charge (2.9) has been established by Vakulenko and Kapitanski [163],

$$E[\mathbf{n}] \geq c|N[\mathbf{n}]|^{3/4}, \tag{2.18}$$

where $c = (3/16)^{3/8}$ [111]. Its derivation is non-trivial and proceeds via considering a sequence of Sobolev inequalities. It is worth noting that a fractional power of the topological charge occurs in this topological bound, whose value is optimal [119]. On the other hand, it seems that the value of c can be improved, that is increased. Ward conjectures [171] that the bound holds for $c = 1$, which has not been proven but is compatible with all the data available. The existence of this bound shows that smooth fields attaining it, if exist, describe topologically stable solitons. Constructing them implies minimizing the energy (2.4) with fixed Hopf charge (2.9). Such minimum energy configurations are sometimes called in the literature Hopf solitons or hopfions, and we shall call them fundamental or ground state hopfions if they have the least possible energy for a given N.

Hopfions have been constructed for the first time for the lowest two values of the Hopf charge, $N = 1, 2$ by Gladikowski and Hellmund [79] and almost simultaneously (although somewhat more qualitatively) by Faddeev and Niemi [64]. Gladikowski and Hellmund used the axial ansatz (2.10) expressed in toroidal coordinates, with $\Theta = \Theta(u, v)$ and $\psi = v + \psi_0(u, v)$, where $\Theta(0, v) = 0$, $\Theta(\infty, v) = \pi$. Assuming the functions $\Theta(u, v)$ and $\psi_0(u, v)$ to be periodic in v, they discretized the variables u, v and numerically minimized the discretized expression for the energy with respect to the lattice cite values of Θ, ψ_0. They found a smooth minimum energy configuration of the $\mathbf{A}_{11}$ type for $N = 1$, while for $N = 2$ they obtained two solutions, $\mathbf{A}_{21}$ and $\mathbf{A}_{12}$, the latter being more energetic than the former.

We have verified the results of Gladikowski and Hellmund by integrating the field equations (2.3) in the static, axially symmetric sector. Using the axial ansatz (2.10), the azimuthal variable φ decouples, and the equations reduce to two coupled PDEs for $\Theta(\rho, z)$, $\psi(\rho, z)$. Unfortunately, these equations are rather complicated and it is not possible to reduce them to ODEs by further separating variables, via passing to toroidal coordinates, say. In fact, we are unaware of any attempts to solve these differential equations. We applied therefore our numerical method described in Section 6 to integrate them, and we have succeeded in constructing the first two fundamental hopfions, $\mathbf{A}_{11}$ and $\mathbf{A}_{21}$. For the $N = 1$ solution the energy density is maximal at the origin and the energy density isosurfaces are squashed spheres, while for the $N = 2$ solution they have toroidal structure (see Fig. 3). For the solutions energies E_N we obtained the values $E_1 = 1.22$, $E_2 = 2.00$. These features

Fig. 3. The energy isosurfaces for the $N = 1$ (left) and $N = 2$ (right) fundamental hopfions.

Fig. 4. Schematic representation of the hopfions as oriented circles.

agree with the results of Gladikowski and Hellmund and with those of Refs. [14,15,158,89,90]. In particular, the same values for the energy are quoted by Ward [172].

Ward also proposes a simple analytic approximation of the solutions based on the rational ansatz formula (2.17) [172]. For $n = m = 1$ this formula gives

$$W = \frac{x + \mathrm{i}y}{f(r) + \mathrm{i}z}\, \mathrm{e}^{\mathrm{i}\alpha} \tag{2.19}$$

where $f(r) = r \cot \chi(r)$. Here the constant phase factor has been introduced to account for the residual O(2) symmetry (2.7). Minimizing the energy with respect to $F(r)$ it turns out that choosing

$$f(r) = 0.453\,(r - 0.878)(r^2 + 0.705r + 1.415) \tag{2.20}$$

gives for the energy a value which is less than 1% above the true minimum, $E_1 = 1.22$ [172]. Eqs. (2.19) and (2.20) provide therefore a good analytic approximation for the $N = 1$ hopfion. They show, in particular, that the position curve of the hopfion is a circle of radius $R = 0.848$ and that for large r the field shows a dipole-type behavior,

$$n^1 + \mathrm{i}n^2 \approx 2W \approx a\,\frac{x + \mathrm{i}y}{r^3}. \tag{2.21}$$

Ward also suggests the moduli space approximation in which the $|N| = 1$ hopfion is viewed as an oriented circle (see Fig. 4). There are six continuous moduli parameters: three coordinates of the circle center, two angles determining the position of the circle axis, and also the overall phase. Choosing arbitrarily a direction along the axis (shown by the vertical arrow in Fig. 4), there are two possible orientations corresponding to the sign of the Hopf charge, changing which is achieved by $W \to W^*$. Although for one hopfion the phase is not important, the relative phases of several hopfions determine their interactions.

Ward conjectures that well-separated hopfions interact as dipoles with the maximal attraction/repulsion when they are parallel/antiparallel, respectively, since the like charges attract in a scalar field theory. He verifies this conjecture numerically, and then numerically relaxes a field configuration corresponding to two mutually attracting hopfions. He discovers two possible outcomes of this process. If the two hopfions are initially located in one plane then they approach each other till the two circles merge to one thereby forming the $\mathbf{A}_{2,1}$ hopfion with $N = 2$. If they are initially oriented along the same line then they approach each other but do not merge even in the energy minimum, where they remain separated by a finite distance. This corresponds to the $\mathbf{A}_{1,2}$ hopfion, which is more energetic but locally stable.

The $\mathbf{A}_{2,1}$ hopfion can be approximated by

$$W = \frac{(x + \mathrm{i}y)^2 \mathrm{e}^{\mathrm{i}\alpha}}{f + \mathrm{i}1.55\, z\, r}, \quad f = 0.23(r - 1.27)(r + 0.44)(r + 0.16)(r^2 - 2.15r + 5.09) \tag{2.22}$$

whose energy is 1.5% above the true minimum, and there is also a similar approximation for the $\mathbf{A}_{1,2}$ hopfion [172].

2.4. Unknots, links and knots

Similarly to the $N = 1, 2$ solutions, hopfions can be constructed within the axial ansatz (2.10) also for higher values of n, m. However, for $N > 2$ they will not generically correspond to the *global* energy minima. This can be understood if we remember that the Hopf charge measures the amount of the twist deformation. Twisting an elastic rod shows that if it is

Fig. 5. Two possible ways to link $N = 1$ hopfions. Left: the total linking number is $2 = 1 + 1$ and the total charge if $N = 1 + 1 + 2 = 4$. Right: the total linking number is $-2 = -1 - 1$ and the total charge is $N = 1 + 1 - 2 = 0$. The numerical relaxation of these configurations gives therefore completely different results [59].

twisted too much then the loop made of it will not be planar, since it will find it energetically favorable to bend toward the third direction. It is therefore expected that the ground state hopfions for higher values of N will not be axially symmetric planar loops, but 3D loops, generically without any symmetries.

The interest towards this issue was largely stirred by the work of Faddeev and Niemi [64,65], who conjectured that higher N hopfions should be not just closed lines but *knotted* closed lines, with the degree of knotedness expressed in terms of the Hopf charge. In other words, they conjectured that there could be a field theory realization of stable knots — the idea that had been put forward by Lord Kelvin in the 19th century [162] but never found an actual realization. This knot conjecture of Faddeev and Niemi had a large resonance and several groups had started large scale numerical simulations to look for knotted hopfions. Such solutions have indeed been found, although not with quite the same properties as had been originally predicted in Refs. [64,65].

The first, really astonishing set of results has been reported by Battye and Sutcliffe [14,15], who managed to construct hopfions up to $N = 8$ and found the first non-trivial knot – the trefoil knot – for $N = 7$. Similar analyses have been then independently carried out by Hietarinta and Salo [89,90] and also by Ward [171,172,176]. All groups performed the full 3D energy minimization starting from an initial field configuration with a given N. Various initial configurations were used, as for example the ones given by the rational ansatz (2.17), supplemented by non-axially symmetric perturbations to break the exact toroidal symmetry. The value of N being constant during the relaxation, the numerical iterations were found to converge to non-trivial energy minima, whose structure was sometimes completely different from that of the initial configuration (an online animation of the relaxation process is available in [59]). Several local energy minima typically exist for a given N, sometimes with almost the same energy, so that it was not always easy to know whether the minima obtained were local or global. Different initial configurations were therefore tried to see if the minimum energy configurations could be reproduced in a different way. As a result, it appears that the global energy minima have now been identified and cross-checked up to $N = 7$ [90,158], after which the analysis has been extended up to $N = 16$ [158]. The properties of the solutions can be summarized as follows.

For $N = 1, 2$ these are the toroidal hopfions of Gladikowski and Hellmund [79], $\mathbf{A}_{11}$ and $\mathbf{A}_{21}$. Although initially obtained within the constrained, axially symmetric relaxation scheme, they also correspond to the global minima of the full 3D energy functional. Axially symmetric hopfions $\mathbf{A}_{m1}$ exist also for higher $N = m$ [14,15], but they no longer correspond to global energy minima. For $N = 3$ the ground state hopfion is not planar and is called in [158] $\tilde{\mathbf{A}}_{31}$, which can be viewed as deformed $\mathbf{A}_{31}$, with a pretzel-like position curve bent in 3D to break the axial symmetry. However, for $N = 4$ the axial symmetry is restored again in the ground state, $\mathbf{A}_{22}$, which seems to have a similarity to the $\mathbf{A}_{12}$ two-ring structure [90,176]. The bent $\tilde{\mathbf{A}}_{41}$ also exists, but its energy is higher.

Up to now all hopfions have been the simplest knots topologically equivalent to a circle, called *unknots* in the knot classification. A new phenomenon arises for $N = 5$, since the fundamental hopfion in this case consists of two linked unknots. This has nothing to do with the linking of preimages determining the value of N. This time the position curve itself consists of two disjoint loops, corresponding to a charge 2 unknot linked to a charge 1 unknot. The Hopf charge is not simply the sum of charges of each component, but contains in addition the sum of their linking numbers due to their linking with the other components. It is worth noting that the linking number of the oriented circles can be positive or negative, depending on how they are linked [89] (see Fig. 5). Using the notation of Ref. [158], the $N = 5$ hopfion can be called $\mathbf{L}^{1,1}_{1,2}$, where the subscripts label the Hopf charges of the unknot components of the link, and the superscript above each subscript counts the extra linking number of that component. The total Hopf charge is the sum of the subscripts plus superscripts. Similarly, for $N = 6$ the ground state hopfion is a link of two charge 2 unknots, so that it can be called $\mathbf{L}^{1,1}_{2,2}$.

For $N = 7$ the true knot appears at last: the ground state configuration corresponds in this case to the simplest non-trivial torus knot: trefoil knot. Let us remind that a (p, q) torus knot is formed by wrapping a circle around a torus p times in one direction and q times in the other, where p and q are coprime integers, $p > q$. One can explicitly parametrize it as $\rho = R + \cos(p\varphi/q), z = \sin(p\varphi/q)$, where $R > 1$. A (p, q) torus knots can also be obtained as the intersection of the unit three sphere $S^2 \in \mathbb{C}^2$ defined by $|\phi|^2 + |\sigma|^2 = 1$ with the complex algebraic curve $\sigma^p + \phi^q = 0$. The trefoil knot is the $(3, 2)$ torus knot, and it determines the profile of the position curve of the $N = 7$ fundamental hopfion denoted $7\mathbf{K}_{3,2}$ in Ref. [158].

Sutcliffe [158] extends the energy minimization up to $N = 16$ specially looking for other knots. For the input configurations in his numerical procedure he uses fields parametrized by the rational map ansatz,

$$W = \frac{\sigma^a \phi^b}{\sigma^p + \phi^q}, \tag{2.23}$$

Table 1
Known Hopf solitons according to Refs. [90,158,15]

N	1	2	2	3	3	4	4	4	5
	$\underline{\mathbf{A}_{1,1}}$	$\underline{\mathbf{A}_{2,1}}$	$\mathbf{A}_{1,2}$	$\underline{\tilde{\mathbf{A}}_{3,1}}$	$\mathbf{A}_{3,1}$	$\underline{\mathbf{A}_{2,2}}$	$\tilde{\mathbf{A}}_{4,1}$	$\mathbf{A}_{4,1}$	$\underline{\mathbf{L}^{1,1}_{1,2}}$
$\mathcal{E}$	1	0.97	0.98	1.00	1.01	1.01	1.03	1.06	1.02
N	5	5	6	6	6	7	7	8	8
	$\tilde{\mathbf{A}}_{5,1}$	$\mathbf{A}_{5,1}$	$\underline{\mathbf{L}^{1,1}_{2,2}}$	$\underline{\mathbf{L}^{1,1}_{1,3}}$	$\mathbf{A}_{6,1}$	$\underline{\mathbf{K}_{3,2}}$	$\mathbf{A}_{7,1}$	$\underline{\mathbf{L}^{1,1}_{3,3}}$	$\mathbf{K}_{3,2}$
$\mathcal{E}$	1.06	1.17	1.01	1.09	1.22	1.01	1.20	1.02	1.02
N	8	9	9	10	10	10	11	11	11
	$\mathbf{A}_{8,1}$	$\underline{\mathbf{L}^{2,2,2}_{1,1,1}}$	$\mathbf{K}_{3,2}$	$\underline{\mathbf{L}^{2,2,2}_{1,1,2}}$	$\mathbf{L}^{2,2}_{3,3}$	$\mathbf{K}_{3,2}$	$\underline{\mathbf{L}^{2,2,2}_{1,2,2}}$	$\mathbf{K}_{5,2}$	$\mathbf{L}^{2,2}_{3,4}$
$\mathcal{E}$	1.40	1.02	1.02	1.02	1.02	1.03	1.02	1.03	1.04
N	11	12	12	12	12	13	13	13	13
	$\mathbf{K}_{3,2}$	$\underline{\mathbf{L}^{2,2,2}_{2,2,2}}$	$\mathbf{K}_{4,3}$	$\mathbf{K}_{5,2}$	$\mathbf{L}^{2,2}_{4,4}$	$\underline{\mathbf{K}_{4,3}}$	χ_{13}	$\mathbf{K}_{5,2}$	$\mathbf{L}^{3,3}_{3,4}$
$\mathcal{E}$	1.05	1.01	1.01	1.04	1.04	1.00	1.03	1.04	1.05
N	14	14	14	15	15	15	16		
	$\underline{\mathbf{K}_{4,3}}$	$\mathbf{K}_{5,3}$	$\mathbf{K}_{5,2}$	$\underline{\chi_{15}}$	$\mathbf{L}^{4,4,4}_{1,1,1}$	$\mathbf{K}_{5,3}$	$\underline{\chi_{16}}$		
$\mathcal{E}$	1.00	1.01	1.05	1.01	1.02	1.02	1.01		

where $0 < a \in \mathbb{Z}$, $0 \leq b \in \mathbb{Z}$ and W, ϕ, σ are defined by Eqs. (2.15) and (2.16). The position curve for such a field configuration coincides with the (p, q) torus knot, since the condition $W = \infty$ reproduces the knot equation. The parameters a, b determine the value of the Hopf charge, $N = aq + bp$ [158]. If p, q are not coprime, then the denominator in (2.23) factorizes and the whole expression describes a link. As a result, fixing a value of N one can construct many different knot or link configurations compatible with this value. Numerically relaxing these configurations, Sutcliffe finds many new energy minima, discovering new knots and links [158]. He also obtains configurations that he calls χ whose position curve seems to self-intersect and so it is not quite clear to what type they belong, unless the self-intersections are only apparent and can be resolved by increasing the resolution.

The properties of all known hopfions, according to the results of Refs. [90,158,15], are summarized in Table 1 and in Fig. 6. Table 1 shows the Hopf charge, the type of the solution, with the ground state configuration in each topological sector underlined, and also the relative energy $\mathcal{E}$ defined by the relation

$$E_N/E_1 = \mathcal{E}N^{3/4}, \tag{2.24}$$

where E_1 is the energy of the $N = 1$ hopfion. Of the two decimal places of values of $\mathcal{E}$ shown in the table the second one is rounded. Different groups give slightly different values for the energy, but one can expect the relative energy to be less sensitive to this. The values of $\mathcal{E}$ for $N \leq 7$ shown in the table correspond to the data of Hietarinta and Salo [90] and of Sutcliffe [158], and it appears that for solutions described by both of these groups these values are the same. The data for $8 \leq N \leq 16$ are given by Sutcliffe [158], apart from those for the $\mathbf{A}_{N,1}$ hopfions for $N = 5, 6, 7, 8$, which are found in the earlier work of Battye and Sutcliffe [15]. Although $\mathbf{A}_{N,1}$ solutions seem to exist also for $N > 8$, no data are currently available for this case. To obtain the energies from Eq. (2.24) one can use the value $E_1 = 1.22$, which is known to be accurate to the two decimal places [172].

As one can see, the hopfion energies follow closely the topological lower bound (2.18). This suggests that the ground state hopfions actually attain this bound, so that they should be topologically stable. According to the data in Table 1 one has $\inf\{\mathcal{E}\} = 0.97$ for $N \leq 16$, and if this is true for all values of N then the optimal value for the constant in the bound (2.18) is $c = E_1 \inf\{\mathcal{E}\} = 1.18$.

A rigorous existence proof for the hopfions was given by Lin and Yang [119], who demonstrate the existence of a smooth least energy configuration in every topological sector whose Hopf charge value belongs to an infinite (but unspecified) subset of $\mathbb{Z}$. This shows that ground state hopfions exist, although perhaps not for any $N \in \mathbb{Z}$. As shown in Ref. [119], their energy is bounded not only below but also *above* as

$$E < C|N|^{3/4}, \tag{2.25}$$

where C is an absolute constant. This implies that knotted solitons are energetically preferred over widely separated unknotted multisoliton configurations when N is sufficiently large. Indeed, for a decay into charge one elementary hopfions the energy should grow at least as N for large N, but it grows slower.

The position curves of the solutions, schematically shown in Fig. 6, present an amazing variety of shapes. It should be stressed though that other characteristics of the solutions, as for example their energy density, do not necessarily show the same knotted pattern. Several types of links and knots appear, and each particular type can appear several times, for different values of the Hopf charge. Intuitively, one can view the position curves as wisps made of two intertwined lines corresponding to preimages of two infinitely close to $-\mathbf{n}_\infty$ points on the target space [158]. Increasing the twist of the wisp

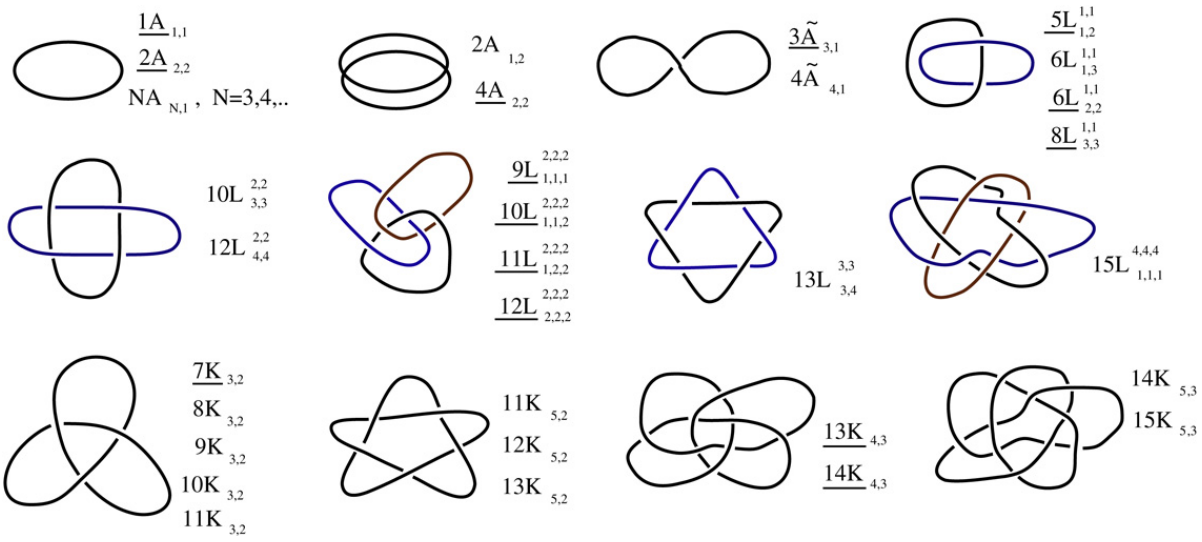

Fig. 6. Schematic profiles of the position curves for the known hopfions (excepting the χ-solutions) according to the results of Refs. [90,158].

increases the Hopf charge, without necessarily changing the topology of the position curve. A more detailed inspection (see pictures in [158]) actually shows that configurations appearing several times in Fig. 6, as for example the trefoil knot $\mathbf{K}_{3,2}$, become more and more distorted by the internal twist as N increases. Finally, for some critical value of N, the excess of the intrinsic deformation makes it energetically favorable to change the knot/link type and pass to other, more complicated knot/link configurations. Estimating the length of the position curves shows that it grows as $N^{3/4}$, so that the energy per unit length is approximately the same for all hopfions [158].

2.5. Conformally invariant knots

Hopf solitons in the Faddeev–Skyrme model, also sometimes called in the literature knot solitons of Faddeev–Niemi, of Faddeev–Skyrme, or of Faddeev–Hopf provide the best known example of knot solitons in field theory. However, there are also other field theory models admitting knotted solitons with a non-zero Hopf index. An interesting example proposed by Nicole [128] is obtained by taking the first term in the Faddeev–Skyrme model (2.1) and raising it to a fractional power,

$$\mathcal{L}_{\text{Nicole}} = \left(-\partial_\mu \mathbf{n}\cdot\partial^\mu \mathbf{n}\right)^{3/2}. \tag{2.26}$$

A similar possibility, suggested by Aratyn, Ferreira and Zimerman (AFZ) [9], uses the second term in the Faddeev–Skyrme Lagrangian,

$$\mathcal{L}_{\text{AFZ}} = \left(\mathcal{F}_{\mu\nu}\mathcal{F}^{\mu\nu}\right)^{3/4}. \tag{2.27}$$

Both of these models are conformally invariant in three spatial dimensions and so the existence of static solitons is not excluded for them by the Derrick argument. In fact, static knot solitons in these models exist and can even be obtained in close analytical form, which is achieved by simply using the axial ansatz (2.10) with the function Θ, ψ expressed in toroidal coordinates Eq. (2.13) according to Eq. (2.14) [8,3]. Curiously, this separates away the v, φ variables in the field equations reducing the problem to an *ordinary* differential equation for $\Theta(u)$ (in the Faddeev–Skyrme theory this does not work). In the AFZ model solutions for $\Theta(u)$ can be expressed in terms of elementary functions for any n, m [8], while in the Nicole model they are obtained numerically [3], apart from the $|n| = |m| = 1$ case, where the solution turns out to be the same in both models and is given by $\tan(\Theta/2) = \sinh u$ [128,9]. These results remain, however, interesting mainly from the purely mathematical point of view at the time being, since it is difficult to justify physically the appearance of the fractional powers in Eqs. (2.26) and (2.27).

Other examples of solitons with a Hopf charge will be discussed in Sections 6.3 and 7.3.2.

2.6. Can one gauge the knot solitons ?

The Faddeev–Skyrme theory is a *global* field model, so that it cannot be a fundamental physical theory like gauge field theory models, but perhaps can be viewed as an effective theory. This suggests using the Faddeev–Skyrme knots for an effective description of some physical objects, and so it has been conjectured by Faddeev and Niemi that they could be used for an effective description of glueballs in the strongly coupled Yang–Mills theory [66,68,153,154,53,69]. This conjecture is very interesting, quite in the spirit of the original Lord Kelvin's idea to view atoms as knotted ether tubes [162], and perhaps it could apply in some form. In fact, when describing the $\eta(1440)$ meson, the Particle Data Group says (see p. 591 in Ref. [60]) that "the $\eta(1440)$ is an excellent candidate for the 0^{-+} glueball in the flux tube model [69]".

Some other physical applications of the global field theory knot solitons could perhaps be found. However, if they could be promoted to *gauge* field theory solutions, then they would be much more interesting physically, since in this case they would find many interesting applications, as for example in the theories of superconductivity and of Bose–Einstein condensation [11,12], in the theory of plasma [67,63], in Standard Model [36,70,130], or perhaps even in cosmology, where they could presumably describe knotted cosmic strings [165]. For this reason it has been repeatedly conjectured in the literature that some analogs of the Faddeev–Skyrme knot solitons could also exist as static solutions of the gauge field theory equations of motion. This conjecture is essentially inspired by the fact that the Faddeev–Skyrme theory already contains something like a gauge field: $\mathcal{F}_{\mu\nu}$. Moreover, we shall now see that changing the variables one can rewrite the theory in such a form that it looks almost identical to a gauge field theory (or the other way round).

2.7. Faddeev–Skyrme model versus semi-local Abelian Higgs model

Let Φ be a doublet of complex scalar fields satisfying a constraint,

$$\Phi = \begin{pmatrix} \phi \\ \sigma \end{pmatrix}, \quad \Phi^\dagger \Phi = |\phi|^2 + |\sigma|^2 = 1, \tag{2.28}$$

such that $\Phi \in S^3$. Let us consider a field theory defined by the Lagrangian density

$$\mathcal{L}[\Phi] = -\frac{1}{4}\,\mathcal{F}_{\mu\nu}\mathcal{F}^{\mu\nu} + (\mathcal{D}_\mu \Phi)^\dagger \mathcal{D}^\mu \Phi \tag{2.29}$$

with $\mathcal{F}_{\mu\nu} = \partial_\mu \mathcal{A}_\nu - \partial_\nu \mathcal{A}_\mu$ and $\mathcal{D}_\mu \Phi = (\partial_\mu - i\mathcal{A}_\mu)\Phi$ and with

$$\mathcal{A}_\mu = -i\Phi^\dagger \partial_\mu \Phi. \tag{2.30}$$

In fact, this theory is again the Faddeev–Skyrme model but rewritten in different variables, since upon the identification

$$n^a = \Phi^\dagger \tau^a \Phi \tag{2.31}$$

(τ^a being the Pauli matrices) the fields $\mathcal{A}_\mu$ and $\mathcal{F}_{\mu\nu}$ coincide with those in (2.1) [141] and the whole action (2.29) reduces (up to an overall factor) to (2.1) [65]. More precisely, (2.31) is the Hopf projection from S^3 parametrized by (ϕ, σ) to S^2 parametrized by the complex projective coordinate ϕ/σ. For example, the axially symmetric fields (2.10) and (2.11) are obtained in this way by choosing the CP^1 variables

$$\phi = \cos\frac{\Theta}{2}\, e^{in\psi}, \quad \sigma = \sin\frac{\Theta}{2}\, e^{im\varphi}, \tag{2.32}$$

such that the phases of ϕ and σ wind, respectively, along the two orthogonal direction as shown in Fig. 2 and the Hopf charge is $N = nm$.

The fields in the static limit, $\Phi = \Phi(\mathbf{x})$, can now be viewed as maps $S^3 \to S^3$, but their energy

$$E[\Phi] = \int \left(|\mathcal{D}_k \Phi|^2 + \frac{1}{4}\,(\mathcal{F}_{ik})^2 \right) \mathrm{d}^3\mathbf{x} \tag{2.33}$$

is still bounded from below as in Eq. (2.18). The topological charge $N = N[\Phi]$, still expressed by Eq. (2.9), is now interpreted as the index of map $S^3 \to S^3$, $N \in \pi_3(S^3) = \mathbb{Z}$. The theory therefore admits the same knot solitons as the original Faddeev–Skyrme model. However, in the new parametrization the theory looks almost like a gauge field theory, in particular it exhibits a local U(1) gauge invariance under $\Phi \to e^{i\alpha}\Phi$, $A_\mu \to A_\mu + \partial_\mu \alpha$.

Let us now compare the model (2.29) to a genuine gauge field theory with the Lagrangian density

$$\mathcal{L}[\Phi, A_\mu] = -\frac{1}{4}\,F_{\mu\nu}F^{\mu\nu} + (D_\mu \Phi)^\dagger D^\mu \Phi - \frac{\lambda}{4}\,(\Phi^\dagger \Phi - 1)^2. \tag{2.34}$$

Here Φ is again a doublet of complex scalar fields, but this time without the normalization condition (2.28), the condition (2.30) being also relaxed, so that A_μ is now an independent field. One has $F_{\mu\nu} = \partial_\mu A_\nu - \partial_\nu A_\mu$ and $D_\mu \Phi = (\partial_\mu - iA_\mu)\Phi$. This semi-local [2] Abelian Higgs model with the $\mathrm{SU}(2)_{\mathrm{global}} \times \mathrm{U}(1)_{\mathrm{local}}$ internal symmetry arises in various contexts, in particular it can be viewed as the Weinberg–Salam model in the limit where the weak mixing angle is $\pi/2$ and the SU(2) gauge field decouples. The non-relativistic limit of this theory is the two-component Ginzburg–Landau model [77].

Let us now consider the limit $\lambda \to \infty$. In this sigma model limit the constraint (2.28) is enforced and the potential term in (2.34) vanishes. The theories (2.29) and (2.34) then look identically the same, the only difference being that in the first case the vector field $\mathcal{A}_\mu$ is defined by Eq. (2.30) and so is composite, while in the second case A_μ is an independent field.

2.8. Energy bound in the Abelian Higgs model

The question now arises: does the gauge field theory (2.34), at least in the limit where $\Phi^\dagger\Phi = 1$, admit knot solitons analogous to those of the global model (2.29) ? If exist, such solutions would correspond to minima of the energy in the theory (2.34) in static, purely magnetic sector,

$$E[\Phi, A_k] = \int \left(|D_k\Phi|^2 + \frac{1}{4}(F_{ik})^2 \right) \mathrm{d}^3\mathbf{x}. \tag{2.35}$$

At first thought, one may think that the answer to this question should be affirmative. Indeed, the energy functionals (2.33) and (2.35) look identical. They have the same internal symmetries and the same scaling behavior under $\mathbf{x} \to \Lambda\mathbf{x}$. The two theories also have the same topology associated to the field Φ, since in both cases $\Phi(\mathbf{x})$ defines a mapping $S^3 \to S^3$ with the topological index (2.9).

The gauged model (2.35) contains in fact even more charges than the global theory (2.33), since it actually has two vector fields: the independent gauge field A_k and the composite field $\mathcal{A}_k = \frac{i}{2}(\partial_k\Phi^\dagger\Phi - \Phi^\dagger\partial_k\Phi)$. It is convenient to introduce their difference $C_k = A_k - \mathcal{A}_k$. Defining the linking number between two vector fields,

$$I[A, B] = \frac{1}{4\pi^2}\int \epsilon_{ijk}A_i\partial_j B_k \,\mathrm{d}^3\mathbf{x}, \tag{2.36}$$

one can construct three different charges,

$$N[\Phi] \equiv I[\mathcal{A}, \mathcal{A}], \quad \mathrm{L} = I[C, A], \quad N_{\mathrm{CS}}[A] \equiv I[A, A], \tag{2.37}$$

which are, respectively, the topological charge (2.9), the linking number between A_k and C_k, and the Chern–Simons number of the gauge field. The following inequality, established by Protogenov and Verbus [137], holds:

$$E[\Phi, A_k] \geq c_1|N|^{3/4}\left(1 - \frac{|\mathrm{L}|}{|N|}\right)^2, \tag{2.38}$$

where c_1 is a positive constant. This can be considered as the generalization of the topological bound (2.18) of Vakulenko–Kapitanski.

Given all these, one may believe that the local theory (2.35) admits topologically stable knot solitons similar to those of the global theory (2.33).

2.9. The issue of charge fixing

The difficulty with implementing the Protogenov–Verbus bound (2.38) in practice is that it contains two different charges, N and L, but without invoking additional physical assumptions there is no reason why L should be fixed while minimizing the energy.

Let us consider first the charge $N = N[\Phi]$. Its variation vanishes identically, so that it does not change under smooth deformations of Φ. It is therefore a genuine topological charge whose value is completely determined by the boundary conditions, and so it should be fixed when minimizing the energy.

Let us now consider the linking number $\mathrm{L} = I[C, A]$. The analogs of this quantity have been studied in the theory of fluids, where they are known to be integrals of motion [178]. In the context of gauge field theory, this quantity is gauge invariant. However, it is not a topological invariant, since its variation does not vanish identically and so it does change under arbitrary smooth deformations of $C_k = A_k - \mathcal{A}_k$. One cannot fix L using only continuity arguments, because there are no topological conditions imposed on A_k, whose arbitrary deformations are allowed. The only topological quantity associated to A_k could be a magnetic charge related to a non-trivial U(1) bundle structure. However, since we are interested in globally regular solutions, the bundle base space is $\mathbb{R}^3$ (or S^3) without removed points, in which case the bundle is trivial.

As a result, on continuity grounds only, one can fix N but not L. But then, as is obvious from Eq. (2.38), there is no non-trivial lower bound for the energy, since one can always choose $\mathrm{L} = N$ in which case the expression on the right in (2.38) vanishes. More precisely, since there are no constraints for A_k, nothing prevents one from smoothly deforming it to zero, after which one can scale away the rest of the configuration. Explicitly, given fields Φ, A_k one can reduce $E[\Phi, A_k]$ to *zero* via a continuous sequence of smooth field deformations preserving the value of the topological charge $N[\Phi]$,

$$E[\Phi(\mathbf{x}), A_k(\mathbf{x})] \to E[\Phi(\Lambda\mathbf{x}), \gamma A_k(\mathbf{x})] \tag{2.39}$$

by taking first the limit $\gamma \to 0$ and then $\Lambda \to \infty$ [74].

The conclusion is that without constraining A_k, with only $N[\Phi]$ fixed, the absolute minimum of $E[\Phi, A_k]$ is zero, so that there can be no absolutely stable knots. To have such solutions, one would need to constraint somehow the vector field A_k, for example it would be enough to ensure that $C_k = A_k - \mathcal{A}_k$ be zero or small. Such a condition is often assumed in the literature [12,11,36,70], but usually simply *ad hoc*. Unfortunately, it cannot be justified on continuity grounds only, without an additional physical input.

2.10. Searching for gauged knots

The above arguments do not rule out all solutions in the theory. Even though the global minimum of the energy is zero, there could still be non-trivial local minima or saddle points. The corresponding static solutions would be metastable or unstable. One can therefore wonder whether such solutions exist. This question has actually a long history, being first addressed by de Vega [49] and by Huang and Tipton [93] over 30 years ago, and being then repeatedly reconsidered by different authors [109,130,74,174,95,57,55,56]. However, the answer is still unknown. No solutions have been found up to now, neither has it been shown that they do not exist.

Trying to find the answer, all the authors were minimizing the energy given by the sum of $E[\Phi, A_k]$ and of a potential term that can be either of the form contained in (2.34) or a more general one. A theory with two vector fields with a local $U(1) \times U(1)$ invariance – Witten's model of superconducting strings [177] – has also been considered in this context [57,55,56]. The energy was minimized within the classes of fields with a given topological charge N and having profiles of a loop of radius R. The resulting minimal value of energy was always found to be a monotonously growing function of R, thus always showing the tendency of the loop to shrink thereby reducing its energy.

These results render the existence of solutions somewhat implausible. However, they do not yet prove their absence. Indeed, local energy minima may be difficult to detect via energy minimization, as this would require starting the numerical iterations in their close vicinity, because otherwise the minimization procedure converges to the trivial global minimum. In other words, one has to choose a good initial configuration. However, since 'there is a lot of room in function space', chances to make the right choice are not high.

It should be mentioned that a positive result was once reported in Ref. [130], were the energy was minimized in the $N = 2$ sector and an indication of a convergence to a non-trivial minimum was observed. However, this result was not confirmed in an independent analysis in Ref. [174], so that it is unclear whether it should be attributed to a lucky choice of the initial configuration or to some numerical artifacts.

3. Knot solitons in gauge field theory

As we have seen, fixing only the topological charge does not guarantee the existence of knot solitons in gauge field theory. In order to obtain such solutions one needs to constraint the gauge field in order that it could not be deformed to zero. Below we describe two known examples of such solutions.

3.1. Anomalous solitons

One possibility to constraint the gauge field is to fix its Chern–Simons number. An example of how this can be done was suggested long ago by Rubakov and Tavkhelidze [143,142], who showed that the Chern–Simons number can be fixed by including fermions into the system. They considered the Abelian Higgs model Eq. (2.34), but with a *singlet* and not doublet Higgs field, augmented by including chiral fermions. In the weak coupling limit at zero temperature this theory contains states with N_F non-interacting fermions and with the bosonic fields being in vacuum, $A_\mu = 0$, $\Phi = 1$. The energy of such states is $E \sim N_F$. Rubakov and Tavkhelidze argued that this energy could be decreased via exciting the bosonic fields in the following way.

Owing to the axial anomaly, when the gauge field A_μ varies, the fermion energy levels can cross zero and dive into the Dirac see. The fermion number can therefore change, but the difference $N_F - N_{CS}$ is conserved. As a result, starting from a purely fermionic state and increasing the gauge field, one can smoothly deform this state to a purely bosonic state, whose Chern–Simon number will be fixed by the initial conditions,

$$N_{CS} = N_F. \tag{3.40}$$

Now, the energy of this state,

$$E[\Phi, A_k] = \int \left(|D_k \Phi|^2 + \frac{1}{4} (F_{ik})^2 + \frac{\lambda}{4} (|\Phi|^2 - 1)^2 \right) \mathrm{d}^3\mathbf{x}, \tag{3.41}$$

can be shown to be bounded from *above* by $E_0 (N_{CS})^{3/4}$ where E_0 is a constant, and so for large $N_F = N_{CS}$ it grows slower than the energy of the original fermionic state, $E \sim N_{CS}$ [143,142]. Therefore, for large enough N_F, it is energetically favorable for the original purely fermionic state to turn into a purely bosonic state. The latter is called *anomalous* [143,142]. The energy of this anomalous state can be obtained by minimizing the functional (3.41) with the Chern–Simons number fixed by the condition (3.40).

Such an energy minimization was carried out in the recent work of Schmid and Shaposhnikov [151]. First of all, they established the following inequality,

$$E[\Phi, A_k] \geq c (N_{CS})^{3/4}, \tag{3.42}$$

which reminds very much of the Vakulenko–Kapitanski bound (2.18) for the Faddeev–Skyrme model, but with the topological charge replaced by N_{CS}. This gives a very good example of how constraining the gauge field can stabilize the

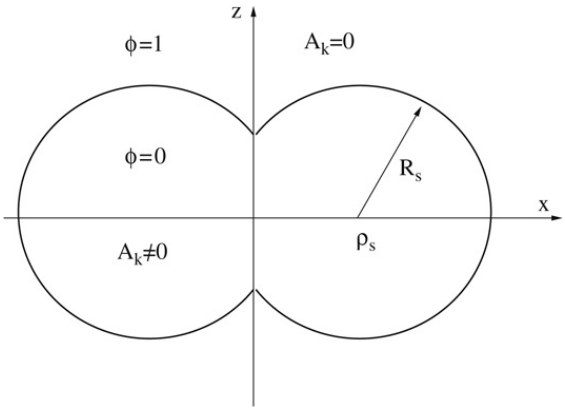

Fig. 7. Spindle torus shape of the anomalous solitons for large N_{CS}.

system: even though in the theory with a singlet Higgs field there is no topological charge similar to the Hopf charge, its role can be taken over by the Chern–Simons charge.

In order to numerically minimize the energy, Schmid and Shaposhnikov considered the Euler–Lagrange equations for the functional

$$E[\Phi, A_k] + \mu \int \epsilon_{ijk} A_i \partial_j A_k \mathrm{d}^3\mathbf{x} \tag{3.43}$$

where $E[\Phi, A_k]$ is given by (3.41) and μ is the Lagrange multiplier. In the gauge where $\Phi = \Phi^* \equiv \phi$ these equations read (with $\vec{A} = A_k$)

$$\Delta\phi - \vec{A}^2\phi - \frac{\lambda}{2}(\phi^2 - 1)\phi = 0, \tag{3.44a}$$

$$\vec{\nabla} \times (\vec{\nabla} \times \vec{A}) + 2\mu\vec{\nabla} \times \vec{A} + 2\phi^2\vec{A} = 0, \tag{3.44b}$$

where $\vec{\nabla}$ and $\Delta = (\vec{\nabla})^2$ are the standard gradient and Laplace operators, respectively. Multiplying Eq. (3.44b) by $\vec{A}$ and integrating gives the expression for the Lagrange multiplier,

$$\mu = \frac{1}{32\pi^2 N_{CS}} \int \left((\nabla \times \vec{A})^2 + |\vec{A}|^2\phi^2 \right) \mathrm{d}^3\mathbf{x}. \tag{3.45}$$

Solutions of the elliptic equations (3.44a) and (3.44b) were studied in [151] in the axially symmetric sector, where $\phi = \phi(\rho, z)$ and $\vec{A} = \vec{A}(\rho, z)$, with the boundary conditions

$$\phi = 1, \quad \vec{A} = 0 \tag{3.46}$$

at infinity and

$$\partial_\rho\phi = \partial_\rho A_z = 0, \quad A_\rho = A_\varphi = 0 \tag{3.47}$$

at the symmetry axis $\rho = 0$. The solutions obtained are quite interesting. They are very strongly localized in a compact region, Ω, of the (ρ, z) plane centered around a point $(\rho_s, 0)$. Inside Ω the field A_k is non-zero, while ϕ is almost constant and very close to zero. As one approaches the boundary of the region, $\partial\Omega$, the field A_k tends to zero, while ϕ is still almost zero. Finally, in a small neighborhood of $\partial\Omega$ whose thickness is of the order of the Higgs boson wavelength, ϕ starts varying and quickly increases up to its asymptotic value. Outside Ω one has everywhere $\phi \approx 1$ and $A_k \approx 0$, such that the energy density is almost zero. The energy for these solutions scales as $(N_{CS})^{3/4}$. For large N_{CS} the region Ω can be described by the simple analytic formula,

$$(\rho - \rho_s)^2 + z^2 < R_s^2, \tag{3.48}$$

where $R_s > \rho_s$. In other words, the 3D domain where the soliton energy is concentrated can be obtained by rotating around the z-axis a disc centered at a point whose distance from the z-axis is less than its radius (see Fig. 7). Such a geometric figure is called spindle torus [151]. The solutions for large N_{CS} are very well approximated by setting $\phi = 1$ and $A_k = 0$ outside the spindle torus, while inside it one has $\phi = 0$ and A_k is obtained by solving the linear equation (3.44b). The spindle torus approximation becomes better and better for large N_{CS}, in which limit Schmid and Shaposhnikov obtain the following asymptotic formulas for the energy and parameters of the torus, which agree very well with their numerics,

$$E = 118\,\lambda^{1/4} M_W (N_{CS})^{3/4}, \quad \rho_s = \frac{1.7}{M_W}\left(\frac{N_{CS}}{\lambda}\right)^{1/4}, \quad R_s = 1.49\rho_s, \tag{3.49}$$

where M_W is the vector field mass.

It is likely that these solutions attain the lower energy bound (3.40), which means that they should be topologically *stable*. It should, however, be emphasized that the anomalous solitons require a rather exotic physical environment, since for them to be energetically favored as compared to the free fermion condensate, the density of the latter should attain enormous values possible perhaps only in the core of neutron stars.

Summarizing, fixing the Chern–Simons number forbids deforming the gauge field to zero and gives rise to stable knot solitons in gauge field theory, even if the Higgs field is topologically trivial. It is unclear whether this result can be generalized within the context of the model (2.34) with two-component Higgs field — since the Protogenov–Verbus formula (2.38) contains not the Chern–Simons number but the linking number L.

3.2. Non-Abelian rings

Another interesting class of objects arises in the non-Abelian gauge field theory, where one can have smooth, finite energy loops stabilized by the magnetic energy.

3.2.1. Yang–Mills–Higgs theory

Let us parametrize the non-Abelian Yang–Mills–Higgs theory for a compact and simple gauge group $\mathcal{G}$ as

$$\mathcal{L}[A_\mu, \Phi] = -\frac{1}{4}\langle F_{\mu\nu}F^{\mu\nu}\rangle + (D_\mu\Phi)^\dagger D^\mu\Phi - U(\Phi). \tag{3.50}$$

Here the gauge field strength is $F_{\mu\nu} = \partial_\mu A_\nu - \partial_\nu A_\mu - \mathrm{ig}[A_\mu, A_\nu] \equiv F^a_{\mu\nu}\mathbf{T}_a$ where $A_\mu = A^a_\mu\mathbf{T}_a$ is the gauge field, $a = 1, 2, \ldots, \dim(\mathcal{G})$, and g is the gauge coupling. The Hermitian gauge group generators $\mathbf{T}_a$ satisfy the relations

$$[\mathbf{T}_a, \mathbf{T}_b] = iC_{abc}\mathbf{T}_c, \quad \mathrm{tr}(\mathbf{T}_a\mathbf{T}_b) = \mathrm{K}\delta_{ab}. \tag{3.51}$$

The Lie algebra inner product is defined as $\langle AB\rangle = \frac{1}{\mathrm{K}}\,\mathrm{tr}(AB) = A^aB^a$. The Higgs field Φ is a vector in the representation space of $\mathcal{G}$ where the generators $\mathbf{T}_a$ act; this space can be complex or real. The covariant derivative of the Higgs field is $D_\mu\Phi = (\partial_\mu - \mathrm{ig}A_\mu)\Phi$ and the Higgs field potential can be chosen as $U(\Phi) = \frac{\lambda}{2}(\Phi^\dagger\Phi - 1)^2$. The Lagrangian is invariant under the local gauge transformations,

$$\Phi \to \mathrm{U}\Phi, \quad A_\mu \to \mathrm{U}\left(A_\mu + \frac{\mathrm{i}}{g}\partial_\mu\right)\mathrm{U}^{-1}, \tag{3.52}$$

where $\mathrm{U} = \exp(\mathrm{i}\alpha^a(x^\mu)T_a) \in \mathcal{G}$. The field equations read

$$\begin{aligned}
&\hat{\mathcal{D}}_\mu F^{\mu\nu} = \mathrm{ig}\left\{(D^\nu\Phi)^\dagger\mathbf{T}_a\Phi - \Phi^\dagger\mathbf{T}_aD^\nu\Phi\right\}\mathbf{T}_a,\\
&D_\mu D^\mu\Phi = -\frac{\partial U}{\partial(\Phi^\dagger\Phi)}\,\Phi,
\end{aligned} \tag{3.53}$$

where $\hat{\mathcal{D}}_\mu = \partial - \mathrm{ig}[A_\mu, \ ]$ is the covariant derivative in the adjoint representation. The energy–momentum tensor is

$$T^\mu_\nu = -\langle F_{\nu\sigma}F^{\mu\sigma}\rangle + (D_\nu\Phi)^\dagger D^\mu\Phi + (D^\mu\Phi)^\dagger D_\nu\Phi - \delta^\mu_\nu\mathcal{L}. \tag{3.54}$$

3.2.2. Monopole rings

The ring solitons in the theory (3.50) have been first constructed by Kleihaus, Kunz and Shnir [106,107] in the case where $\mathcal{G} = \mathrm{SU}(2)$ and the Higgs field is in its adjoint, $\Phi \equiv \Phi^a$, such that the gauge group generators are 3×3 matrices with components $(\mathbf{T}_a)_{bc} = -i\epsilon_{abc}$. The fundamental solutions in this theory are the magnetic monopoles of 't Hooft and Polyakov [160,136], while the ring solitons are more general solutions. Specifically, in the static, axially symmetric and purely magnetic case it is consistent to choose the following ansatz for the fields in spherical coordinates:

$$\begin{aligned}
&A_\mu\mathrm{d}x^\mu = (K_1\mathrm{d}r - (1-K_2)\mathrm{d}\vartheta)\mathbf{T}_\varphi + m(K_3\mathbf{T}_r + (1-K_4)\mathbf{T}_\vartheta)\sin\vartheta\,\mathrm{d}\varphi,\\
&\mathbf{T}_a\Phi^a = \phi_1\mathbf{T}_r + \phi_2\mathbf{T}_\vartheta,
\end{aligned} \tag{3.55}$$

where functions $K_1, K_2, K_3, K_4, \phi_1, \phi_2$ depend on r, ϑ and are subject of suitable boundary conditions at the symmetry axis and at infinity [106,107]. Here

$$\begin{aligned}
&\mathbf{T}_r = \sin(k\vartheta)\cos(m\varphi)\mathbf{T}_1 + \sin(k\vartheta)\sin(m\varphi)\mathbf{T}_2 + \cos(k\vartheta)\mathbf{T}_3,\\
&\mathbf{T}_\vartheta = \frac{1}{k}\frac{\partial}{\partial\vartheta}\mathbf{T}_r, \quad \mathbf{T}_\varphi = \frac{1}{m\sin\vartheta}\frac{\partial}{\partial\varphi}\mathbf{T}_r,
\end{aligned} \tag{3.56}$$

with $k, m \in Z$. Using the gauge-invariant tensor

$$H_{\mu\nu} = \Phi^aF^a_{\mu\nu} - \epsilon_{abc}\Phi^aD_\mu\Phi^bD_\nu\Phi^c \tag{3.57}$$

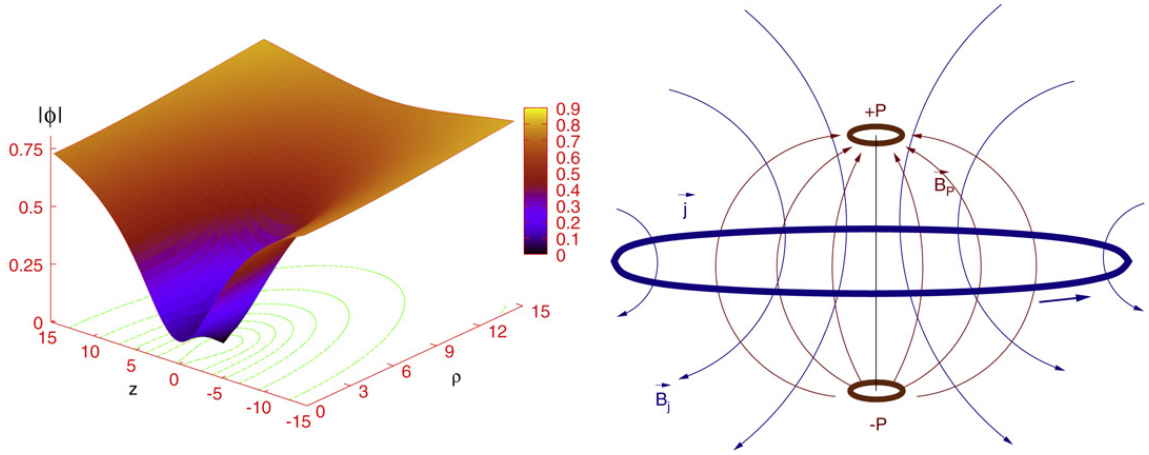

Fig. 8. Left: Higgs field amplitude for the $k = 2$, $m = 3$ monopole ring solution in the limit where the Higgs field potential is zero. $|\Phi|$ vanishes at a point in the (ρ, z) plane away from the z-axis, which corresponds to a ring. Right: schematic shape of charge/current distribution for this solution.

and its dual, $\tilde{H}_{\mu\nu} = \frac{1}{2}\epsilon_{\mu\nu\alpha\beta}H_{\alpha\beta}$, one can define the electric and magnetic currents, respectively, as

$$j_\mu = \partial^\alpha H_{\alpha\beta}, \qquad \tilde{j}_\mu = \partial^\alpha \tilde{H}_{\alpha\beta}. \tag{3.58}$$

It turns out that the solutions depend crucially on values of k, m in (3.55). In particular, their magnetic charge is given by

$$\mathcal{Q} = \frac{m}{2}[1 - (-1)^k]. \tag{3.59}$$

The following solutions are known in the limit of vanishing Higgs potential (for a generic potential their structure is more complicated) [106,107]:

$k = 1, m = 1$ — the spherically symmetric 't Hooft–Polyakov monopole.

$k = 1, m > 1$ — multimonopoles.

$k > 1, m = 1, 2$ — monopole–antimonopole sequences.

$k = 2l \geq 2, m \geq 3$ — monopole vortex rings.

In the first three cases the Higgs field has discrete zeros located at the z-axis. Solutions of the last type are especially interesting in the context of our discussion, since zeros of the Higgs fields in this case are not discrete but continuously distributed along a circle (for $k = 2$) around the z-axis (see Fig. 8). Solutions in this case can be visualized as stationary rings stabilized by the magnetic energy. The mechanism of their stabilization is quite interesting and can be elucidated as follows [155,156]. If one studies the profiles of the currents (3.58) for these solutions, it turns out that both the magnetic charge density $\tilde{j}_0$ and the electric current density j_k have ring shape distributions, as qualitatively shown in Fig. 8.

Although the total magnetic charge is zero, locally the charge density is non-vanishing and the system can be visualized as a pair of magnetically charged rings with opposite charge located at $z = \pm z_0$, accompanied by a circular electric current in the $z = 0$ plane. The two magnetic rings create a magnetic field orthogonal to the $z = 0$ plane. This magnetic field forces the electric charges in the plane to Larmore orbit, which creates a circular current. The Biot–Savart magnetic field produced by this current acts, in its turn, on the magnetic rings keeping them away from each other, so that the whole system is in a self-consistent equilibrium [155] (assuming the magnetic rings to be rigid).

It is, however, unlikely that this sophisticated balance mechanism stabilizing the rings against contraction could also guarantee their stability with respect to all possible deformations. In fact, the monopole–antimonopole solution is known to be unstable [161], while the monopole rings can be viewed as generalizations of this solution. They are therefore likely to be saddle points of the energy functional and so they should be unstable as well.

3.2.3. *Sphaleron rings*

Very recently, a similar ring construction was carried out by Kleihaus, Kunz and Leissner [101] within the context of the Yang–Mills–Higgs theory (3.50) with $\mathcal{G} = \mathrm{SU}(2)$ and with the Higgs field in its fundamental complex doublet representation, where $\mathbf{T}_a = \frac{1}{2}\tau_a$. This theory can be viewed as the $\mathrm{SU}(2) \times \mathrm{U}(1)$ Weinberg–Salam theory in the limit where the weak mixing angle vanishes and the U(1) gauge field decouples. Kleihaus, Kunz and Leissner used exactly the same field ansatz (3.55), only modifying the Higgs field as

$$\Phi = (\phi_1 \mathbf{T}_r + \phi_2 \mathbf{T}_\vartheta)\Phi_0, \tag{3.60}$$

where Φ_0 is a constant 2-vector. As in the monopole case, in this case too the solutions depend strongly on the choice of the integers k and m in Eq. (3.56). The fundamental solutions in this case are the sphalerons — unstable saddle point configurations that can be smoothly deformed to vacuum. They can be characterized by the Chern–Simons number, given

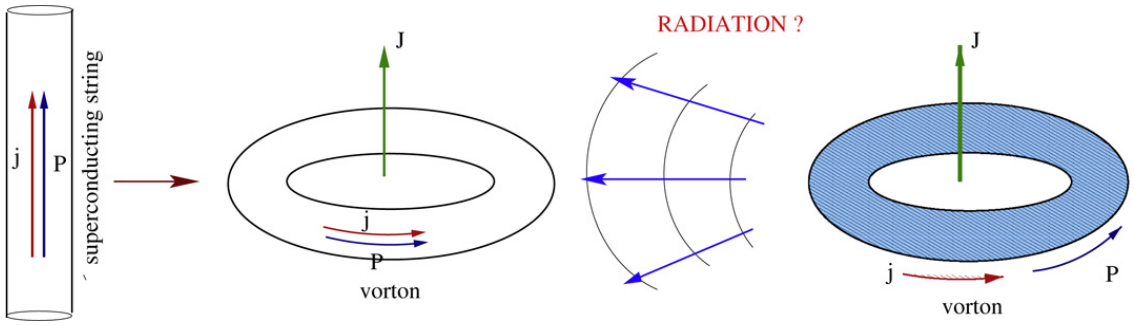

Fig. 9. One can make a loop from a vortex carrying a current j and momentum P. It will have an angular momentum, but it may be radiating.

by the same formula as the magnetic charge in the monopole case, up to the factor 1/2, so that half-integer values are now allowed: $\mathcal{Q} = m[1 - (-1)^k]/4$.

Setting $k = m = 1$ gives the Klinkhamer–Manton sphaleron [108], in which case the Higgs field vanishes at one point. Choosing $k = 1, m > 1$ or $k > 1, m = 1$ gives multisphalerons or sphaleron–antisphaleron solutions for which the Higgs field has several isolated zeros located at the symmetry axis [101]. A new type of solution arises for $k \geq 2, m \geq 3$, in which case the Higgs field vanishes on one or more rings centered around the symmetry axis. In this respect these sphaleron rings are quite analogous to the monopole rings. It is unclear at the moment whether their existence can be qualitatively explained by a mechanism similar to that for the monopole rings, shown in Fig. 8.

Since sphalerons are unstable objects, it is very likely that sphaleron rings are also unstable. However, similar to the sphalerons, they could perhaps be interesting physically as mediators of baryon number violating processes [108].

4. Angular momentum and radiation in field systems

We are now passing to the spinning systems with the ultimate intention to discuss spinning vortex loops stabilized by the centrifugal force — vortons. As was already said in the Introduction, usually vortons are considered within a qualitative macroscopic description as loops made of vortices and stabilized by rotation. This description is suggestive, but it does not take into account the radiation damping. At the same time, the presence of the vorton angular momentum requires some internal motions in the system (see Fig. 9), as for example circular currents, and these are likely to generate radiation carrying away both the energy and angular momentum. It is therefore plausible that macroscopically constructed vortex loops will not be stationary field theory objects, but at best only quasistationary, with a finite lifetime determined by the radiation rate.

The best way to decide whether vortons are truly stationary or only quasistationary is to explicitly resolve the corresponding field theory equations. The current situation in this direction is not, however, very suggestive. Within the original local U(1) × U(1) Witten's model of superconducting cosmic strings [177] vorton solutions have never been constructed. To the best of our knowledge, the only explicit vorton solutions have been presented by Lemperier and Shellard [118] within the global version of Witten's model, and also by Battye, Cooper and Sutcliffe [17] in a special limit of the same global model. In addition, vortons in a $(2 + 1)$-dimensional field theory toy model have been recently analyzed [19].

Lemperier and Shellard [118] considered the full hyperbolic evolution problem for the fields, with the initial data corresponding to a vortex loop. Evolving dynamically this loop in time, they saw it oscillate around a visibly stationary equilibrium position, and they could follow these oscillations for several dozen characteristic periods of the system. This suggests that vortons exist and are stable against perturbations. However, one cannot decide on these grounds whether the equilibrium configurations are truly stationary or only quasistationary, since the radiation damping could be non-zero but too small to be visible in their numerics. In addition, Lemperier and Shellard did not actually consider precisely the global version of Witten's model (see Eq. (6.138)), but, in order to improve the numerics, added to it a Q-ball-type interaction term of the form $|\phi|^6|\sigma|^2$, where ϕ, σ are the two scalars in the model.

Battye, Cooper and Sutcliffe [17] did not study Witten's model but minimized the energy of a non-relativistic Bose–Einstein condensate, which seems to be mathematically equivalent to solving equations of Witten's model in a special limit. They found non-trivial energy minima saturated by configurations of vorton type, which again suggests that vortons exist, at least in this limit. Moreover, this suggests that they are indeed non-radiative — since being already in the energy minimum they cannot lose energy anymore. It would therefore be interesting to construct these solutions in a different way, extending the analysis to the full Witten's model.

The method we shall employ below to study truly non-radiating vortons will be to construct them as stationary solutions of the elliptic boundary value problem obtained by separating the time variable. However, first of all we need to understand how in principle a non-radiating field system can have a non-zero angular momentum. Both angular momentum and radiation are associated to some internal motions in the system, and it is not completely clear how to reconcile the presence of the former with the absence of the latter.

4.1. Angular momentum for stationary solitons

In what follows we shall be considering field theory systems obeying the following four conditions:

(1) stationarity
(2) finiteness of energy
(3) axial symmetry
(4) non-vanishing angular momentum

The angular momentum is defined as the Noether charge associated to the global spacetime symmetry generated by the axial Killing vector $K = \partial/\partial\varphi$,

$$J = \int T^0_\varphi \mathrm{d}^3\mathbf{x}. \tag{4.61}$$

Let us discuss the first three conditions.

(1) A system is stationary if its energy–momentum tensor T^μ_ν does not depend on time. According to the standard definition of symmetric fields [71], for stationary fields the action of time translations can be compensated by internal symmetry transformations.

If all internal symmetries of the theory are local, then there is a gauge where the compensating symmetry transformation is trivial, so that the stationary fields are time-independent. We shall call them *manifestly* stationary. If the theory contain also global internal symmetries and if the compensating symmetry transformation is global, then its action cannot be trivialized and so the action of time translations will be non-trivial. The fields will explicitly depend on time in this case, typically via time-dependent phases, and we shall call them *non-manifestly* stationary.

For example, in a system with two complex scalars coupled to a U(1) gauge field one cannot gauge away simultaneously phases of both scalars. A non-manifestly stationary field configuration will then be $\phi_1(\mathbf{x}), \phi_2(\mathbf{x})\mathrm{e}^{\mathrm{i}\omega t}, A_\mu(\mathbf{x})$. However, if there is only one scalar, then it is always possible to gauge away its time-dependent phase.

(2) Even if T^μ_ν is time-independent, one can still have a constant radiation flow compensated by the energy inflow from infinity. However, if the energy is finite, then the fields fall-off fast enough at infinity to eliminate this possibility.

In principle, one can also have situations where T^μ_ν is time-dependent, but radiation is nevertheless absent, as for the breathers in $1+1$ dimensions [139]. However, such cases are probably less typical and we shall not discuss them.

(3) It is intuitively clear that asymmetric spinning systems will more likely radiate than symmetric ones. It is therefore most natural to assume spinning non-radiating solitons to be axially symmetric. The axially symmetry can be manifest or non-manifest. In fact, it appears that the axial symmetry condition can sometimes be relaxed, but such a possibility seems to be more exotic and will be discussed below only very briefly in Section 5.3.

Let us now analyze possibilities for condition (4) to coexist with (1)–(3).

4.1.1. The case of manifest symmetries — no go results

In theories where *all* internal symmetries are local the stationary field are time-independent. Can one have an angular momentum in this case?

In fact, even without an explicit time dependence one can have a non-vanishing field momentum expressed by the Poynting vector, $\vec{\mathcal{E}} \times \vec{\mathcal{B}}$, and this could give a contribution to the angular momentum,

$$\int \vec{r} \times (\vec{\mathcal{E}} \times \vec{\mathcal{B}})\, \mathrm{d}^3\mathbf{x}. \tag{4.62}$$

If the theory contains gauged scalars, they will give an additional contribution. If there exists a stationary, globally regular, finite energy on-shell configuration for which the integral (4.61) is non-zero, this would correspond to a rotating and non-radiating soliton. The existence of such solutions is not *a priori* excluded. However, it turns out that for a number of physically interesting cases they can be ruled out.

Specifically, since the time translations and spatial rotations commute, the system is not only manifestly stationary but also manifestly axially symmetric [71]. It turns out that the latter condition allows one to transform the volume integral in Eq. (4.61) to a surface integral, which is often enough to conclude that $J = 0$.

To me more precise, let us consider the Yang–Mills–Higgs theory (3.50). If the fields (A_μ, Φ) are manifestly invariant under the action of a Killing symmetry generator $K = \partial/\partial s$, then there is a gauge where they do not depend on the corresponding spacetime coordinate s and their Lie derivatives along K vanish, $\pounds_K A_\mu = \pounds_K \Phi = 0$. In some other gauge the fields could depend on s, but only in such a way that [71]

$$\pounds_K A_\mu = \hat{\mathcal{D}}_\mu W(K), \quad \pounds_K \Phi = \mathrm{i}gW(K)\Phi. \tag{4.63}$$

Here $W(K)$ takes its values in the Lie algebra of the gauge group and transforms as connection under gauge transformations. If $K = \partial/\partial\varphi$ is the axial Killing vector and $W_\varphi \equiv W(K)$, then in spherical coordinates these conditions reduce to

$$\partial_\varphi A_\mu = \hat{\mathcal{D}}_\mu W_\varphi, \quad \partial_\varphi \Phi = \mathrm{i}gW_\varphi \Phi. \tag{4.64}$$

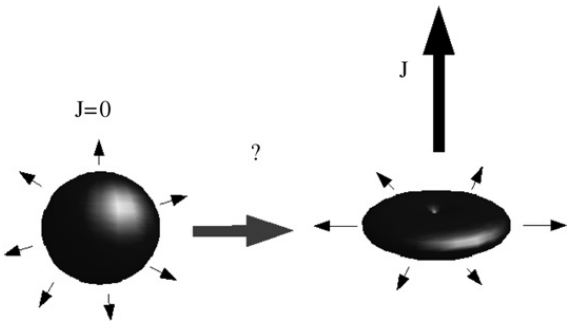

Fig. 10. Do static solitons admit stationary, spinning generalizations?

If these conditions are fulfilled, then it is straightforward to check with the field equations (3.53) that the T^0_φ component of the energy–momentum tensor (3.54) has a total derivative structure [50,169],

$$T^0_\varphi = \partial_k \langle (W_\varphi - A_\varphi) F^{0k} \rangle . \tag{4.65}$$

Since both A_φ and W_φ transform as connections under gauge transformations, their difference is gauge covariant, so that this formula is gauge invariant. For globally regular solutions the electric field $\mathcal{E}^k = F^{0k}$ is everywhere bounded, which allows one to transform the volume integral of T^0_φ to a surface integral over the boundary of $\mathbb{R}^3$ at infinity. This gives the surface integral representation for the angular momentum

$$J = \oint \langle (W_\varphi - A_\varphi) \vec{\mathcal{E}} \rangle \, \mathrm{d}\vec{S}. \tag{4.66}$$

This formula imposes rather strong restrictions on the existence of spinning solitons. For example, it shows that if the electric field $\mathcal{E}$ decays at infinity faster than $1/r^2$, such that the electric charge is zero, then $J = 0$. A non-zero electric charge is therefore necessary to have a non-zero angular momentum [50]. Similarly, using the asymptotic conditions in the far field zone, one can show that for a number of important cases the asymptotic behavior of the fields does not allow for the surface integral to be non-zero.

Specifically, one can consider any known static, spherically symmetric soliton, as for example the 't Hooft–Polyakov monopole, and ask if it admits stationary, spinning generalizations (see Fig. 10)? For example, the static Schwarzschild black hole solution of Einstein's equation in General Relativity can be generalized to the manifestly stationary, spinning Kerr black hole. One can wonder if similar generalizations are possible for solitons in non-linear field theories in Minkowski space. If they exist, then in the far field zone their fields should approach those of the original static soliton, so that they should be spherically symmetric, up to small corrections which could contribute to the surface integral (4.66). Since the corrections are small, their most general form can be determined from the linearized field equations [169].

Surprisingly, one discovers in this way that none of the well-known solitons in the gauge field theory (3.50) with gauge group SU(2), as for example the magnetic monopoles of 't Hooft–Polyakov [160,136], dyons of Julia–Zee [98], and sphalerons of Klinkhamer–Manton [108], admit spinning generalizations within the manifestly stationary and manifestly axisymmetric sector [50,51,169]. The picture in Fig. 10 thus does not apply for these solitons. If the gauge symmetry is completely broken in the Higgs vacuum, as for the sphalerons, then the fields approach their vacuum values exponentially fast and the surface integral vanishes. For the monopoles and dyons there is a long-range field associated with the unbroken U(1), so that some additional analysis is required to show that in the asymptotic region there are actually no field modes giving a non-zero contribution to the surface integral [169].

As a result, the best known SU(2) solitons cannot spin in the manifestly stationary and manifestly axisymmetric sector. This restricts rather strongly the existence of spinning solitons with manifest symmetries, although does not rule them out completely. Such solutions might exist in theories with other gauge groups. Their explicit examples in U(1) gauge field theories will be presented below. Non-manifestly symmetric rotational excitations could perhaps exist for the sphalerons, since only an SU(2) part of their U(2) internal symmetry is gauged. A more exotic possibility to have stationary rotation without axial symmetry will be briefly discussed in Section 5.3.

4.1.2. The case of non-manifest symmetries

More general possibilities to have spinning solitons arise in theories where *not all* internal symmetries are local, since in this case the conditions (4.63) can be generalized as

$$\pounds_K A_\mu = \hat{\mathcal{D}}_\mu W(K), \quad \pounds_K \Phi = \mathrm{i}gW(K)\Phi + \mathrm{i}T(K)\Phi, \tag{4.67}$$

where $T(K)$ is a function of the *global* symmetry generators. One can gauge away $W(K)$ but not $T(K)$, so that the action of the Killing symmetry will always be non-trivial, since Φ will depend explicitly on the corresponding spacetime coordinate s as

$$\Phi(s) = \mathrm{e}^{\mathrm{i}sT(K)}\Phi_0. \tag{4.68}$$

This means that the s-dependence is equivalent to a sequence of internal symmetry transformations, in which case the invariant objects like T^{μ}_{ν} will not depend on s at all. Such a symmetry can be called *non-manifest*. Non-manifestly stationary and non-manifestly axisymmetric fields would typically depend on t, φ via the complex phase factor

$$\exp\{\mathrm{i}(\omega t + m\varphi)\}, \tag{4.69}$$

in which case one can say that it is the phase that spins. The angular momentum in this case cannot be totally expressed by a surface integral and will contain a volume integral contribution, in which case typically $J \sim \omega m$.

As a result, one can have $J \neq 0$. However, the absence of radiation is not yet guaranteed. Separating the time variable makes the equations elliptic, but with the mass term(s) modified as

$$M^2 \to M^2 - \omega^2, \tag{4.70}$$

where M^2 collectively denotes masses of the field excitations in the asymptotic zone. Now, if the equations admit globally regular solutions with

$$\omega^2 < M^2 \tag{4.71}$$

then these solutions will behave asymptotically as $\exp\{-\sqrt{M^2-\omega^2}\ r\}$ and there will be no radiation. On the other hand, if $\omega^2 > M^2$ then solutions in the asymptotic region will oscillate as $\exp\{\pm\mathrm{i}\sqrt{\omega^2-M^2}\ r\}$ thus showing the presence of the ingoing and outgoing radiation, even though T^{μ}_{ν} is time-independent, so that the total energy will be infinite. As a result, the no-radiation condition (4.71) becomes crucial in this case.

4.1.3. Spinning solitons as solutions of elliptic equations

Summarizing the above discussion, one can conclude that the existence of non-radiating spinning solitons, although not forbidden, is not guaranteed either. Even for known static solitons their spinning generalizations may or may not exist, and if they do exist, this should be considered as something exceptional rather than the general rule. At first view, such a conclusion may seem to contradict our experience, since normally one knows that compact objects can spin. However, we are not saying that generic field theory solitons cannot spin. They always can, but it seems that they should generically radiate at the same time. One can always 'give a kick' to any static soliton, as for example to the magnetic monopole or to any of the knotted solitons of Faddeev–Skyrme shown in Fig. 6, so that they will start spinning. However, at the same time they will start radiating away all the received energy and angular momentum, till they relax back to the original static, non-spinning configuration. It seems that 'spinning and radiating' represents the generic way the field systems behave, while 'spinning without radiating' should rather be considered as something exceptional, possible only in some special field theory models.

Perhaps the best way to really establish the existence of spinning and non-radiating solitons would be to construct them as solutions of the elliptic boundary value problem obtained by separating the time variable. In gauge field theory, as for example in the local $\mathrm{U}(1) \times \mathrm{U}(1)$ Witten's model [177], one could look for manifestly stationary and axisymmetric vortons, in which case there is no radiation. However, since the angular momentum in this case can be expressed by the surface integral (4.66) and so is determined only by the asymptotic behavior of the fields, there are higher chances that it could vanish. For global field theories one could consider systems with non-manifest symmetries, in which cases there are better chances to have a non-zero angular momentum, but also higher chances to have radiation, unless the no-radiation condition (4.71) is fulfilled.

5. Explicit examples of stationary spinning solitons

Before coming to vortons, one can wonder, in view of the above discussion, if there exist at all any known examples of non-radiating spinning solitons. As we said, for the $\mathrm{SU}(2)$ magnetic monopoles, dyons and sphalerons there are no spinning generalizations, at least in the manifestly stationary and manifestly axisymmetric case. Nevertheless, explicit examples of spinning solitons in Minkowski space in $3+1$ dimensions exist and below we shall review all known solutions of this type. These are the spinning Q-balls, spinning Skyrmions and also rotating monopole–antimonopole pairs, apart from the vortons. Interestingly, it seems that spinning solitons are in some sense more easily constructed in curved space, because the spinning degrees of freedom can be naturally associated to the non-radiative dipole moment of gravitational field. For this reason a number of articles cited below actually describe the Minkowski space spinning solitons only as a special limit of the more general, self-gravitating configurations.

5.1. Q-balls

This is important for our discussion example which shares many features with the vortons. At the same time, spinning Q-balls are simpler than vortons, and so they can be used to introduce a number of notions to be applied later. We shall therefore discuss them in some detail.

Q-balls have been introduced by Coleman [39]. These are non-topological solitons [116] found in a theory with a single complex scalar field with the Lagrangian density

$$\mathcal{L}_Q[\Phi] = \partial_\mu \Phi^* \partial^\mu \Phi - U(|\Phi|), \tag{5.72}$$

the corresponding field equation being

$$\partial_\mu \partial^\mu \Phi + \frac{\partial U}{\partial |\Phi|^2}\, \Phi = 0, \tag{5.73}$$

while the energy–momentum tensor

$$T_{\mu\nu} = \partial_\mu \Phi^* \partial_\nu \Phi + \partial_\nu \Phi^* \partial_\mu \Phi - g_{\mu\nu} \mathcal{L}_Q. \tag{5.74}$$

The potential U should have the absolute minimum, $U(0) = 0$, and should also satisfy the condition

$$\omega_-^2 = \min_f \frac{U(f)}{f^2} < \omega_+^2 = \frac{1}{2} \frac{\mathrm{d}^2 U}{\mathrm{d}f^2}\bigg|_{f=0}, \tag{5.75}$$

whose meaning will be explained below. The value of ω_+ determines the mass of the field quanta, $M = \omega_+$. For the condition (5.75) to be fulfilled U should (if it is even in $|\Phi|$) contain powers of $|\Phi|$ higher than four, which means that the theory cannot be renormalizable [39]. A convenient choice is

$$U = \lambda |\Phi|^2 (|\Phi|^4 - a|\Phi|^2 + b), \tag{5.76}$$

where λ, a, b are positive constants, so that $\omega_+^2 = \lambda b$ and $\omega_-^2 = \omega_+^2 (1 - a^2/4b)$. In our numerics below we shall always choose $\lambda = 1$, $a = 2$, $b = 1.1$ [168], which is not a restriction (for $\omega_- \neq 0$) since λ, a can be changed by rescaling the coordinates and field, while the mass $M = \sqrt{\lambda b}$ enters the field equation (5.83) only in the combination $M^2 - \omega^2$ where ω is another free parameter.

The global invariance of the theory under $\Phi \to \Phi \mathrm{e}^{\mathrm{i}\alpha}$ implies the conservation of the Noether charge

$$Q = \mathrm{i} \int (\partial_t \Phi^* \Phi - \Phi^* \partial_t \Phi) \mathrm{d}^3 \mathbf{x}. \tag{5.77}$$

The scaling argument of Derrick applies for the theory (5.72) and rules out all static solutions with finite energy. Therefore, in order to circumvent this argument, solutions should depend on time,

$$\Phi = \phi(\mathbf{x}) \mathrm{e}^{\mathrm{i}\omega t}, \tag{5.78}$$

in which case the Noether charge is

$$Q = 2\omega \int \phi^2 \mathrm{d}^3 \mathbf{x} \equiv 2\omega \mathcal{N}. \tag{5.79}$$

In what follows we shall assume ω to be positive. More explicitly, with

$$E_2 = \int (\nabla \phi)^2 \mathrm{d}^3 \mathbf{x}, \qquad E_0 = \int U \mathrm{d}^3 \mathbf{x}, \tag{5.80}$$

the Lagrangian reads

$$L = \int \mathcal{L}_Q \, \mathrm{d}^3 \mathbf{x} = \omega^2 \mathcal{N} - E_0 - E_2. \tag{5.81}$$

Under scale transformations $\mathbf{x} \to \Lambda \mathbf{x}$ one has $L \to \Lambda^3 (\omega^2 \mathcal{N} - E_0) - \Lambda E_2$ so that L will be stationary for $\Lambda = 1$ if the virial relation is fulfilled,

$$3\omega^2 \mathcal{N} = 3E_0 + E_2, \tag{5.82}$$

which is only possible (for $E_0 \neq 0$, $E_2 \neq 0$) if $\omega \neq 0$.

Q-balls are finite energy solutions of the Lagrangian field equations for the ansatz (5.78),

$$\left(\Delta + \omega^2\right) \phi = \frac{\partial U}{\partial |\phi|^2}\, \phi. \tag{5.83}$$

Even though Φ depends on time, $T_{\mu\nu}$ is time-independent — the system is non-manifestly stationary. Equivalently, Q-balls can be obtained by minimizing the total energy

$$E = \int T_0^0 \mathrm{d}^3 \mathbf{x} = \int (\omega^2 |\phi|^2 + |\nabla \phi|^2 + U) \mathrm{d}^3 \mathbf{x} \equiv \omega^2 \mathcal{N} + E_0 + E_2 \tag{5.84}$$

by keeping fixed the charge Q. Indeed, rewriting the energy as

$$E = \frac{Q^2}{4\mathcal{N}} + E_0 + E_2 \tag{5.85}$$

shows that minimizing E with Q fixed is equivalent to extremizing L, since

$$\delta E = -\frac{Q^2}{4\mathcal{N}^2}\,\delta\mathcal{N} + \delta(E_0 + E_2) = -\omega^2\delta\mathcal{N} + \delta(E_0 + E_2) = -\delta L, \tag{5.86}$$

so that the on-shell condition $\delta L = 0$ follows from $\delta E = 0$. It is also instructive to see how the same thing comes about within the Lagrange multiplier method. Introducing

$$E_Q = \int (\omega^2|\phi|^2 + |\nabla\phi|^2 + U)\mathrm{d}^3\mathbf{x} + \mu\left(2\omega\int |\phi|^2\mathrm{d}^3\mathbf{x} - Q\right), \tag{5.87}$$

the condition $\partial E_Q/\partial\mu = 0$ fixes the charge, the condition $\partial E_Q/\partial\omega = 0$ gives $\mu = -\omega$ ensuring that $E_Q = L + \text{const.}$, so that the condition $\delta E_Q/\delta\phi = 0$ reproduces the field equation.

Equivalently, one can minimize the potential energy of the field, $E_0 + E_2$, by keeping fixed

$$\mathcal{N} = \int |\phi|^2\mathrm{d}^3\mathbf{x} \tag{5.88}$$

via extremizing the functional

$$E_{\mathcal{N}} = \int (|\nabla\phi|^2 + U)\mathrm{d}^3\mathbf{x} + \mu_1\left(\int |\phi|^2\mathrm{d}^3\mathbf{x} - \mathcal{N}\right). \tag{5.89}$$

The condition $\partial E_{\mathcal{N}}/\partial\mu_1 = 0$ imposes the constraint (5.88), while the condition $\delta E_{\mathcal{N}}/\delta\phi = 0$ reproduces the field equation (5.83) with $\omega^2 = -\mu_1$. The time dependence of the solutions is very implicit in this approach, since ω appears only as a Lagrange multiplier. It follows from Eq. (5.86) that

$$\omega^2 = \frac{\partial(E_0 + E_2)}{\partial\mathcal{N}}, \tag{5.90}$$

so that fixing $\mathcal{N}$ fixes also the charge $Q = 2\omega(\mathcal{N})\mathcal{N}$. In the non-relativistic theory $\mathcal{N}$ can be viewed as the particle number (see Section 7.1).

Let us also note that using the charge definition (5.79) and the virial relation (5.82) the energy (5.84) can be rewritten as

$$E = \omega Q + \frac{2}{3}E_2. \tag{5.91}$$

Q-balls could exist in the supersymmetric extensions of Standard Model [113] and could perhaps contribute to the dark matter [114].

5.1.1. Non-spinning Q-balls

Let us briefly consider the simplest spherically symmetric Q-balls [39], since this will help to understand more complex, spinning solutions. Setting $\Phi = \mathrm{e}^{\mathrm{i}\omega}f(r)$, the real amplitude $f(r)$ satisfies the equation

$$f'' + \frac{2}{r}f' + \omega^2 f = \frac{1}{2}\frac{\partial U}{\partial f}. \tag{5.92}$$

For the energy to be finite f should vanish at infinity, so that for large r one has

$$f \sim \frac{1}{r}\,\exp\{-\sqrt{M^2 - \omega^2}\,r\}. \tag{5.93}$$

Solutions of Eq. (5.92) comprise an infinite family labeled by an integer $n = 0, 1, \ldots$ counting the nodes of $f(r)$ [168] (see Fig. 11). The energy increases with n. These solutions admit a simple qualitative interpretation [39], since Eq. (5.92) is then equivalent to

$$f'^2 + U_{\text{eff}}(f) = \tilde{E} - 4\int_0^r f'^2\,\frac{\mathrm{d}r}{r}. \tag{5.94}$$

This describes a particle moving with friction in 1D potential $U_{\text{eff}}(f) = \omega^2 f^2 - U(f)$ shown in Fig. 11, the integration constant $\tilde{E}$ playing a role of the total energy. At the 'moment' $r = 0$ the 'particle' rests at a point with coordinate f_0 close to the potential maximum A (see Fig. 11), so that its energy is $\tilde{E} = U_{\text{eff}}(f_0)$. Then it starts moving to the left, dissipating its energy as it goes. One can adjust the value of f_0 so that for $r \to \infty$ it dissipates all its energy and arrives at the local

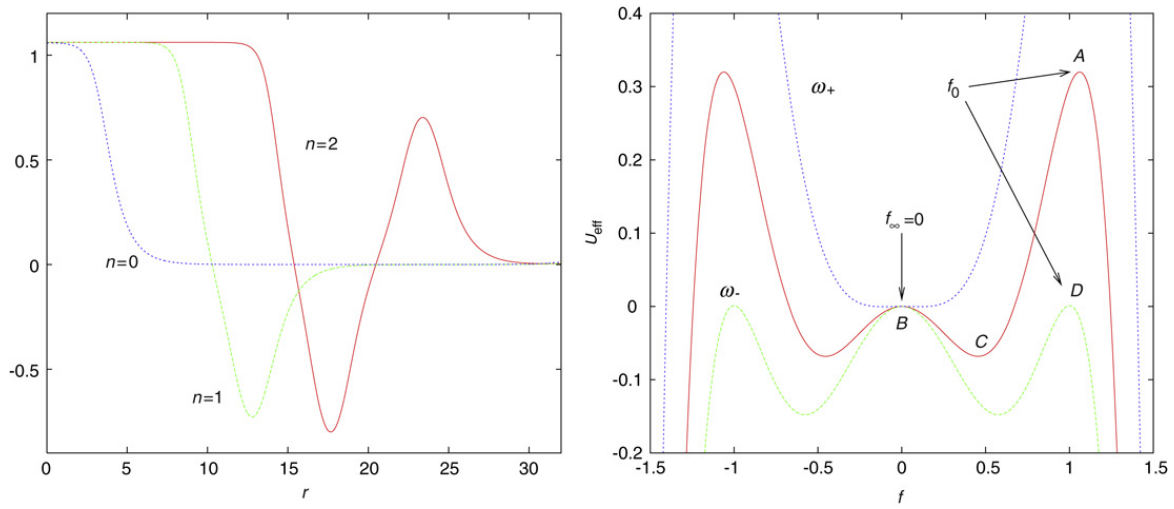

Fig. 11. Left: the amplitude $f(r)$ for the $n = 0, 1, 2$ spherically symmetric Q-balls with $\omega = 0.2$. Right: the effective potential $U_{\rm eff}$ in Eq. (5.94) for three values of ω.

maximum B of the potential with zero total energy to rest there — either directly or after n oscillations between the two potential hills.

It follows that ω should belong to the interval $\omega_- < \omega < \omega_+$, the condition Eq. (5.75) making sure that this interval is non-empty. Q-balls become large as $\omega \to \omega_\pm$, their charge and energy growing without bounds.

As $\omega \to \omega_-$ the maximum A of the potential descends towards the position D. The 'particle' then stays for a 'long time' at D, till the friction term becomes suppressed by the $1/r$ factor. Then it starts moving, crosses the potential well in a finite 'time' Δr and asymptotically approaches the potential maximum B. In the simplest $n = 0$ case solutions in this limit can be described by a smoothed step function,

$$f(r) \approx f_0 \Theta(R - r), \tag{5.95}$$

where $R \to \infty$ as $\omega \to \omega_-$ and $f' \approx f_0/\Delta r$ in a region of a fixed size $\Delta r \ll R$ around $r = R$. This is sometimes called Q-balls in the thin wall approximation [39]. Their charge $Q \sim R^3$ while $E_2 \sim R^2$ so that for large R one can neglect the second term in Eq. (5.91), which gives for their energy $E = \omega_- Q$. The same value is obtained inserting Eq. (5.95) to Eq. (5.85), neglecting the E_2 term and minimizing with respect to R, f_0.

When $\omega \to \omega_+$ the local minimum C of the potential approaches the local maximum B. The potential in their vicinity becomes approximately $U_{\rm eff} \approx f^2(f^2 - M_\omega^2)$ with $M_\omega^2 = \omega_+^2 - \omega^2$. Inserting this to Eq. (5.94) gives Q-balls in the thick wall approximation [112],

$$f(r) \approx \sqrt{2} M_\omega\, y(M_\omega r), \tag{5.96}$$

where $y(x)$ fulfills $y'' + (2/x)y' + (y^2 - 1)y = 0$. Solutions of this equation satisfy $y(0) = y_n$ and $y \sim e^{-x}$ for large x (one has $y_0 = 4.33$). Although $f \sim M_\omega$ is small in this case, the typical configuration radius $R \sim 1/M_\omega$ is large. The charge is also large, $Q \sim 1/M_\omega$, while $E_2 \sim M_\omega$, so that one can again neglect the second term in Eq. (5.91), which gives for the energy $E = \omega_+ Q$.

5.1.2. Spinning Q-balls

The spinning, axially symmetric generalizations for the spherically symmetric Q-balls have been constructed by Volkov and Wohnert [168] and have been analyzed also in Refs. [10,102,103,30]. These non-manifestly stationary and non-manifestly axisymmetric solutions provide the first explicitly constructed example of stationary, spinning solitons in Minkowski space in a relativistic field theory in $3 + 1$ spacetime dimensions. They have the typical ring structure, very similar to that for vortons, and they can also have the same topology as vortons. They admit simple generalizations to the gauged case. Spinning Q-balls thus provide a simple prototype example of vortons. Their analogs also exist in the context of non-linear optics [125], where they describe spinning light pulses (see Section 7.2).

Spinning Q-balls have a spinning phase: the field being non-manifestly stationary and non-manifestly axisymmetric,

$$\Phi = \mathrm{e}^{\mathrm{i}(\omega t + m\varphi)} f(r, \vartheta). \tag{5.97}$$

The real field amplitude $f(r, \vartheta)$ satisfies the equation

$$\left(\Delta - \frac{m^2}{r^2 \sin^2 \vartheta} + \omega^2\right) f = \frac{1}{2}\frac{\partial U}{\partial f}. \tag{5.98}$$

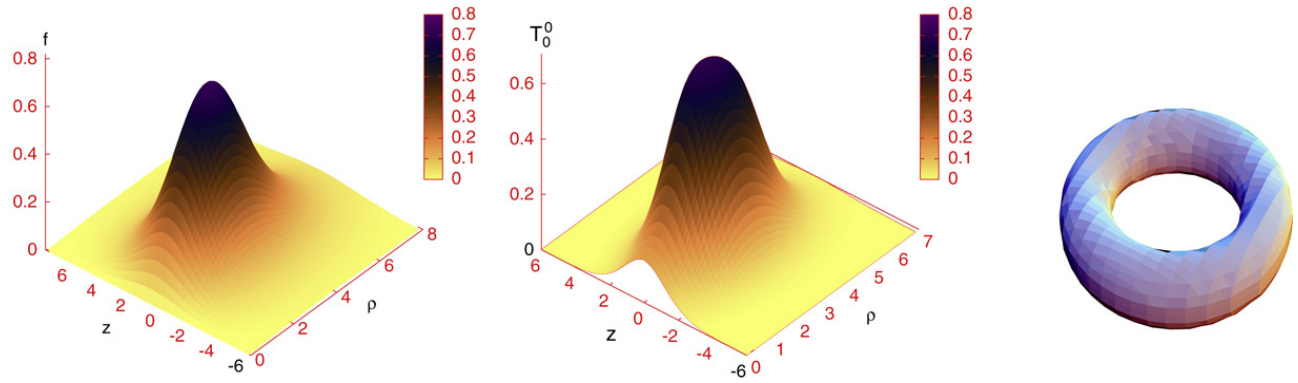

Fig. 12. The amplitude $f(r,\vartheta)$, energy density T_0^0 and the energy isosurface with $T_0^0 = 0.65$ for the 1^+ spinning Q-ball with $\omega = 0.9$.

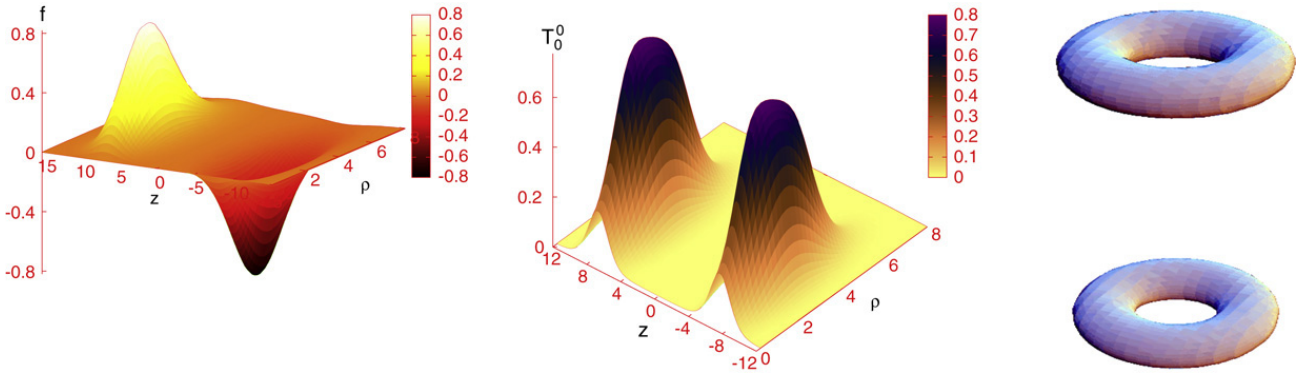

Fig. 13. The amplitude $f(r,\vartheta)$, energy density T_0^0 and the energy isosurface with $T_0^0 = 0.65$ for the 1^- spinning Q-ball with $\omega = 0.9$.

For $m \neq 0$ the energy will be finite if only f vanishes at the symmetry axis, while at infinity the asymptotic behavior (5.93) still applies. The energy–momentum T^μ_ν depends only on r, ϑ and the angular momentum is

$$J = \int T^0_\varphi \, \mathrm{d}^3\mathbf{x} = 2m\omega \int f^2 \mathrm{d}^3\mathbf{x} = 2m\omega\mathcal{N}, \tag{5.99}$$

so that it is classically quantized as

$$J = mQ. \tag{5.100}$$

In view of this relation, spinning Q-balls correspond to minima of energy with fixed angular momentum. They could therefore be obtained by extremizing

$$E = \frac{J^2}{4m^2 \int f^2 \, \mathrm{d}^3\mathbf{x}} + \int \left((\nabla f)^2 + \frac{m^2 f^2}{r^2 \sin^2\vartheta} + U \right) \mathrm{d}^3\mathbf{x} \tag{5.101}$$

with constant J, m, the corresponding extremum condition being given by Eq. (5.98). A direct minimization of this functional carried out in Ref. [10] (although for a different choice of the potential U) suggests that its extrema exist but seem to have negative directions. One should therefore integrate the field equation to construct these solutions.

Taking into account the boundary conditions at the z-axis and at infinity, Eq. (5.98) with $m \neq 0$ admits two different types of solutions determined by the behavior of f under $z \to -z$ [168].

For even-parity solutions, called m^+, the amplitude $f(r,\vartheta)$, energy–momentum and charge densities are maximal in the equatorial plane and the energy is concentrated in a toroidal region encircling the z-axis (see Fig. 12).

For odd-parity solutions, called m^-, the amplitude $f(r,\vartheta)$ vanishes in the equatorial plane, while the energy–momentum and charge densities show two maxima located symmetrically with respect to the plane, so that the solutions exhibit in this case a double torus or dumbbell-like structure (see Fig. 13).

Apart from choosing the parity and the value of m, solving the differential equation (5.98) also requires choosing ω^2 as an input parameter, the energy and charge being computed from the numerical output. As in the spherically symmetric case, spinning solutions are also found to exist only in a finite frequency range, $\omega_- < \omega < \omega_+$. Here $\omega_+ = M$ as in Eq. (5.75), while ω_- seems to be m-dependent. As ω approaches the limiting values, the energy and charge seem to grow without bounds (see Fig. 14), while somewhere in between there is a critical value of frequency, ω_{crit}, for which both $E(\omega)$ and $Q(\omega)$ attain their minimal values. This behavior is found for all m [102] and it is qualitatively the same as in the $m = 0$ case.

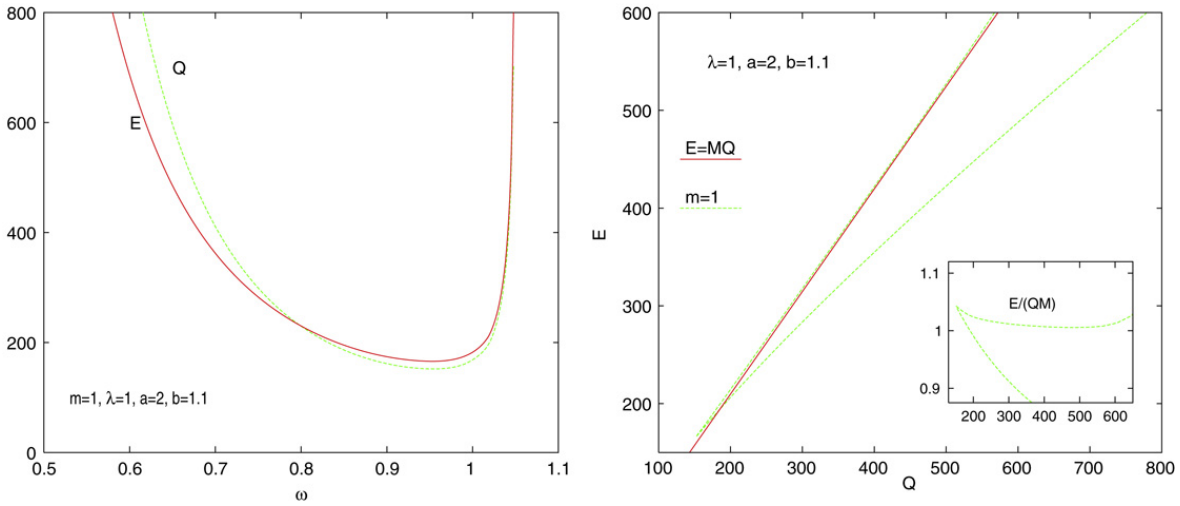

Fig. 14. Energy and charge $E(\omega)$, $Q(\omega)$ (left) and $E(Q)$ (right) for the 1^+ spinning Q-balls. For large Q one has $E(Q) = \omega_- Q$ and $E(Q) = \omega_+ Q$ for the lower an upper branch, respectively. The upper branch solutions are unstable, since $E/(MQ) > 1$, while the lower branch solutions are stable for large enough Q.

The existence of a minimal value of the Q-ball charge implies that the angular momentum (5.100) cannot be arbitrarily small. Q-balls cannot therefore rotate slowly. They show a *discrete* spectrum of spinning excitations.

Although it is difficult to qualitatively analyze the behavior of the $m \neq 0$ solutions, there are some analogies with the $m = 0$ case. Specifically, Q-balls become large as $\omega \to \omega_\pm$. For $\omega \to \omega_-$ they can be viewed as squashed spheroids, homogeneously filled inside, which reminds of the thin wall approximation. Unfortunately, an analog of the step function solution (5.95) does not directly apply for $m \neq 0$, since the function f cannot be constant inside the ball because it must vanish at the symmetry axis. Instead, f increases as one moves away from the axis and reaches maximal values at the surface of the spheroids, after which it rapidly goes to zero. The energy density is approximately constant inside the spheroid, with a slight increase at its surface, and rapidly vanishes outside it. For $\omega \to \omega_+$ solutions also become large spheroids, but this time they are hollow, with the maximal energy density concentrated at the surface and being close to zero everywhere else. It seems that the thick wall approximation (5.96) can be directly generalized to the axially symmetric case to give $f(r,\theta) \approx \sqrt{2} M_\omega\, y(M_\omega r, \theta)$ where $M_\omega \to 0$ and $y(r,\theta)$ fulfills $(\Delta - \frac{m^2}{r^2 \sin^2\theta} + y^2 - 1)y = 0$.

If one considers Q and not ω as the solution parameter then, using $E(\omega)$ and $Q(\omega)$ to express E in terms of Q, one discovers that the function $E(Q)$ is double-valued with a cusp, as shown in Fig. 14 [102]. For a given Q there are thus two different spinning Q-ball solutions with different energies. Solutions from the less energetic branch correspond to the $\omega < \omega_{\rm crit}$ parts of the $E(\omega)$, $Q(\omega)$ curves in Fig. 14. As in the $m = 0$ case, the plots shown in Fig. 14 demonstrate for large Q the linear dependence, $E = \omega_\pm Q$. This can again be explained by the general relation (5.91), implying that for large Q one can neglect the gradient energy E_2 as compared to Q.

The existence of two different solutions with the same Q suggests that the more energetic of them is unstable. In fact, it follows from Eq. (5.91) that the energy-to-charge ratio for Q-balls is $E/Q = \omega + 2E_2/3Q$. For the upper branch solutions one has $\omega \to \omega_+ = M$ for large Q, implying that $E/Q = M + O(Q^{-2})$ where the subleading term can in principle be positive or negative, depending on the details of the Q-ball potential. In the present case it is positive, as can be seen in Fig. 14, so that the upper branch Q-balls are unstable with respect to decay into free particles. The same argument for the lower branch solutions gives $E/Q = \omega_- < M$ for large Q, so that they cannot decay into free particles. However, there can be other decay modes, and so the stability analysis is needed. In fact, the $m = 0$ lower branch Q-balls are known to be stable [44]. The stability analysis of the even parity solutions with $m \neq 0$ will be described in Section 7.2. It seems that for $|m| = 1$ the lower branch solutions are stable only for large enough Q, while already for $|m| = 2$ all of them are unstable – they seem to decay by splitting into several non-spinning Q-balls.

It is plausible that spinning generalizations could also be constructed for the excited spherically symmetric Q-balls with $n > 0$. The complete family of spinning Q-balls should therefore contain not only $m^\pm$ solutions, but also the excited $(n, m^\pm)$ solutions with $n = 1, 2, \ldots$ for which the amplitude $f(r,\vartheta)$ exhibits nodes. More precisely, parametrizing the (ρ, z) plane by a complex variable $w = \rho + iz$, one can expect the amplitude $f(w)$ of the (n, m^+) and (n, m^-) solutions to have the same zeros as, respectively, $\Re(F_n^+(w))$ and $\Im(F_n^-(w))$, where

$$F_n^\pm(w) = \prod_{j=1}^{n} \alpha_j^\pm (w - \rho_j^\pm), \tag{5.102}$$

with some suitably chosen $\alpha_j^\pm \in \mathbb{C}$ and $\rho_j^\pm > 0$. However, very little is known about such excited solutions at present.

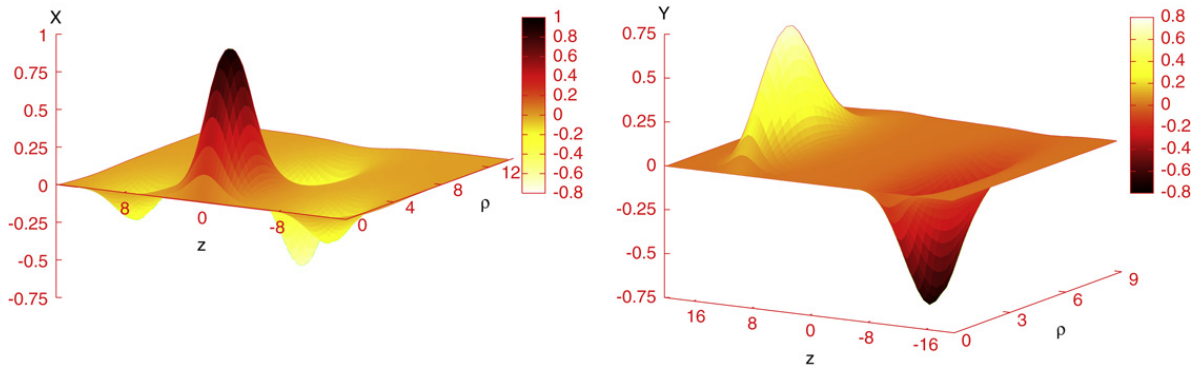

Fig. 15. Profiles of the (1, 1) twisted Q-ball with $\omega = 0.9$.

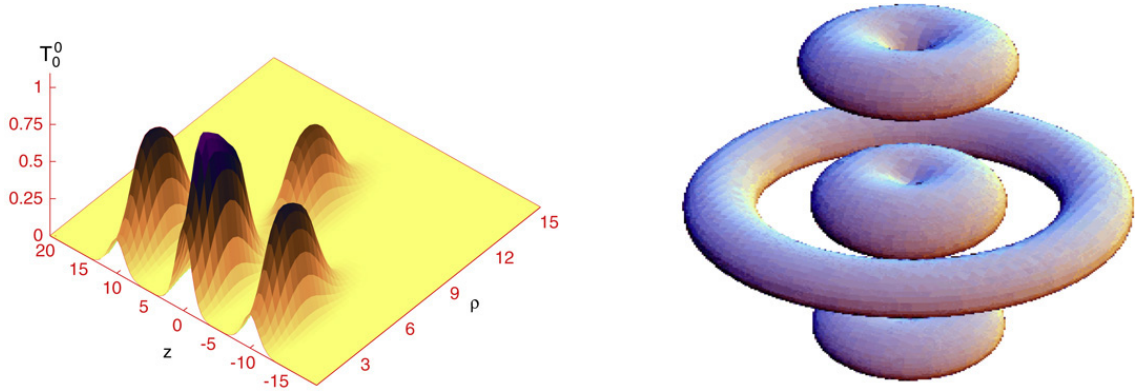

Fig. 16. Energy density for the (1, 1) twisted Q-ball with $\omega = 0.9$ (left) and the isosurfaces of constant energy density with $T_0^0 = 0.3$ (right).

5.1.3. Twisted Q-balls

Here and in the next subsection we briefly describe our new results on further generalizations of the spinning Q-balls, not yet discussed in the literature. Let us consider again the theory (5.72), but generalize the field ansatz to include an independent phase,

$$\Phi = \mathrm{e}^{\mathrm{i}(\omega t + m\varphi - n\psi(r,\theta))} f(r,\theta) \equiv (X(r,\vartheta) + \mathrm{i}Y(r,\vartheta))\mathrm{e}^{\mathrm{i}(\omega t + m\varphi)}. \tag{5.103}$$

We require the phase function $\psi(r,\vartheta)$ to increase by 2π after one revolution around the contour C shown in Fig. 2. The overall phase $\omega t + m\varphi - n\psi(r,\theta)$ then winds around the circle S and along the contour C, exactly as for the Faddeev–Hopf field Eq. (2.10). For regular fields $f(r,\vartheta)$ vanishes at C and has n zeros inside C. The solutions are thus characterized by two integers (n, m) giving rise to the 'topological charge' $N = nm$, although now this does not represent a genuine topological invariant. We shall call Q-balls with $N \neq 0$ twisted, by analogy with twisted loops in the Faddeev–Hopf theory, while those with $N = n = 0$ described above will be called simply spinning or 'non-twisted'.

The field equations read

$$\left(\Delta - \frac{m^2}{r^2\sin^2\vartheta} + \omega^2\right) X = \frac{1}{2}\frac{\partial U(\sqrt{X^2+Y^2})}{\partial X},$$
$$\left(\Delta - \frac{m^2}{r^2\sin^2\vartheta} + \omega^2\right) Y = \frac{1}{2}\frac{\partial U(\sqrt{X^2+Y^2})}{\partial Y}, \tag{5.104}$$

where one can require X, Y to be symmetric and antisymmetric, respectively, with respect to reflections in the equatorial plane. The simplest twisted solutions are obtained for $n = m = 1$ and are shown in Fig. 15.

The profiles of the energy density look spectacular; see Fig. 16. It is unclear at present whether these solutions are dynamically stable, but they certainly exist as solutions of the elliptic system (5.104). The twisted Q-balls are much more heavy than the non-twisted ones. For example, for $\omega = 0.9$ we found for the twisted (1, 1) solution the energy $E = 929.34$, while the non-twisted 1^+ and 1^- spinning Q-balls have, respectively, $E = 169.27$ and $E = 338.66$.

5.1.4. Spinning gauged Q-balls

Another possibility to generalize the spinning Q-balls is to couple them to a gauge field within the theory

$$\mathcal{L}_{\mathrm{gQ}}[A_\mu, \Phi] = -\frac{1}{4}F_{\mu\nu}F^{\mu\nu} + \mathcal{L}_{\mathrm{Q}}[\Phi]. \tag{5.105}$$

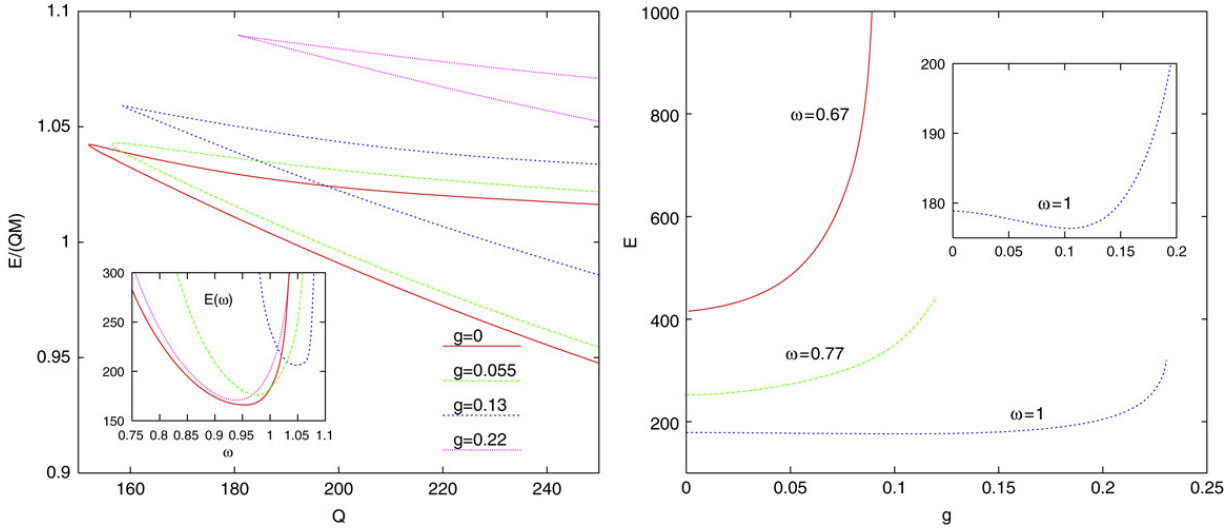

Fig. 17. Left: the energy $E(\omega)$ and $E(Q)/(QM)$ for several values of g for the 1^+ gauged Q-balls. Right: the energy $E(g)$ for several values of ω for the 1^+ solutions. The plots of $Q(\omega)$ and $Q(g)$ look qualitatively similar.

Here $F_{\mu\nu} = \partial_\mu A_\nu - \partial_\nu A_\mu$ while $\mathcal{L}_Q[\Phi]$ is the same Q-ball Lagrangian as in (5.72) but with the derivatives of Φ replaced by the covariant derivatives, $\partial_\mu \Phi \to D_\mu \Phi = (\partial_\mu - igA_\mu)\Phi$ where g is the gauge coupling constant. This theory is in fact the U(1) version of the general gauge field model (3.50). The local gauge transformations (3.52) now read $\Phi \to \Phi e^{ig\alpha}$, $A_\mu \to A_\mu + \partial_\mu \alpha$ while the field equations (3.53) assume the form

$$\partial^\mu F_{\mu\nu} = ig\left\{(D_\mu\Phi)^*\Phi - \Phi^*(D_\mu\Phi)\right\} \equiv gj_\nu,$$
$$D_\mu D^\mu \Phi = -\frac{\partial U}{\partial|\Phi|^2}\Phi. \tag{5.106}$$

The conserved Noether charge analogous to the Q-ball charge Eq. (5.77) is

$$Q = \int j_0 \, d^3\mathbf{x} = \frac{1}{g}\oint \vec{\varepsilon}\, d\vec{S} \equiv \frac{4\pi Q_{el}}{g}, \tag{5.107}$$

where Q_{el} is the electric charge. Spherically symmetric solutions of this model were discussed in Ref. [115].

We make the ansatz

$$A_\mu dx^\mu = A_0(r,\vartheta)dt + A_\varphi(r,\vartheta)\sin\theta d\varphi, \quad \Phi = f(r,\vartheta)e^{i(m\varphi+\omega t)}, \tag{5.108}$$

with real $f(r,\vartheta)$, and require the gauge field to vanish at infinity, while at the z-axis $A_\varphi = \partial_\theta A_0 = 0$. Although Φ depends on t, φ, this dependence can be gauged away, so that the system is manifestly stationary and manifestly axially symmetric. Numerically solving the field equations gives spinning Q-balls with a long-range gauge field which behaves for large r as ($\mathbf{m}$ being the magnetic dipole moment)

$$A_0 = \frac{Q_{el}}{r} + \cdots, \quad A_\varphi = \frac{\mathbf{m}\sin\theta}{r^2} + \cdots. \tag{5.109}$$

In the limit $g \to 0$ they reduce to the non-gauged spinning Q-balls. It seems that solutions exist if only g does not exceed a certain maximal value $g_{max}(\omega)$ (see Fig. 17). This feature can be understood qualitatively [115]: since Q-balls can be viewed as condensate states of mutually attracting scalar particles, gauging them creates an electric repulsion that destroys the condensate for large enough g.

Since the symmetries of the solutions are manifest, one can use the surface integral formula (4.66) for the angular momentum. Applying the symmetry equations (4.64) to the ansatz (5.108) gives $W_\varphi = m/g$, inserting which to (4.66) and using (5.109) yields

$$J = \oint\left(\frac{m}{g} - A_\varphi\right)\vec{\varepsilon}\,d\vec{S} = \frac{4\pi Q_{el} m}{g} = Qm. \tag{5.110}$$

This shows that spinning is possible in manifestly stationary and manifestly axially symmetric systems where all the spinning phases can be gauged away.

As seen in Fig. 17, the dependence of solutions on ω is similar to that in the ungauged case: they exist for a limited range of ω. Expressing E in terms of Q gives again a two-branch function $E(Q)$, the solutions from the lower branch being stable for large enough Q with respect to decay into free particles. E, Q cannot be arbitrarily large for $g \neq 0$, since the electric and

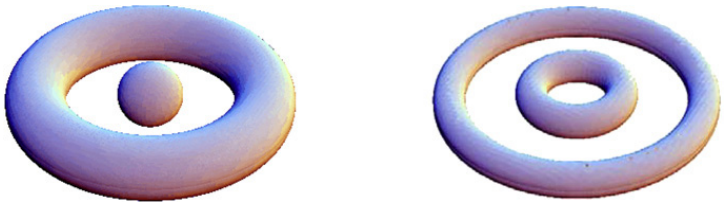

Fig. 18. Energy isosurfaces with $T_0^0 = 0.1$ for the $m_1 = 0$, $m_2 = 3$ 'Saturn' (left) and with $T_0^0 = 0.3$ for the $m_1 = 1$, $m_2 = 3$ bi-ring (right) solutions in the theory (5.111).

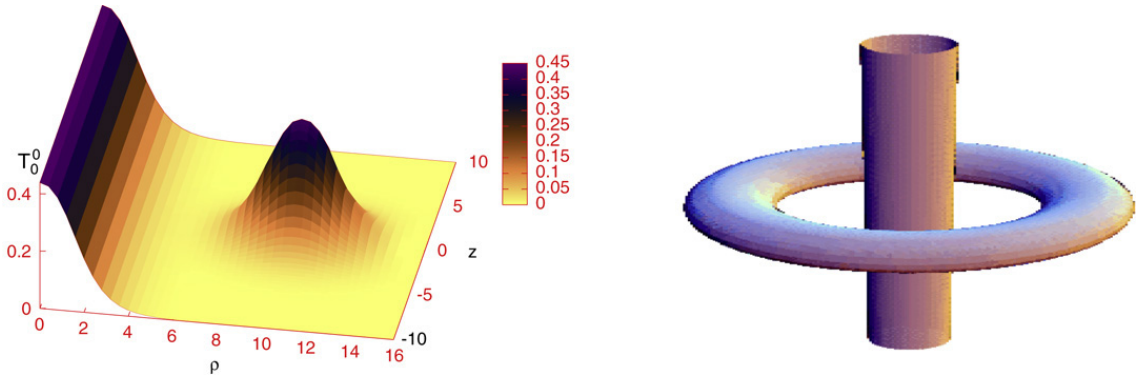

Fig. 19. The energy density T_0^0 and the $T_0^0 = 0.1$ energy isosurface for the $m_1 = 0$, $m_2 = 3$ 'hoop' solution in the theory (5.111).

scalar field contributions to the energy grow as $Q_{\rm el}^2 \sim Q^2$ and Q, respectively, and so for large Q the electric term dominates and destroys the soliton.

For small g solutions can be represented as $\Phi = \Phi^{(0)} + g^2\Phi^{(2)} + \cdots$ and $A_\mu = gA_\mu^{(1)} + \cdots$ where $\Phi^{(0)}$ is the non-gauged Q-ball. The energy is $E(g) = E^{(0)} + g^2E^{(2)} + \cdots$ and calculating $E^{(2)}$ reveals that it is not sign definite — due to the electric field contribution. The plots in Fig. 17 show that it can be both positive and negative, depending on the solution.

5.1.5. *Spinning interacting Q-balls*

Yet another way to generalize Q-balls is to couple to each other several copies of the theory. This allows one to consider 'non-linear superpositions' of individual Q-balls. Although this idea has already been considered in the literature [30], we have reconsidered it and found some curious solutions which could be interesting in the context of our discussion. In the simplest case one can choose

$$L[\Phi_1, \Phi_2] = L_Q(\Phi_1) + L_Q(\Phi_2) - \gamma|\Phi_1|^2|\Phi_2|^2, \tag{5.111}$$

where $L_Q(\Phi_1)$ and $L_Q(\Phi_2)$ are two copies of the Q-ball Lagrangian (5.72). Setting

$$\Phi_1 = e^{i(\omega_1 t + m_1\varphi)}f_1(r,\theta), \quad \Phi_2 = e^{i(\omega_2 t + m_2\varphi)}f_2(r,\theta), \tag{5.112}$$

it is interesting to consider solutions with $m_1 \neq m_2$. Choosing $\omega_1 = \omega_2 = 1$, $\gamma = 1$ and restricting to the even parity sector, we find solutions of the 'Saturn type', with a central concentration of the energy density produced by the first scalar with $m_1 = 0$ and surrounded by a ring created by the second scalar with $m_2 > 0$ (Fig. 18), solutions for $m_2 > m_1 > 0$ with bi-ring profiles (Fig. 18), as well as solutions describing a superposition of a straight 'Q-ball vortex' with $m_1 = 0$ 'hooped' by a Q-ball ring with $m_2 > 0$ (Fig. 19).

5.2. *Skyrmions*

The first known example of topological solitons in $3+1$ dimensions was suggested almost 50 years ago within the non-linear relativistic field theory model proposed by Skyrme [157]. These solitons are now called skyrmions. Skyrme himself considered them as field theoretic realizations of baryons. Nowadays the Skyrme model is regarded as an effective, low energy approximation of QCD [5,4]. In this approximation the static skyrmions are promoted to spinning objects by making use of the effective rigid body approximation that will be considered below. The masses of the spinning skyrmions obtained in this way are then compared to the hadron masses.

The question of whether spinning skyrmions really exist as stationary field theory objects was addressed only very recently in Ref. [18], whose authors constructed spinning skyrmions by applying the same mechanism as for the Q-balls and arrived at conclusions which differ considerably from those obtained within the rigid body approximation.

Since there exist excellent descriptions of the Skyrme model and its solutions in the literature [120,121], we shall very briefly summarize only the features essential for our discussion. The fundamental field variables in the theory comprise an SU(2)-valued matrix $U(x^\mu)$ which satisfies field equations for the Lagrangian

$$\mathcal{L}_S[U] = \mathrm{tr}\left(\frac{1}{2}\,\partial_\mu U^\dagger \partial^\mu U + \frac{1}{8}\,[\partial_\mu U^\dagger,\, \partial_\nu U][\partial^\mu U^\dagger,\, \partial^\nu U]\right). \tag{5.113}$$

It is convenient to introduce a pure gauge SU(2) connection,

$$\mathbf{A}_\mu = iU^\dagger \partial_\mu U \equiv \tau^a \mathbf{A}^a_\mu, \quad \partial_\mu \mathbf{A}_\nu - \partial_\nu \mathbf{A}_\mu = i[\mathbf{A}_\mu, \mathbf{A}_\nu], \tag{5.114}$$

in terms of which the field equations read

$$\partial^\mu \left(\mathbf{A}_\mu - \frac{1}{4}\,[[\mathbf{A}_\mu, \mathbf{A}_\nu], \mathbf{A}^\nu]\right) = 0. \tag{5.115}$$

The energy for static fields is

$$E[U] = \int \mathrm{tr}\left(\frac{1}{2}(\mathbf{A}_k)^2 - \frac{1}{8}([\mathbf{A}_i, \mathbf{A}_k])^2\right) \mathrm{d}^3\mathbf{x}. \tag{5.116}$$

For the energy to be finite the field $U(\mathbf{x})$ should approach a constant value at infinity, which can be chosen to be the unit matrix, so that $\lim_{|\mathbf{x}|\to\infty} U(\mathbf{x}) = 1$. This allows one to replace $\mathbb{R}^3$ by its one-point compactification S^3. Since SU(2) is topologically also S^3 it follows that any finite energy field configuration can be viewed as a map, $U(\mathbf{x}) : S^3 \to S^3$, and can therefore be characterized by the integer degree of map,

$$N[U] = \frac{\mathrm{i}}{24\pi^2} \int \mathrm{tr}\left(\epsilon_{ijk}\mathbf{A}_i\mathbf{A}_j\mathbf{A}_k\right) \mathrm{d}^3\mathbf{x}. \tag{5.117}$$

This topological charge is called in Skyrme theory 'baryon number'. Fixing it the energy obeys the Bogomol'nyi-type inequality

$$E[U] \geq 12\sqrt{2}\pi^2 |N[U]|, \tag{5.118}$$

which can be easily obtained by rearranging terms in the integrand in (5.116). The existence of this lower bound suggests looking for energy minimizers in each topological sector.

It will be convenient for what follows to parametrize the matrix U in terms of two complex scalar fields ϕ, σ subject to the normalization condition $|\phi|^2 + |\sigma|^2 = 1$ as

$$U = \begin{pmatrix} \phi & \mathrm{i}\sigma^* \\ \mathrm{i}\sigma & \phi^* \end{pmatrix}. \tag{5.119}$$

Simplest skyrmions are spherically symmetric, $U = \exp(\mathrm{i}\chi(r)\,\mathbf{x}\cdot\boldsymbol{\tau}/r)$, hence

$$\phi = \cos\chi(r) + \mathrm{i}\sin\chi(r)\cos\vartheta, \quad \sigma = \sin\chi(r)\sin\vartheta\,\mathrm{e}^{\mathrm{i}\varphi}. \tag{5.120}$$

Inserting this to Eq. (5.115) the variables separate and the equations reduce to an ODE for $\chi(r)$. This equation admits globally regular solutions with the boundary conditions $\chi(0) = N\pi$ and $\chi(\infty) = 0$ for any value of the topological charge N. However, it seems that only for $N = \pm 1$ these solutions correspond to the absolute energy minimum, while those for $|N| > 1$ are local minima or saddle points. Global energy minima for $|N| > 1$ are not spherically symmetric and can be obtained by directly minimizing the energy (5.116). For $|N| = 2$ they are axially symmetric, with the constant baryon number isosurfaces having toroidal shape, so they are somewhat similar to knots. However, higher charge skyrmions do not resemble knots at all and look like polyhedral shells. Their detailed description can be found in the monograph [121].

5.2.1. Skyrme versus Faddeev–Skyrme

It is worth emphasizing the similarity between the Skyrme and Faddeev–Skyrme models. Both can be represented in the form (up to normalization)

$$\mathcal{L}[\boldsymbol{\phi}] = \partial_\mu\boldsymbol{\phi}\cdot\partial^\mu\boldsymbol{\phi} - \frac{1}{4}\,(\partial_\mu\boldsymbol{\phi}\cdot\partial^\mu\boldsymbol{\phi})^2 + \frac{1}{4}\,(\partial_\mu\boldsymbol{\phi}\cdot\partial_\nu\boldsymbol{\phi})(\partial^\mu\boldsymbol{\phi}\cdot\partial^\nu\boldsymbol{\phi}) \tag{5.121}$$

where $\boldsymbol{\phi}$ is a vector normalized by the condition $\boldsymbol{\phi}\cdot\boldsymbol{\phi} = 1$. In the Faddeev–Skyrme case one has $\boldsymbol{\phi} = \phi^a$ with $a = 1, 2, 3$ so that the target space is S^2. In the Skyrme model one has $\boldsymbol{\phi} = (\phi^0, \phi^a)$ with $a = 1, 2, 3$ so that the target space is S^3, the Skyrme field being $U = \phi^0 + \mathrm{i}\phi^a\tau^a$. One can also construct a generalized theory whose target space 'interpolates' between S^2 and S^3 and so it includes both models as special cases [175].

The Faddeev–Skyrme model can be regarded as a consistent truncation of the Skyrme theory. Specifically, if $\mathbf{n} = n^a$ is a solution of the Faddeev–Skyrme model, then $\boldsymbol{\phi} = (0, n^a)$ solves the equations of the Skyrme model. As a result, knot solitons can be embedded into the Skyrme model [123,37], although their stability properties will then be different.

Another embedding of knot solitons into Skyrme theory is obtained by expressing the fields $\mathcal{A}_\mu$ and $\mathbf{n}$ in terms of the CP^1 coordinates ϕ, σ using Eqs. (2.28), (2.30) and (2.31). The Skyrme field U is then given by Eq. (5.119). Although this correspondence does not map solutions to solutions, the advantage now is that the baryon number $N[U]$ is exactly equal to the Hopf charge $N[\mathbf{n}]$. This follows from the fact that $\mathbf{A}^3_\mu = -\mathcal{A}_\mu$ and $\mathcal{F}_{\mu\nu} = 2(\mathbf{A}^1_\mu \mathbf{A}^2_\nu - \mathbf{A}^1_\nu \mathbf{A}^2_\mu)$ due to Eq. (5.114). With this, the expression (5.117) for the baryon number exactly reduces to the expression (2.9) for the Hopf charge. For example, using the parametrization (2.32) for the CP^1 scalars ϕ, σ with the Hopf charge $N[\mathbf{n}] = nm$ gives with (5.119) the Skyrme field U with $N[U] = nm$.

The Hopf charge $N[\mathbf{n}]$ will determine in this case also the winding number of the pure gauge field $\mathbf{A}_k = iU^\dagger \partial_k U$. If $\mathbf{n}$ is an energy minimizer then the pure gauge $\mathbf{A}_k$ is maximally abelian [164].

The correspondence can also be used in the opposite direction to construct $\mathbf{n}$ with a given Hopf charge out of U with a given baryon number. If U is spherically symmetric, then $\mathbf{n}$ is axially symmetric, as can be seen comparing Eqs. (5.120) and (2.16). Using approximations for U gives in this way approximate solutions for $\mathbf{n}$ [173].

5.2.2. Spinning skyrmions

Let us consider the $N = 1$ static, spherically symmetric skyrmion described by Eq. (5.120). Its spinning analog in the rigid body approximation is obtained by simply replacing in Eq. (5.120)

$$\varphi \to \varphi + \omega t, \tag{5.122}$$

which gives a non-zero value to the angular momentum. It is in fact precisely this type of approximation that is often implicitly assumed in the literature when talking about spinning solitons. In this approximation spinning solitons do not change their shape and the radiation effects are neglected, which are natural assumptions if the rotation is slow. However, if ω is not small, then this description does not approximate the true spinning solutions any more but simply gives field configurations with $J \neq 0$. If one uses them as initial data, then their temporal evolutions will be certainly accompanied by radiation carrying J away, and it is not clear if the system will finally relax to a state with $J \neq 0$.

In order to construct truly spinning skyrmions with $N = 1$, Battye, Krusch and Sutcliffe (BKS) [18] generalize the spherically symmetric ansatz (5.119) and (5.120) to the axially symmetric, non-manifestly stationary one, which can be parametrized as

$$\phi = \cos\frac{\Theta}{2}\, e^{i\psi}, \qquad \sigma = \sin\frac{\Theta}{2}\, e^{i(\varphi+\omega t)}. \tag{5.123}$$

It is instructive to compare this with the ansatz (2.32) for the axially symmetric hopfions with $m = n = 1$. They also add to the Lagrangian (5.113) the mass term

$$M^2\,\mathrm{tr}(U-1). \tag{5.124}$$

Instead of solving the field equations for $\Theta(r,\vartheta)$, $\psi(r,\vartheta)$ they minimize the energy with fixed J, whose expression is similar to the one in Eq. (5.101). The frequency ω for their solutions is a parameter in the interval

$$0 \leq \omega^2 < M^2, \tag{5.125}$$

both the energy and angular momentum increasing with ω. The latter feature is very interesting — for spinning skyrmions J is a continuous parameter that can be arbitrarily small, so that they can rotate slowly. To compare, Q-balls cannot rotate slowly. Although BKS do not emphasize this, it seems that both E and J should blow up as $\omega^2 \to M^2$ since the fields localized by the factor $\exp(-\sqrt{M^2-\omega^2}\, r)$ become then long range.

Trying to adjust M^2 and the energy scale to reproduce the pion and hadron masses and their spins, BKS discover that this requires moving to the parameter region where deviations of spinning skyrmions from spherical symmetry are large. They conclude that the rigid body approximation does not provide an adequate description of spinning skyrmions.

The results of BKS have been confirmed by solving the field equations by Ioannidou, Kleihaus and Kunz [94] (who studied in fact gravity-coupled skyrmions, but considered the Minkowski space limit as well).

The spinning skyrmions have been obtained by BKS by minimizing the energy within the axially symmetric ansatz (5.123). Strictly speaking, this does not exclude the possibility of non-axially symmetric instabilities. However, since the non-spinning skyrmions are stable, one can expect that at least for small J their spinning analogs should be stable as well.

Spinning solitons have also been studied in the context of the baby Skyrme model [133,25]. This is simply the Faddeev–Skyrme model restricted to $2+1$ spacetime dimensions and written in the form (5.121) with an additional mass term $M^2(\boldsymbol{\phi}^3 - 1)$. Spinning fields are then chosen to be

$$\boldsymbol{\phi}^1 + i\boldsymbol{\phi}^2 = \sin\Theta(\rho) e^{i(\omega t+\varphi)}, \quad \boldsymbol{\phi}^3 = \cos\Theta(\rho). \tag{5.126}$$

The field equations reduce in this case to an ODE for $\Theta(\rho)$ whose solutions are easy to study. Solutions exist for $\omega < M$ and both E and J blow up as $\omega \to M$.

Trying to further increase ω, solutions become oscillatory, since one has $\Theta \sim \exp(-\sqrt{M^2-\omega^2}\,\rho)$ for large ρ, both E and J being then infinite. However, one can consider the initial data of the form (5.126), where $\omega > M$ and $\Theta(\rho)$ vanishes identically for large ρ. E, J will then be finite. Evolving these data in time, the system radiates away a fraction of its energy and angular momentum and relaxes to a stationary, rotating configuration with $\omega < M$ [133].

5.2.3. Spinning gauged skyrmions

Spinning solutions have also been constructed within the gauged version of the Skyrme model [31] by Radu and Tchrakian [138]. These solutions are manifestly stationary and manifestly axisymmetric. Parametrizing the Skyrme field U in terms of two complex scalars ϕ, σ according to Eq. (5.119), the gauged Skyrme model is obtained from the Skyrme model as

$$\mathcal{L}_{\rm gS}[A_\mu, \phi, \sigma] = -\frac{1}{4} F_{\mu\nu}F^{\mu\nu} + \mathcal{L}_{\rm S}[\phi, \sigma]. \tag{5.127}$$

Here $\mathcal{L}_{\rm S}$ is the Skyrme Lagrangian (5.113) with the mass term (5.124) included, $F_{\mu\nu} = \partial_\mu A_\nu - \partial_\nu A_\mu$, and the derivatives of the field σ in $\mathcal{L}_{\rm S}[\phi, \sigma]$ are replaced by the covariant derivatives, $\partial_\mu\sigma \to (\partial_\mu - {\rm i}gA_\mu)\sigma$, while the derivatives ϕ do not change, so that the theory is invariant under local U(1) gauge transformations

$$A_\mu \to A_\mu + \partial_\mu\alpha, \quad \sigma \to {\rm e}^{{\rm i}\alpha}\sigma, \quad \phi \to \phi. \tag{5.128}$$

Radu and Tchrakian [138] generalize the ansatz (5.123) as

$$A_\mu {\rm d}x^\mu = A_0 {\rm d}t + A_\varphi \sin\vartheta\, {\rm d}\varphi, \quad \phi = \cos\frac{\Theta}{2}\,{\rm e}^{{\rm i}\psi}, \quad \sigma = \sin\frac{\Theta}{2}\,{\rm e}^{{\rm i}(m\varphi+\omega t)}, \tag{5.129}$$

where $A_0, A_\varphi, \Theta, \psi$ depend on r, ϑ. This ansatz is manifestly stationary and manifestly axially symmetric, since its t, φ-dependence can be removed by a gauge transformation. The topological charge (5.117) is $N = m$. Integrating the field equations gives globally regular solutions with finite energy and a long-range gauge field, which is at large r

$$A_0 = \frac{Q_{\rm el}}{r} + \ldots, \qquad A_\varphi = \frac{\mathbf{m}}{r^2}\sin\vartheta + \ldots, \tag{5.130}$$

where $Q_{\rm el}$, $\mathbf{m}$ are the electric charge and dipole moment. This feature is similar to that for the gauged Q-balls in Eq. (5.109). The angular momentum can be calculated in the same way as in Eq. (5.110), with a similar result,

$$J = \frac{4\pi Q_{\rm el} m}{g}. \tag{5.131}$$

However, unlike for Q-balls, J can be arbitrarily small if ω is small. The dependence of solutions on ω is qualitatively similar to that for the global skyrmions: they exist only for a finite frequency range, both E and J growing with ω. For $\omega = 0$ the solutions reduce to the non-spinning gauged skyrmions found in Ref. [134].

The stability of spinning gauged skyrmions has not been studied. They probably have less chance to be stable than their global counterparts — since gauging introduces additional degrees of freedom that can produce instabilities.

5.3. Rotating monopole–antimonopole pairs

There are other known solutions with non-zero angular momentum. They are manifestly stationary and manifestly axisymmetric, but they describe rotations in multisoliton systems and not spinning of a single soliton. Let us consider the already mentioned above monopole–antimonopole solutions in the Yang–Mills–Higgs theory (3.50). Their existence was demonstrated by Taubes [161] and they were explicitly constructed by Kleihaus and Kunz [100] within the ansatz (3.55) with $k = 2$, $m = 1$. These solutions are static, purely magnetic and manifestly axisymmetric (since their φ-dependence can be gauged away) and with vanishing magnetic charge. The Higgs field Φ shows two simple zeros at two spatial points separated by a finite distance (see Fig. 20). These two points correspond to the positions of the monopole and antimonopole. The analysis of the charge and current distributions similar to that described in Section 3.2 shows that the system also contains a circular electric current, as shown in Fig. 20. The magnetic field created by this current acts against the Coulombian attraction between the monopole and antimonopole, which presumably stabilizes the system.

Since there is no electric field for these solutions, their angular momentum (4.66) is zero. However, in the limit where the Higgs potential vanishes, the Lagrangian (3.50) admits the global symmetry [27,40]

$$A_0 \to A_0\cosh\gamma + \Phi\sinh\gamma, \quad \Phi \to \Phi\cosh\gamma + A_0\sinh\gamma, \quad A_k \to A_k, \tag{5.132}$$

and this allows one to produce solutions with an electric field starting from purely magnetic solutions. As was noticed in [88], this transformation may also generate a non-zero angular momentum

$$J \sim \sinh\gamma, \tag{5.133}$$

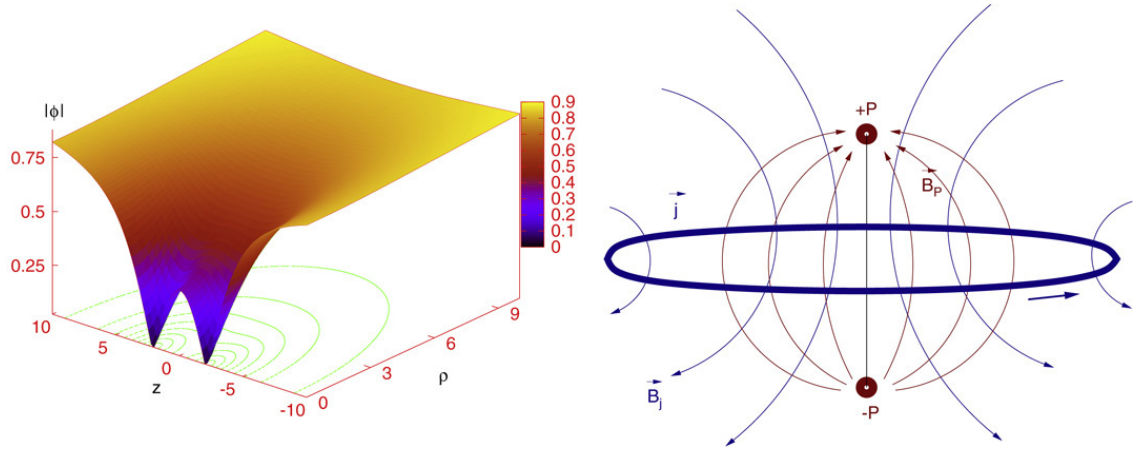

Fig. 20. Left: the Higgs field amplitude for the monopole–antimonopole solution in the limit where the Higgs field potential vanishes. It is shown only for a limited region around the origin, while at infinity it approaches the unit value. Right: the charge and current distributions for this solution exhibits essentially the same structure as for the monopole rings, shown in Fig. 8.

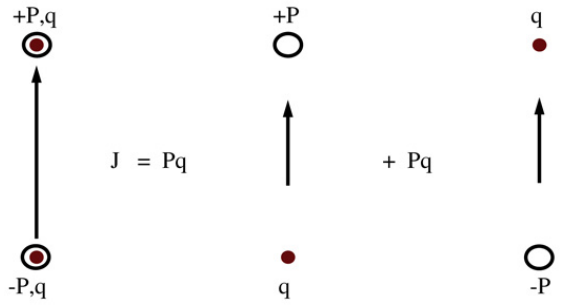

Fig. 21. Schematic visualization of the rotating monopole–antimonopole pair as superposition of a monopole–electric charge pair $(+P, q)$ and an antimonopole–electric charge pair $(-P, q)$, both of which making the same contribution to the angular momentum.

provided that the original purely magnetic solution is not spherically symmetric and does not satisfy the first-order Bogomol'nyi equations [27]. The latter condition excludes from consideration the (multi)monopole solutions of these equations. However, applying the symmetry (5.132) to the monopole–antimonopole solution, which does not fulfill the Bogomol'nyi equations and whose Higgs field is long range in the limit of vanishing Higgs potential, gives an electrically charged system, since both monopole and antimonopole then receive an electric charge of the same sign [85]. The total electric charge calculated with the gauge-invariant definition (3.58) is $Q_{\rm el} \sim \sinh\gamma$, and applying the surface integral formula (4.66) gives the angular momentum [51]

$$J = \frac{4\pi Q_{\rm el}}{g} \tag{5.134}$$

directed along the symmetry axis passing through the monopole and antimonopole.

It is interesting to understand the origin of this angular momentum. If it was an orbital angular momentum, then it would be orthogonal to the monopole–antimonopole symmetry axis, but it is parallel to it instead. Let us remember that a static system containing an electric charge q and a magnetic charge P has an angular momentum $J = Pq$ independent of the distance between the charges and directed from q to P [38]. This angular momentum can be obtained by integrating the Poynting vector as in Eq. (4.62). We know that a rotating monopole–antimonopole pair contains two magnetic charges of the opposite sign and two electric charges of the same sign. It can therefore be visualized as a superposition of two pairs, $(+P, q)$ and $(-P, q)$, both of which making *the same* contribution to the angular momentum, as shown in Fig. 21.

A similar construction of rotating solutions can be carried out using other known static solutions of the non-Abelian theory (3.50), as for example the monopole rings described in Section 3.2, also for the generic Higgs field potential [131, 105]. It turns out that the following general relation holds

$$J = \frac{2\pi m Q_{\rm el}}{g}\left[1 + (-1)^k\right] \tag{5.135}$$

where m, k are the winding numbers in the ansatz (3.56) [131,51,105]. Therefore, using Eq. (3.59), the angular momentum is zero in the presence of a non-vanishing magnetic charge, even though $T^0_\varphi \neq 0$ [105], while the relation (5.131) is still valid for solutions with zero magnetic charge.

Since they are related to the monopole–antimonopole solution known to be unstable [161], rotating monopole–antimonopole pairs are very probably unstable as well. However, the mechanism of their rotation is interesting and suggests, in particular, a possibility to have stationary, non-radiating spinning solitons *without* axial symmetry.

Specifically, in theories without radiation, as in classical mechanics, steadily rotating bodies can be totally asymmetric. However, if they carry an electric charge distribution, say, then their electric dipole momentum will depend on time, hence producing radiation, unless they are axially symmetric. This suggests that non-radiating spinning field systems should be axially symmetric — the assumption usually made when studying spinning solitons.

An interesting illustration of this has been found by Hen and Karliner [87], who analyze situations where rapidly spinning systems can lose axial symmetry. A classical example of this phenomenon is provided by the rotating Jacobi ellipsoids in Newtonian gravity — a theory without radiation. Hen and Karliner study spinning baby skyrmions on a *compact* (sphere or disk) 2D space, in which case there is no radiation, and find that the system loses axial symmetry for large enough J. However, as was discussed above, in the limit of infinite $\mathbb{R}^2$, when radiation can exist, spinning baby skyrmions remain axially symmetric for any value of J [133] — since otherwise they would radiate.

Now, the rotating monopole–antimonopole pairs suggest a possibility to have non-radiating, non-axially symmetric rotation even in theories with radiation. This can be achieved by simply taking three or more dyons not aligned along one direction. Of course, this should be realized by constructing a smooth, static, non-axially symmetric, finite energy solutions in a non-Abelian gauge field theory. If they exist, they may have a non-zero J due to the same mechanism as for the rotating monopole–antimonopole pairs.

6. Vortons

We are now ready to explicitly construct vortons as localized, finite energy solutions of the elliptic field equations. By construction, they are stationary and non-radiating. Our results can be viewed as complementary to those obtained by Battye, Cooper and Sutcliffe [17] (although in a completely different context) and by Lemperier and Shellard [118].

6.1. The Witten model

Vortons were originally suggested [46,48,45,47] in the context of Witten's model of superconducting cosmic strings [177]. This model contains two Abelian vectors $A^{(a)}_\mu (a = 1, 2)$ interacting with two complex scalars ϕ and σ with the Lagrangian density

$$\mathcal{L}_W = -\frac{1}{4}\sum_{a=1,2} F^{(a)}_{\mu\nu}F^{(a)\mu\nu} + D_\mu\phi^* D^\mu\phi + D_\mu\sigma^* D^\mu\sigma - U. \tag{6.136}$$

Here $F^{(a)}_{\mu\nu} = \partial_\mu A^{(a)}_\nu - \partial_\nu A^{(a)}_\mu$ are the Abelian field strengths, the gauge covariant derivatives of the scalars are $D_\mu\phi = (\partial_\mu - \mathrm{i}g_1 A^{(1)}_\mu)\phi$ and $D_\mu\sigma = (\partial_\mu - \mathrm{i}g_2 A^{(2)}_\mu)\sigma$ where g_1 and g_2 are the gauge coupling constants. The scalar field potential is

$$U = \frac{1}{4}\lambda_\phi(|\phi|^2 - \eta_\phi^2)^2 + \frac{1}{4}\lambda_\sigma|\sigma|^2(|\sigma|^2 - 2\eta_\sigma^2) + \gamma|\phi|^2|\sigma|^2, \tag{6.137}$$

where λ_ϕ, λ_σ, η_ϕ, η_σ and γ are positive constants. This theory is invariant under local U(1) × U(1) gauge transformations, so that there are two conserved Noether currents.

The theory admits stationary, cylindrically symmetric solutions of the vortex type, supporting a constant non-zero value of one of the Noether currents [177,13,86,91,46,7,132]. These are the superconducting cosmic strings. Vortons are supposed to be loops made of these strings.

Within the full gauged model (6.136) explicit vorton constructions have never been attempted — due to the complexity of the problem. However, the problem simplifies in the global limit of this model, for $g_1 = g_2 = 0$. The gauge fields then decouple and the theory reduces to

$$\mathcal{L} = \partial_\mu\phi^*\partial^\mu\phi + \partial_\mu\sigma^*\partial^\mu\sigma - U \tag{6.138}$$

so that the U(1) × U(1) internal symmetry becomes global. This global theory still keeps some essential features of the original local model. In particular, it still admits superconducting vortex solutions, even though the corresponding current is now global and not local. One can therefore study global vortons made of these vortices, which was in fact the subject of Refs. [17,118]. Below we shall construct the global vortons as stationary solutions of the field equations in the model (6.138), which has not been done before. The question of whether these solutions can be generalized within the full gauged model (6.136) remains open.

One can absorb η_ϕ in the definition of ϕ, σ in (6.138) to achieve $\eta_\phi = 1$. Since the overall normalization of the potential could be changed by rescaling the spacetime coordinates, $x^\mu \to \Lambda x^\mu$, one can impose one more condition on the remaining four parameters λ_ϕ, λ_σ, η_σ, γ, although we do not use this option.

A minimal value of the potential is achieved for $|\phi| = \eta_\phi = 1$ and $|\sigma| = 0$, in which case $U = 0$. This minimum is global if $4\gamma^2 > \lambda_\sigma \lambda_\phi$. The perturbative spectrum of field excitations around this vacuum consists of two massless Goldstone particles, corresponding to excitations of the phases of the fields, and of two Higgs bosons with the masses

$$M_\phi = \sqrt{\lambda_\phi}, \qquad M_\sigma = \sqrt{\gamma - \frac{1}{2}\lambda_\sigma \eta_\sigma^2}. \tag{6.139}$$

The global U(1) × U(1) symmetry of the theory, $\phi \to \phi e^{i\alpha_1}$, $\sigma \to \sigma e^{i\alpha_2}$, leads to the conserved currents

$$j^\mu_{(\phi)} = 2\Re(i\phi^* \partial^\mu \phi), \qquad j^\mu_{(\sigma)} = 2\Re(i\sigma^* \partial^\mu \sigma), \tag{6.140}$$

with $\partial_\mu J^\mu_{(\phi)} = \partial_\mu J^\mu_{(\sigma)} = 0$. The energy–momentum tensor is

$$T_{\mu\nu} = \partial_\mu \phi^* \partial_\nu \phi + \partial_\nu \phi^* \partial_\mu \phi + \partial_\mu \sigma^* \partial_\nu \sigma + \partial_\nu \sigma^* \partial_\mu \sigma - g_{\mu\nu} \mathcal{L}, \tag{6.141}$$

where $g_{\mu\nu}$ is the spacetime metric.

The Lagrangian field equations in the theory (6.138) read

$$\partial_\mu \partial^\mu \phi + \frac{\partial U}{\partial |\phi|^2}\phi = 0, \qquad \partial_\mu \partial^\mu \sigma + \frac{\partial U}{\partial |\sigma|^2}\sigma = 0. \tag{6.142}$$

Expressing the complex scalar fields in terms of their amplitudes and phases as

$$\phi = f_1 e^{i\psi_1}, \qquad \sigma = f_2 e^{i\psi_2}, \tag{6.143}$$

Eqs. (6.142) assume the form ($a = 1, 2$)

$$\partial_\mu \partial^\mu f_a = (\partial_\mu \psi_a \partial^\mu \psi_2) f_a - \frac{1}{2}\frac{\partial U}{\partial f_a}, \quad \partial_\mu (f_a^2 \partial^\mu \psi_a) = 0. \tag{6.144}$$

These equations admit cylindrically symmetric vortex solutions discussed by several authors (see e.g. [46,118,84]). For these solutions one has

$$\phi = f_1(\rho) e^{in\varphi}, \quad \sigma = f_2(\rho) e^{i(pz+\omega t)}, \tag{6.145}$$

where $n \in \mathbb{Z}$ and $p, \omega \in \mathbb{R}$, with $0 \leftarrow f_1(\rho) \to 1$ and $f_2(0) \leftarrow f_2(\rho) \to 0$ as $0 \leftarrow \rho \to \infty$, respectively. The field ϕ thus vanishes in the vortex core and approaches the finite vacuum value at infinity, while σ develops a non-zero condensate value in the core and vanishes at infinity. The fields ϕ, σ are sometimes referred to as vortex field and condensate field, respectively. The phase of ϕ changes by $2\pi n$ after one revolution around the vortex, while the phase of σ increases along the vortex. The z-dependence of the condensate field gives rise to a non-zero momentum along the vortex, $P = \int T^0_z d^3x \sim p$.

The qualitative vorton construction usually discussed in the literature suggests taking a piece of length L of the vortex and identifying its extremities to form a loop. The momentum along the vortex will then circulate along the loop, thus becoming an angular momentum, and the centrifugal force which arises is supposed to be able to compensate the tension of the loop, thereby producing an equilibrium configuration. The coordinate z along the vortex then becomes periodic and can be replaced by the azimuthal angle φ, so that p will have to assume discrete values, $p = 2\pi m/L$ with $m \in \mathbb{Z}$. The central axis of the vortex where the field ϕ vanishes then becomes a circle of radius $R = L/2\pi$.

6.2. Vorton topology and boundary conditions

The above considerations suggest describing the vortons by the ansatz

$$\phi = f_1(\rho, z) e^{i\psi_1(\rho,z)}, \quad \sigma = f_2(\rho, z) e^{im\varphi + i\omega t}. \tag{6.146}$$

The phase of σ increases by $2\pi m$ after one revolution around the z-axis, so that $f_2(\rho, z)$ should vanish at the axis for the field to be regular there. The phase ψ_1 increases by $2\pi n$ after one revolution around the boundary C of the (ρ, z) half-plane, which is the z-axis plus the infinite semi-circle (see Fig. 22). The regularity condition then implies that $\phi(\rho, z)$ must have n zeros somewhere inside C. Therefore any vorton configuration can be characterized by a pair of integers (n, m), which we shall call, respectively, vortex winding number and azimuthal winding number.

It is instructive to compare these boundary conditions to those for the Faddeev–Hopf knots in Eq. (2.32). They are the same — the phases of ϕ, σ wind, respectively, along the orthogonal directions shown in Fig. 2. The vortons and knots have therefore similar topology. This suggests introducing the 'topological charge' analogous to the Hopf charge (2.12)

$$N = nm. \tag{6.147}$$

Strictly speaking, this quantity will be topologically invariant, that is unchanged under arbitrary continuous field deformations, only in the sigma model limit defined by the condition (6.168). However, we shall call it topological charge in all cases and shall require the vortons to have $N \neq 0$.

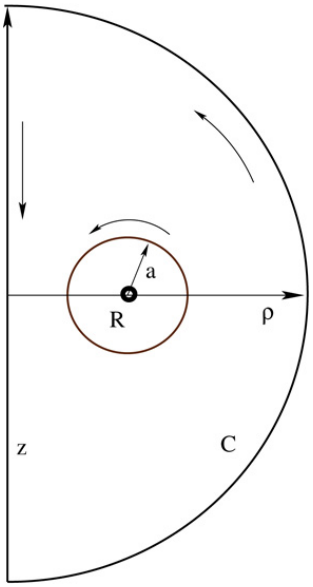

Fig. 22. Vorton topology. The phase of ϕ increases by $2\pi n$ after one revolution around the boundary C of the half-plane, ϕ then vanishing n times somewhere inside C. In the simplest $n = 1$ case the zero is located at a point $(R, 0)$ corresponding to the vortex center. The vortex has a characteristic thickness a.

Let us pass in (6.146) to spherical coordinates,

$$\phi = f_1(r,\vartheta)e^{i\psi_1(r,\vartheta)}, \quad \sigma = f_2(r,\vartheta)\exp[i(m\varphi+\omega t)]. \tag{6.148}$$

Inserting this to Eq. (6.144) gives

$$\begin{aligned}
&\Delta f_1 - \left((\nabla\psi_1)^2 + \frac{\lambda_\phi}{2}(f_1^2-1) + \gamma f_2^2\right) f_1 = 0,\\
&\Delta f_2 - \left(\frac{m^2}{r^2\sin^2\vartheta} - \omega^2 + \frac{\lambda_\sigma}{2}(f_2^2-\eta_\sigma^2) + \gamma f_1^2\right) f_2 = 0,\\
&\nabla(f_1^2\nabla\psi_1) = 0.
\end{aligned} \tag{6.149}$$

At infinity the fields are required to approach the vacuum values, $f_1 \to 1, f_2 \to 0$. One finds for large r

$$\begin{aligned}
&\psi_1 = \frac{A\cos\vartheta}{r^2} + \cdots, \quad f_2 = \frac{B}{r}\exp(-\sqrt{M_\sigma^2-\omega^2}\, r) + \ldots,\\
&f_1 = 1 + \frac{A^2}{r^6}(1+3\cos^2\vartheta) + \cdots + \frac{C}{r}\exp(-M_\phi\, r) + \ldots,
\end{aligned} \tag{6.150}$$

where A, B, C are integration constants and the dots denote the subleading terms. These asymptotic expansions show the presence of two massive Higgs modes and a long-range massless Goldstone mode. The second Goldstone field is not excited within the ansatz (6.148). Introducing the notation

$$X = f_1\cos\psi_1, \qquad Y = f_1\sin\psi_1, \qquad Z = f_2, \tag{6.151}$$

the equations assume the form

$$\begin{aligned}
\Delta X &= \left(\frac{\lambda_\phi}{2}(X^2+Y^2-1) + \gamma Z^2\right) X,\\
\Delta Y &= \left(\frac{\lambda_\phi}{2}(X^2+Y^2-1) + \gamma Z^2\right) Y,\\
\Delta Z &= \left(\frac{m^2}{r^2\sin^2\vartheta} - \omega^2 + \frac{\lambda_\sigma}{2}(Z^2-\eta_\sigma^2) + \gamma(X^2+Y^2)\right) Z.
\end{aligned} \tag{6.152}$$

Using Eq. (6.150), one has at large r

$$X = 1 + O(r^{-4}), \qquad Y = O(r^{-2}), \qquad Z \sim \frac{1}{r}\exp(-\sqrt{M_\sigma^2-\omega^2}\, r). \tag{6.153}$$

Introducing

$$E_2 = \int (|\nabla\phi|^2 + |\nabla\sigma|^2)\mathrm{d}^3\mathbf{x}, \quad E_0 = \int U\mathrm{d}^3\mathbf{x}, \quad \mathcal{N} = \int Z^2\mathrm{d}^3\mathbf{x}, \tag{6.154}$$

the energy is

$$E = \int T_0^0\mathrm{d}^3\mathbf{x} = \omega^2\mathcal{N} + E_2 + E_0, \tag{6.155}$$

while the Lagrangian

$$L = \int \mathcal{L}\,\mathrm{d}^3\mathbf{x} = \omega^2\mathcal{N} - E_2 - E_0. \tag{6.156}$$

One of the two Noether charges is non-vanishing,

$$Q = \int \mathrm{d}^3\mathbf{x} J^0_{(\sigma)} = 2\omega\mathcal{N}, \tag{6.157}$$

and this gives rise to the angular momentum

$$J = \int T^0_\varphi\mathrm{d}^3\mathbf{x} = mQ. \tag{6.158}$$

Rescaling the spatial coordinates as $\mathbf{x} \to \Lambda\mathbf{x}$, the Lagrangian L should be stationary, which implies the virial relation

$$E_2 = 3(\omega^2\mathcal{N} - E_0). \tag{6.159}$$

The presence of the term $(m^2Z^2/r^2\sin^2\vartheta)$ in $|\nabla\sigma|^2$ requires that for finite energy fields one should have $Z = 0$ at the z-axis. Let us now remember that the phase ψ_1 of $\phi = X + \mathrm{i}Y = f_1\mathrm{e}^{\mathrm{i}\psi_1}$ should increase by $2\pi n$ after one revolution around the boundary of the (ρ, z) half-plane. Since one has $X = 1$, $Y = 0$ at $r \to \infty$, it follows that the phase is constant at infinity, so that it can only change along the z-axis (see Fig. 22). Therefore,

$$\psi_1(\rho = 0, z = \infty) - \psi_1(\rho = 0, z = -\infty) = -2\pi n, \tag{6.160}$$

from where it follows that the functions X and Y have (at least) $2n$ and $2n + 1$ zeros at the z-axis, respectively. Such a behavior is compatible with the assumption that X is symmetric and Y is antisymmetric under $z \to -z$. Assuming that Z is symmetric, one arrives at the following parity conditions,

$$X(r, \vartheta) = X(r, \pi - \vartheta), \qquad Y(r, \vartheta) = -Y(r, \pi - \vartheta), \qquad Z(r, \vartheta) = Z(r, \pi - \vartheta), \tag{6.161}$$

which allow one to restrict in the analysis the range of ϑ to the interval $[0, \pi/2]$. Summarizing everything together, solutions of Eqs. (6.152) should satisfy the following boundary conditions.

At the symmetry axis, $\vartheta = 0$, functions X, Y should have, respectively, n and $n - 1$ zeros for $0 < r < \infty$, and one should also have

$$\partial_\vartheta X = \partial_\vartheta Y = Z = 0. \tag{6.162}$$

At the origin, $r = 0$,

$$\partial_r X = Y = Z = 0. \tag{6.163}$$

At infinity, $r = \infty$,

$$X = 1, \quad Y = Z = 0. \tag{6.164}$$

In the equatorial plane, $\vartheta = \pi/2$,

$$\partial_\vartheta X = \partial_\vartheta Z = Y = 0. \tag{6.165}$$

6.3. The sigma model limit

We have succeeded for the first time to solve the equations in the special limit of the theory obtained by choosing the parameters in the potential (6.137) as

$$\lambda_\sigma = \lambda_\phi = \beta, \quad \eta_\sigma = 1, \quad \gamma = \frac{1}{2}\beta + \gamma_0, \tag{6.166}$$

such that the potential becomes

$$U = \frac{\beta}{4}(|\phi|^2 + |\sigma|^2 - 1)^2 + \gamma_0|\phi|^2|\sigma|^2. \tag{6.167}$$

Taking $\beta \to \infty$ enforces the constraint

$$|\phi|^2 + |\sigma|^2 = 1 \tag{6.168}$$

and the theory (6.138) becomes a sigma model,

$$\mathcal{L} = \partial_\mu\phi^*\partial^\mu\phi + \partial_\mu\sigma^*\partial^\mu\sigma - \gamma_0|\phi|^2|\sigma|^2. \tag{6.169}$$

This model is simpler than the full theory (6.138). It has less degrees of freedom and no free parameters, since the value of γ_0 can be changed by rescaling the spacetime coordinates. The field mass M_σ determined by (6.139) reduces now to $\sqrt{\gamma_0}$, while the mass M_ϕ becomes infinite, which means that field degrees of freedom violating the constraint (6.168) are excluded from the dynamics. The theory therefore contains only one massive particle and two Goldstone bosons in the spectrum. It is worth noting that $N = mn$ now becomes genuinely topological charge, invariant under arbitrary smooth field deformations.

It is convenient to use the Lagrange multiplier method by adding to the Lagrangian (6.169) a term $\mu(1 - |\phi|^2 - |\sigma|^2)$ and varying with respect to ϕ, σ and μ. Using the same ansatz (6.148) and (6.151) as before gives

$$\begin{aligned}
\Delta X &= \left(\gamma_0 Z^2 + \mu\right) X, \\
\Delta Y &= \left(\gamma_0 Z^2 + \mu\right) Y, \\
\Delta Z &= \left(\frac{m^2}{r^2\sin^2\vartheta} - \omega^2 + \gamma_0(X^2 + Y^2) + \mu\right) Z
\end{aligned} \tag{6.170}$$

and also

$$X^2 + Y^2 + Z^2 - 1 = 0. \tag{6.171}$$

Multiplying the three equations (6.170), respectively, by X, Y, Z and taking their sum and using the constraint (6.171) one finds the expression for the Lagrange multiplier,

$$\mu = X\Delta X + Y\Delta Y + Z\Delta Z - 2\gamma_0(X^2 + Y^2)Z^2 - \left(\frac{m^2}{r^2\sin^2\theta} - \omega^2\right)Z^2 - \frac{1}{2}\Delta(X^2 + Y^2 + Z^2), \tag{6.172}$$

where the last term on the right has been added in order to cancel the second derivatives contained in the first three terms. Inserting this to (6.170), the constraint (6.171) will be imposed automatically on the solutions, so that it can be excluded from considerations from now on.

The boundary conditions for Eqs. (6.170) are given by Eqs. (6.162)–(6.165). The regularity condition $Z|_{\theta=0,\pi} = 0$ imposes the constraint $X^2 + Y^2 = 1$ on the z-axis. In addition, since at the origin one has $Y = 0$, the constraint requires that $X^2 = 1$, and so one can choose

$$X|_{r=0} = -1. \tag{6.173}$$

Since one has $X|_{r=\infty} = +1$, this will guarantee a non-zero value of n, which is the principal advantage of the sigma model theory (6.169).

In fact, making sure that the phase of ϕ winds $n \neq 0$ times around the contour C is not simple. This condition can be naturally implemented in toroidal coordinates (2.13), but these coordinates are somewhat singular at infinity. Spherical or cylindrical coordinates are better suited for numerics, but the field topology is then determined by zeros of the X, Y amplitudes (see Eq. (6.160)), whose number cannot be generically prescribed, since they are able to disappear during numerical iterations. Now, the condition (6.173) enforces a non-trivial field topology at least in the $n = 1$ case.

We can now solve the problem. Starting from a field configuration satisfying the boundary conditions (6.162)–(6.165) and (6.173) we numerically iterate it until the convergence is achieved. The resulting solutions are qualitatively very similar to the generic vortons described in detail below, and they also agree with the 'skyrmions' in the theory of Bose–Einstein condensation previously obtained in a completely different way by Battye, Cooper and Sutcliffe [17]. The latter issue will be discussed below in more detail.

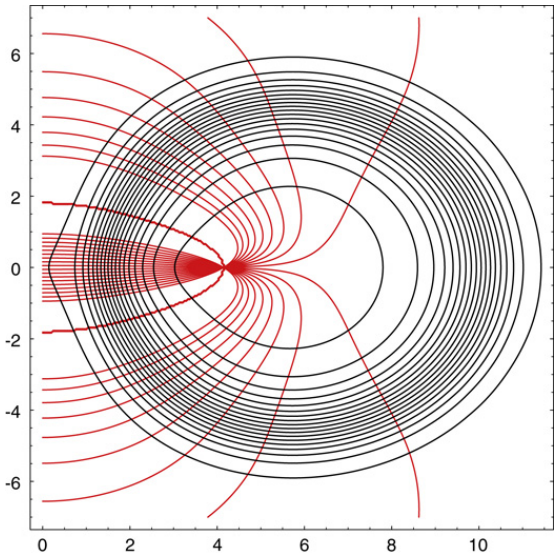

Fig. 23. Levels of constant amplitude $|\phi|$ (closed lines) and phase ψ_1 (radial lines, red online) on the ρ (horizontal direction)–z (vertical direction) plane for the vortex field $\phi = |\phi| \exp(i\psi_1)$ corresponding to the vorton solution with $n = 1, m = 2, \omega = 0.85, \lambda_\phi = 41.12, \lambda_\sigma = 40, \eta_\sigma = 1, \gamma = 22.3$.

6.4. Explicit vorton solutions

Having obtained vortons in the sigma model limit, we can use them as the starting profiles in order to iteratively descend from infinite to finite values of β in the potential (6.167), thus relaxing the sigma model condition. After this, we can relax also the conditions (6.166), thereby recovering vorton solutions within the full original theory (6.138).

In our numerics we use the program FIDISOL (written in Fortran), based on the iterative Newton–Raphson method. A detailed presentation of the FIDISOL code is given in [152,150]. In this approach the field equations are discretized on a (r, ϑ) grid with $N_r \times N_\vartheta$ points, and the resulting system is iterated until convergence is achieved. The grid spacing in the r-direction is non-uniform, while the values of the grid points in the angular direction are given by $\vartheta_k = (k-1)\pi/(2(N_\vartheta - 1))$. Instead of r, a new radial variable x is introduced which maps the semi-infinite region $[0, \infty)$ to the finite interval $[0, 1]$. There are various possibilities for such a mapping, a flexible enough choice being $x = r/(c+r)$, where c is a properly chosen constant. Typical grids for the $n = 1$ solutions have around 200×30 points. The typical numerical error for the solutions is estimated to be of order 10^{-3}. In addition, the virial relation (6.159) was also monitored. The deviation from unity of the ratio $E_2/3(\omega^2 \mathcal{N} - E_0)$ is less than 10^{-3} for most of the solutions we have considered.

As a result, for given values of the parameters λ_ϕ, λ_σ, η_σ and γ in the potential, we can specify the azimuthal winding number m and the frequency ω and obtain a vorton solution. The value of n, the charge Q and energy E are computed from the numerical output. A complete analysis of the parameter space of solutions is a time consuming task that we did not aim at. Instead, we analyzed in detail a few particular classes of solutions, which hopefully reflects the essential properties of the general pattern.

We mainly considered the case where the function X vanishes once at the positive z semi-axis, which corresponds to the vortex winding number $n = 1$. The amplitude of the scalar field ϕ has in this case one zero located on a circle in the $\vartheta = \pi/2$ plane. The corresponding vorton topology can be illustrated by the diagram in Fig. 23, where the level lines of the complex vortex function $\phi = |\phi| \exp(i\psi_1)$ are shown. The levels of constant amplitude, $|\phi|$, are closed lines encircling the center of the vortex where ϕ vanishes. Emanating from this center there are lines of constant phase. The phase, ψ_1, increases by 2π after one revolution around the center.

All vortons have toroidal distributions of the energy density and charge. It seems that they do not exist for arbitrary values of the parameters of the model but only for some regions in the parameter space. In Figs. 24 and 25 the 3D plots of X, Y, Z and also of $|\phi| = \sqrt{X^2 + Y^2}$ for a typical solution with $m = 2$ are presented. One can see that these functions exhibit a strong dependence both on ρ and z, with the zero of $|\phi|$ located in the $z = 0$ plane at $R \simeq 0.82$.

In Figs. 26 and 27 the 2D profiles of X, Y, Z and $|\phi|$ for a typical $m = 1$ solution for several values of ϑ are shown; these pictures remain qualitatively the same for higher values of m. As seen in these plots, the space can be partitioned into three regions. In the first region, located near the origin, the functions X, Y, Z present a strong variation, with Y approaching its extremum. The second region is located inside the vortex, where X stays very close to zero, while the field Z is almost constant and close to its maximal value. As seen in the insertion in the first plot, X crosses zero value with a non-zero first derivative, as it should, since the degree of zero of ϕ at the vortex center should be one. In the third region, outside the vortex ring, the fields approach the vacuum values. Both X and Z show strong variations in a transition domain between second and third regions. We notice also that the value of X at the origin, which was -1 in the sigma model limit, is now different and contained in the interval $(-1, -0.5)$ for all solutions we have found.

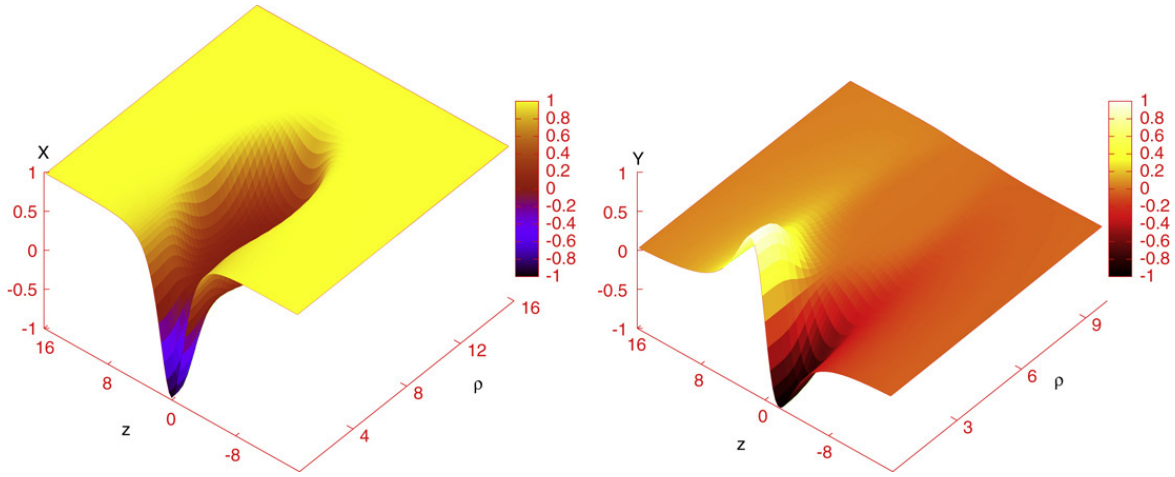

Fig. 24. The amplitudes $X(\rho, z)$, $Y(\rho, z)$ for the typical vorton solution; here $n = 1, m = 2, \omega = 0.85, \lambda_\phi = 41.12, \lambda_\sigma = 40, \eta_\sigma = 1, \gamma = 22.3$.

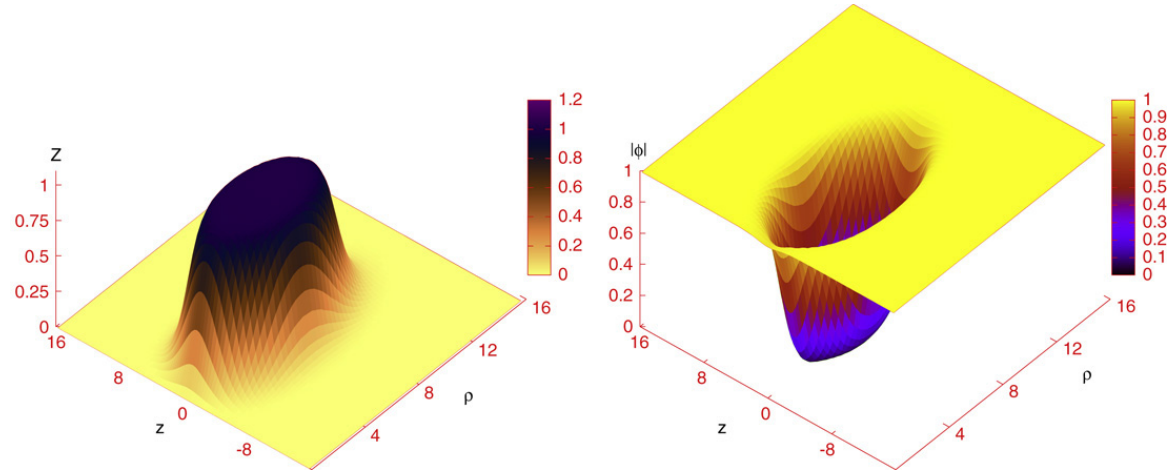

Fig. 25. The amplitudes $Z(\rho, z)$ and $|\phi(\rho, z)|$ for the same solution as in Fig. 24.

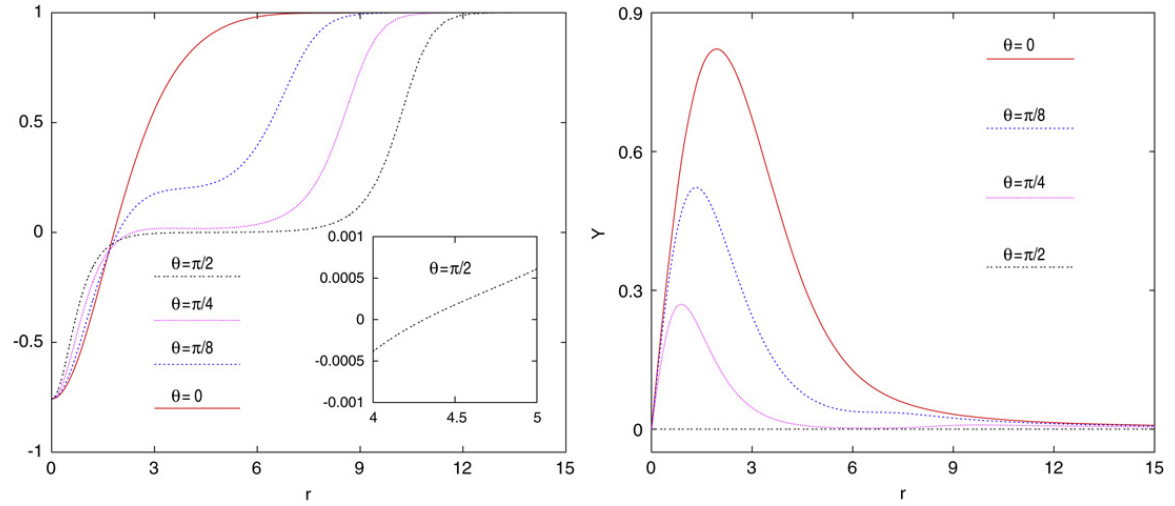

Fig. 26. Profiles of $X(r, \vartheta)$, $Y(r, \vartheta)$ for fixed ϑ for the $n = m = 1$ vorton solution with $\omega = 0.8, \lambda_\phi = 33.26, \lambda_\sigma = 32.4, \eta_\sigma = 1, \gamma = 18.4$.

For the $m = 1$ solutions the energy density is maximal at the origin. Emanating from this central maximum there is a toroidal shell of energy containing the ring of radius R where ϕ vanishes (see Fig. 28). When m increases R grows, whereas the height of the maximum at the origin decreases (see Fig. 28), so that the shape of the energy density resembles a hollow tube (see Fig. 30). There is, however, an almost constant energy density inside the tube, whose value decreases with m. As

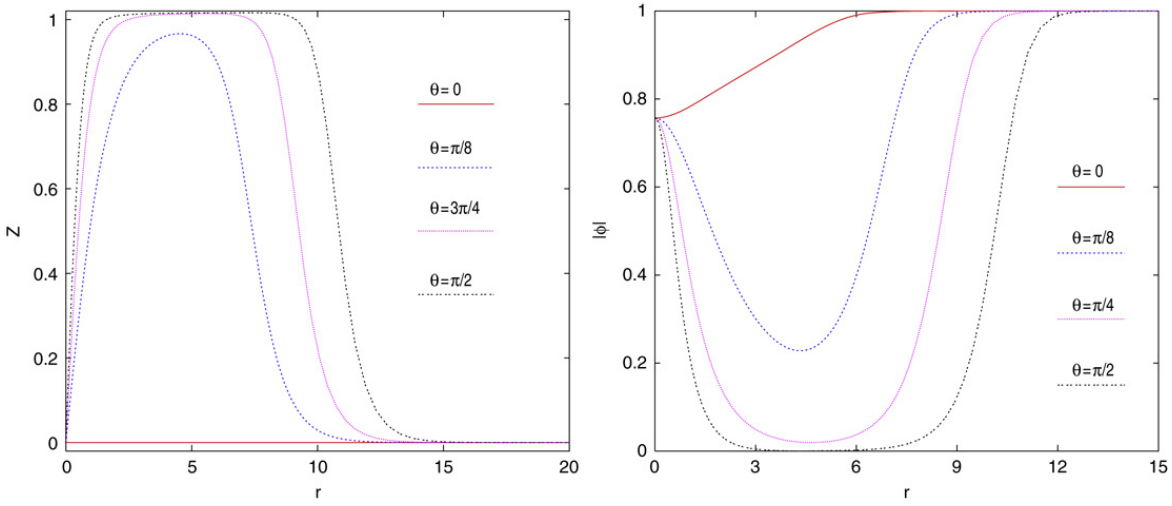

Fig. 27. Profiles of $Z(r,\vartheta)$, $|\phi(r,\vartheta)|$ for fixed values of ϑ for the same solution as in Fig. 26.

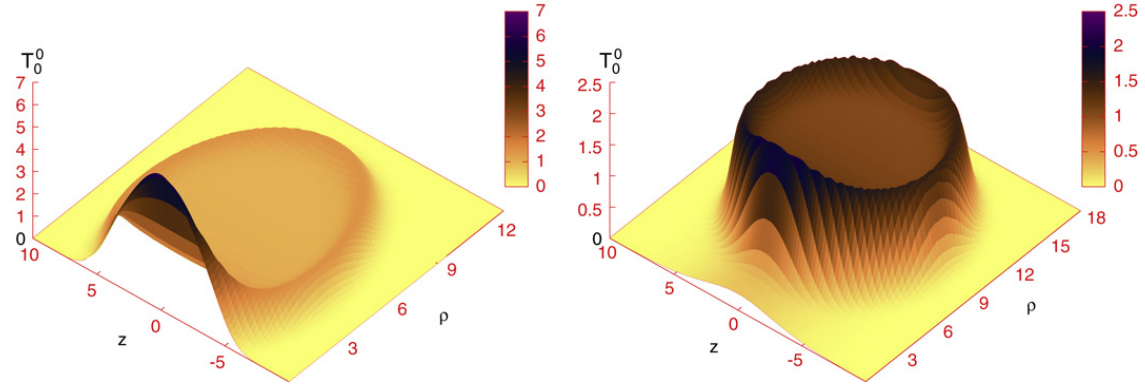

Fig. 28. The energy density T_0^0 for the $n=m=1$ (left) and $n=1, m=3$ (right) vortons with $\omega=0.8, \lambda_\phi=39.25, \lambda_\sigma=38.4, \eta_\sigma=1, \gamma=21.39$.

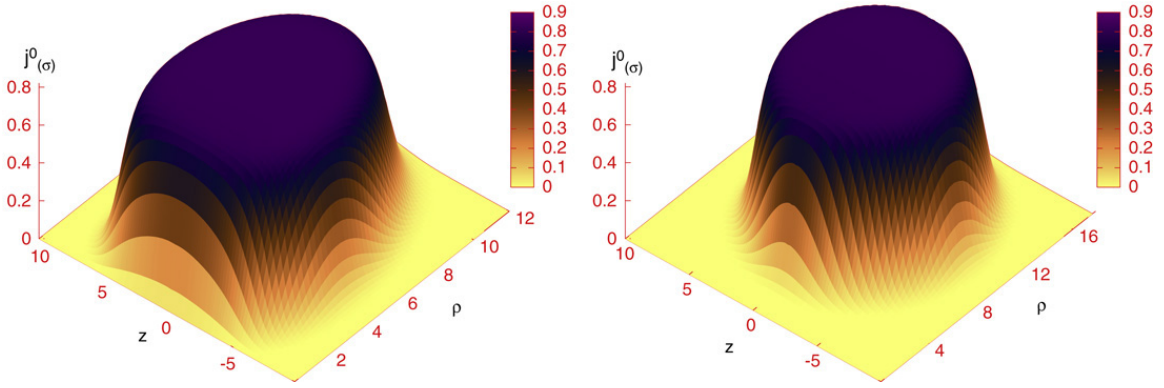

Fig. 29. The charge density for the same solutions as in Fig. 28.

seen in Fig. 29, the charge of the solutions, although also localized in a compact region, does not present the tube structure of the energy density.

Nontrivial vorton solutions are likely to exist for all values of m. We have studied solutions up to $m=5$, but beyond this value the numerical accuracy of our procedure decreases drastically. The energy of the solutions increases with m, and for solutions with the same ω one has $E(m) < mE(m=1)$. All solutions we have found have the ratio R/a between 1 and 1.5, so that the radius of the vortex ring is almost the same as the thickness of the vortex. The construction of vortons in the thin ring limit, for $R \gg a$, remains a numerical challenge.

Fig. 30 (right) shows the energy E and charge Q as functions of the frequency ω for $m=2$ vortons. These functions are actually quite similar to those found in the Q-ball case. As one can see, solutions exist for a limited range of frequencies, $\omega_- < \omega < \omega_+$. Unfortunately, the numerical accuracy decreases considerably near the limits of this interval. However, it seems that both $Q(\omega)$ and $E(\omega)$ diverge in these limits, as in the Q-ball case.

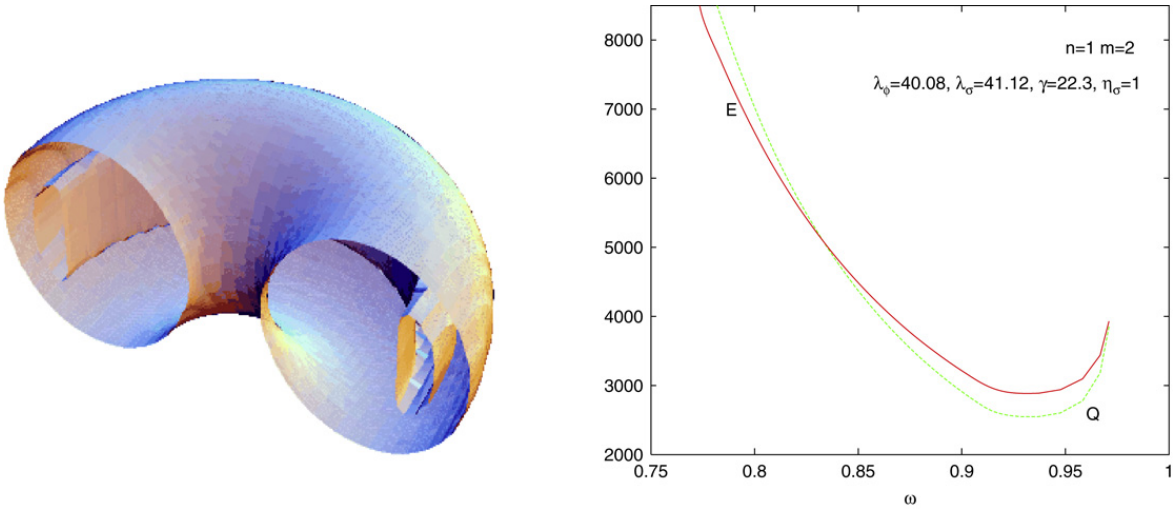

Fig. 30. Left: the surface of constant ($T_0^0 = 1.05$) energy density for the same $n = 1$, $m = 3$ vorton solution as in Fig. 28. It has the structure of a torus containing inside another toroidal surface. Right: the energy $E(\omega)$ and charge $Q(\omega)$ for the $n = 1$, $m = 2$ vorton solutions.

In analogy with Q-balls, the vortons become large as $\omega \to \omega_{\pm}$. However, it is not the vorton radius R that becomes large, since it appears to be not very sensitive to ω and remains finite and non-zero when ω approaches its limiting values. It appears that the torus thickness increases for $\omega \to \omega_{\pm}$ so that its volume grows, thereby increasing the energy and charge. Both E and Q assume their minimal values at $\omega = \omega_{\rm crit}$. The dependence $E(Q)$ appears to be double-valued, very similar to the one shown in Fig. 14 for Q-balls, again exhibiting two branches with a cusp. Solutions with $\omega < \omega_{\rm crit}$ are less energetic than those for $\omega > \omega_{\rm crit}$ and with the same Q.

Using again the analogy with Q-balls, it seems likely that only solutions from the lower branch can be stable, probably those for large enough charge. Stable vortons certainly exist, perhaps not for all values of the parameters of the potentials, but at least for large enough values, when the theory approaches the sigma model limit. Vortons in the sigma model limit are stable, since, as will be discussed below, they can be obtained via 3D energy minimization [17]. This suggests that they should remain stable at least when they are close to this limit.

Although we did not study in detail the dependence of the solutions on the parameters of the potential, one should mention that for $\eta_\sigma \simeq 1$ and $\omega \simeq 0.85$ (the values we mainly considered) we could find solutions only for $\lambda_\phi \gtrsim 22$, while the ratio $\lambda_\phi/\lambda_\sigma$ was always close to one. In other words, our vortons are not that far from the sigma model limit, which suggests that they could be stable.

Vortons with $n > 1$ also exist, and we were able to construct them for $n = 2$. For these solutions there are two concentric rings in the $\vartheta = \pi/2$ plane where $|\phi|$ vanishes. All $n = 2$ solutions we have found have very large values of $\lambda_\phi, \lambda_\sigma, \gamma$.

Finally, an interesting class of solutions of Eqs. (6.152) is obtained by setting $Y = 0$, which means that the phase of ϕ is trivial and so $n = 0$. Such solutions have not been discussed in the literature. Although $m \neq 0$ in this case, one has $N = nm = 0$, and so according to our definition these solutions are not vortons, since they are 'topologically trivial'. However, they also have a ring structure, resembling somewhat spinning Q-balls. One can view them as 'ϕ-dressed' Q-balls made of the complex σ field, the non-renormalizable $|\sigma|^6$ term in the Q-balls potential being replaced by the interaction with a real scalar field ϕ, as was first suggested in Ref. [75].

7. Ring solitons in non-relativistic systems

So far we have been considering relativistic ring solitons that could be relevant in models of high energy physics. At the same time, similar objects also exist in non-relativistic physics, and below we shall consider some of them which are most closely related to our previous discussion.

A famous example of soliton-type toroidal systems is provided by the magnetically confined plasma in the TOKAMAK's. However, since considering this subject would lead us far beyond the scope of our present discussion, we shall restrict ourselves to simply giving a reference to a recent review [28]. In addition, since the external field is necessary to confine the plasma in this case, this example does not quite fit in with our discussion, because we are considering closed, self-interacting systems. Another example of plasma confinement, although somewhat controversial, but which could perhaps be explained by some solitonic structures, is provided by the phenomenon of ball lightning (see [82] for a bibliography). It has in fact been conjectured that some analogs of Faddeev–Skyrme solitons in plasma might be responsible for their existence [67,63], although we are unaware of any confirmations of this conjecture via constructing explicit solutions.

Field theory models of condensed matter physics are more closely related to our discussion. As in the relativistic case, they can be either theories with local gauge invariance, as for example the Ginzburg–Landau theory of superconductivity [77], or models with global internal symmetries, as in the Gross–Pitaevskii [78,135,83] theory of Bose–Einstein condensation.

It has been conjectured that some analogs of the Faddeev–Skyrme knot solitons could exist in the multicomponent Ginzburg–Landau models [11]. However, we are again unaware of any explicit solutions, and moreover, as was discussed above, their existence is not very plausible, at least in the purely magnetic case. On the other hand, global models of condensed matter physics do admit ring-type solitons.

7.1. Vortons versus 'skyrmions' in Bose–Einstein condensates

Surprisingly, it turns out that the above described vortons in the global limit of Witten's model can also be considered as solutions of the Gross–Pitaevskii (GP) equation,

$$\mathrm{i}\frac{\partial \Psi_a}{\partial t} = \left(-\frac{1}{2}\,\Delta + V(\mathbf{x}) + \frac{1}{2}\sum_b \kappa_{ab}|\Psi_b|^2\right)\Psi_a. \tag{7.174}$$

This equation, also called non-linear Schrödinger equation, provides an effective description of the Bose–Einstein condensates. Here Ψ_a are the condensate order parameters, $V(\mathbf{x})$ is the external trapping potential and κ_{ab} describes interactions between different condensate components. In the case of a two-component condensate the indices a, b assume values 1, 2.

Let

$$\phi = \phi(\mathbf{x}), \quad \sigma = \sigma(\mathbf{x})\mathrm{e}^{\mathrm{i}\omega t} \tag{7.175}$$

be a solution of the Eqs. (6.142) of the global model of Witten (6.138) in the case where the parameters in the potential (6.137) are related as

$$\lambda_\phi = \lambda_\sigma \eta_\sigma^2. \tag{7.176}$$

Then setting

$$\Psi_1 = \mathrm{e}^{-\mathrm{i}\frac{\lambda_\phi}{4}t}\,\phi(\mathbf{x}), \qquad \Psi_2 = \mathrm{e}^{-\mathrm{i}\left(\frac{\lambda_\phi}{4}+\frac{\omega^2}{2}\right)t}\,\sigma(\mathbf{x}) \tag{7.177}$$

gives a solution of the GP equation (7.174) in the case where

$$V(\mathbf{x}) = 0, \quad \kappa_{11} = \frac{\lambda_\phi}{2}, \quad \kappa_{22} = \frac{\lambda_\sigma}{2}, \quad \kappa_{12} = \kappa_{21} = \gamma. \tag{7.178}$$

It follows that any vorton solution satisfying the condition (7.176) (this condition is typically not difficult to achieve numerically) provides a solution to the Gross–Pitaevskii equation and hence can be interpreted in terms of condensed matter physics.

In particular, the condition (7.176) is achieved in the sigma model limit (6.166) and (6.168), in which case one obtains solutions of the GP equation with

$$V(\mathbf{x}) = \kappa_{11} = \kappa_{22} = 0, \quad \kappa_{12} = \kappa_{21} = \gamma_0 \tag{7.179}$$

by setting $\Psi_1 = \phi(\mathbf{x})$, $\Psi_2 = \mathrm{e}^{-\mathrm{i}\frac{\omega^2}{2}t}\,\sigma(\mathbf{x})$. Remarkably, solutions of the GP equation in this case have been independently studied by Battye, Cooper and Sutcliffe (BCS) [17], so that we can compare our results in Section 6.3 with theirs. They parametrize the fields as

$$\phi(\mathbf{x}) = \cos\frac{\Theta}{2}\,\mathrm{e}^{\mathrm{i}n\psi}, \qquad \sigma(\mathbf{x}) = \sin\frac{\Theta}{2}\,\mathrm{e}^{\mathrm{i}m\varphi}, \tag{7.180}$$

which exactly coincides with the parametrization Eq. (2.32) of the Faddeev–Hopf field. Instead of directly solving the GP equation, BCS minimize the energy

$$E_2 + E_0 = \int (|\nabla\phi|^2 + |\nabla\sigma|^2 + \gamma_0|\phi|^2|\sigma|^2)\mathrm{d}^3\mathbf{x} \tag{7.181}$$

in a given N sector by keeping fixed the particle number

$$\mathcal{N} = \int |\sigma|^2 \mathrm{d}^3\mathbf{x}. \tag{7.182}$$

They call the resulting configurations $\phi_{\mathcal{N}}(\mathbf{x})$, $\sigma_{\mathcal{N}}(\mathbf{x})$ 'skyrmions' — because Eq. (7.180) agrees with the skyrmion parametrization (5.123). At first view it is not completely obvious how these 'skyrmions' are related to our vortons $\phi_\omega(\mathbf{x})$, $\sigma_\omega(\mathbf{x})$ obtained by solving Eqs. (6.170) for a given ω. However, these are actually the same solutions. In particular, the profiles of the vortons described in the previous sections, their energy density distributions, are similar to those for the 'skyrmions' given in Ref. [17].

The two different ways to obtain the solutions, either by minimizing the energy or via solving the equations, are actually equivalent.[1] This issue has in fact already been discussed above in the Q-ball context. Q-balls can be obtained either by solving Eq. (5.83), which gives $\phi_\omega(\mathbf{x})$, or via minimizing the truncated energy functional $E_0 + E_2$ (5.89) with the particle number $\mathcal{N}$ Eq. (5.88) fixed, which gives $\phi_\mathcal{N}(\mathbf{x})$. Once one knows the value $\omega = \omega(\mathcal{N})$, obtained either with the formula (5.90) or from the virial relation (5.82), the two results can be related to each other: $\phi_\omega(\mathbf{x}) = \phi_{\omega(\mathcal{N})}(\mathbf{x}) = \phi_\mathcal{N}(\mathbf{x})$.

Similarly, the BCS skyrmions $\phi_\mathcal{N}(\mathbf{x})$, $\sigma_\mathcal{N}(\mathbf{x})$ can be related to our vortons $\phi_\omega(\mathbf{x})$, $\sigma_\omega(\mathbf{x})$ by simply establishing the relation $\omega(\mathcal{N})$. The knowledge of ω is important to make sure that the no radiation condition

$$\omega^2 \leq M_\sigma^2 = \gamma_0 \tag{7.183}$$

is fulfilled, which is the case for our solutions, while their profiles agree with the features described by BCS in [17]. This provides an independent confirmation of our numerical results described in Section 6.3. Since they can be obtained by the 3D energy minimization, these solutions are stable.

Apart from the work of BCS there have been other studies of 'skyrmions' in Bose–Einstein condensates [149,147,144, 99,124]. Such solutions have been constructed by numerically resolving the GP equation for more general choices of $V(\mathbf{x})$ and κ_{ab} and also for more than two condensate components. Possibilities for an experimental creation and observation of such objects have also been discussed [146,145]. In all studies the solutions are typically presented for the winding numbers $n = 1$, with the exception of Ref. [144], where results for $n = 2$ are reported, although without giving many details.

7.2. Spinning rings in non-linear optics — Q-balls as light bullets

Yet another application of the ring solitons considered above arises in the theory of light propagating in media whose polarization vector $\vec{\mathcal{P}}$ depends non-linearly on the electric field $\vec{\mathcal{E}}$. The sourceless Maxwell equations become in this case non-linear and in a number of important cases they can be reduced to a non-linear Schrödinger (NLS) equation similar to the Gross–Pitaevskii equation (7.174). For a Kerr medium, when the non-linear part of $\vec{\mathcal{P}}$ is cubic in $\vec{\mathcal{E}}$, the NLS equation has exactly the same structure as Eq. (7.174), but for more general media it can have different non-linearities. Soliton solutions of this NLS equation describe non-linear light pulses, sometimes called light bullets, which are very interesting from the purely theoretical viewpoint and which can actually be observed, as for example in the optical fibers. Unfortunately, discussing these issues in more detail would lead us away from our subjects, and so we simply refer to a monograph [6] on optical solitons.

Most of the known solitons of the NLS equation describe plane waves or cylindrical beams of light [6]. However, solutions describing solitons localized in all three dimensions are also known, they have been studied by Mihalache et al. [125]. These solutions describe spinning rings, which is very interesting in the context of our discussion.

Mihalache et al. consider light pulses travelling in the z direction with a group velocity V in a medium with cubic and quintic non-linearities. After a suitable rescaling of the coordinates and fields, the envelope of the pulse, Ψ, satisfies the equation [125]

$$\mathrm{i}\frac{\partial\Psi}{\partial z} = \left(-\frac{\partial^2}{\partial x^2} - \frac{\partial^2}{\partial y^2} - \frac{\partial^2}{\partial \zeta^2} + |\Psi|^4 - |\Psi|^2\right)\Psi \tag{7.184}$$

where $\zeta = z - Vt$. Solutions of this equation, numerically constructed in Ref. [125], describe 'spinning light bullets'. Interestingly, it turns out that these solitons correspond to the spinning Q-balls already described above.

Specifically, let us rename the variables as $z \to t$, $\zeta \to z$ and set $\Psi = \exp\{\mathrm{i}(\omega^2 - M^2)t\}\phi$. Eq. (7.184) then assumes the form

$$\mathrm{i}\dot{\phi} = (-\Delta + |\phi|^4 - |\phi|^2 + M^2 - \omega^2)\phi. \tag{7.185}$$

Let us now consider Eq. (5.73) describing Q-balls with the potential (5.76). We notice that rescaling the spacetime coordinates and the field as $x^\mu \to \Lambda_1 x^\mu$, $\Phi \to \Lambda_2\Phi$ is equivalent to changing the values of the parameters λ, a in the potential. Therefore, as long as they do not vanish, one can choose without any loss of generality $\lambda = 1/3$, $a = 3/2$. Setting then $\Phi = \mathrm{e}^{\mathrm{i}\omega t}\phi$, Eq. (5.73) assumes the form

$$-\ddot{\phi} - 2\mathrm{i}\omega\dot{\phi} = (-\Delta + |\phi|^4 - |\phi|^2 + M^2 - \omega^2)\phi, \tag{7.186}$$

with $M^2 = \lambda b$. We see that if $\dot{\phi} = 0$ then Eqs. (7.185) and (7.186) become identical. They have therefore the same solutions. We thus conclude that the Q-balls solutions discussed in Section 5.1 can describe light pulses in non-linear media. The solutions found in Ref. [125] correspond to the simplest m^+, that is non-twisted, even parity Q-balls. Let us remind that for a given m these solutions can be parametrized by the value of ω varying within the range $\omega_-^2(m) < \omega^2 < \omega_+^2 = M^2$.

Mihalache et al. also study the dynamical stability of the solutions by analysing their small perturbations [125]. Perturbing in Eq. (7.185) the field as $\phi \to \phi + \delta\phi$ and linearizing with respect to $\delta\phi$ gives

$$\mathrm{i}\dot{\delta\phi} = \hat{\mathcal{D}}[\phi]\delta\phi, \tag{7.187}$$

[1] We thank Richard Battye for explaining this point to us.

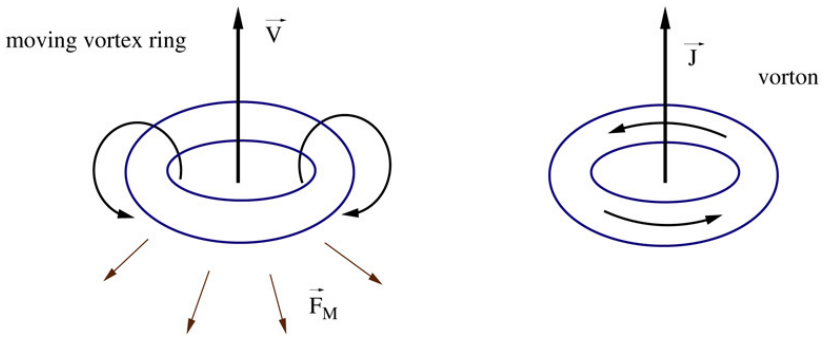

Fig. 31. Moving vortex rings are stabilized by an analog $\vec{F}_M$ of the Magnus force produced by the phase rotation *around* the vortex core. Vortons are stabilized by the centrifugal force produced by the phase rotation *along* the vortex.

where $\hat{\mathcal{D}}[\phi]$ is a linear differential operator. If the spectrum of this operator is known,

$$\hat{\mathcal{D}}[\phi]\xi_\lambda = \lambda\xi_\lambda, \tag{7.188}$$

then Eq. (7.187) is solved by setting $\delta\phi = \exp\{i\lambda t\}\xi_\lambda$. It follows that if there are complex eigenvalues λ with a negative imaginary part, then the perturbations grow for $t \to \infty$ and so the background is unstable. Mihalache et al. study the spectral problem (7.188) and find complex eigenvalues for all spinning solitons with $m = 2$. They also integrate Eq. (7.184) to trace the full non-linear perturbation dynamics, and they observe that the spinning toroidal soliton splits into *three* individual non-spinning spheroidal pieces [125]. However, they find that the $m = 0, 1$ solitons can be stable, both at the linear and non-linear levels, if ω is less than a certain value $\omega_*(m) < M$ but still within the domain of the solution existence, $\omega_-(m) < \omega < \omega_*(m)$. According to their results, for $m = 0$ one has $\omega_* = \omega_{\rm crit}$, which is the value where $E(\omega)$, $Q(\omega)$ pass through the minimum (see Fig. 14). For $m = 1$ the stability region shrinks, since $\omega_* < \omega_{\rm crit}$, so that not all parts of the less energetic solution branch (see Fig. 14) correspond to stable solutions.

These results are very interesting, since they allow us to draw certain conclusions about stability of the relativistic Q-balls. Linearizing Eq. (7.186) gives

$$-\delta\ddot{\phi} - 2i\omega\delta\dot{\phi} = \hat{\mathcal{D}}[\phi]\delta\phi, \tag{7.189}$$

whose solution is $\delta\phi = \exp\{i\gamma t\}\xi_\lambda$ with $\gamma = -\omega \pm \sqrt{\lambda + \omega^2}$. All eigenmodes with complex λ therefore correspond to complex γ and so to unstable modes. In addition, there could be unstable modes with real $\lambda < -\omega^2$, since γ would then be complex. As a result, the relativistic Q-balls have the same unstable modes as their non-relativistic optical counterparts (although with different instability growth rates) and perhaps also some additional instabilities.

It follows that the 2^+ spinning Q-balls are unstable, while the 1^+ ones, if they belong to the lower solution branch and their charge is large enough, should be stable (unless they have negative modes with $\lambda < -\omega^2$). The latter conclusion agrees with the results shown in Fig. 14.

As was said above, Q-balls corresponding to the lower solution branch in Fig. 14 cannot decay into free particles. As we now see, this property does not yet guarantee their stability, since there can be other decay channels. Their non-relativistic optical counterparts can decay into several solitonic constituents. In order to see if the same could be true for the relativistic Q-balls, one should integrate the full time evolutions equation (7.186). The existence of negative modes for spinning Q-balls is also suggested by the results of Refs. [10,16].

The results of Ref. [125] have been generalized in Refs.[126,127] to describe the case of light pulses with two independent polarizations and also for more general non-linearities of the medium.

7.3. Moving vortex rings

For the sake of completeness, we would also like to consider another well-known type of ring solitons: moving vortex rings in continuous media. Although they are stabilized by the interaction with the medium and not by intrinsic forces, their structure can be quite similar to that for the other solitons considered above.

A vortex ring moving in a medium encounters the 'wind' that produces a circulation around the vortex core, giving rise to the Magnus force — the same force that acts on a spinning ping-pong ball in the direction orthogonal to its velocity. This force is directed outwards orthogonally to the ring velocity, stabilizing the ring against shrinking (see Fig. 31). As a result, the ring travels with a constant speed (if there is no dissipation), dynamically keeping a constant radius, so that in the comoving reference frame its configuration is stationary.

The moving vortex rings are best known in fluid dynamics, as for example smoke rings. The vortices themselves correspond in this case to their traditional definition — these are line-type objects containing a non-zero rotation of the fluid in their core, as for example swirls in water or tornadoes. Vortices and vortex rings can be created in the wake of rigid bodies travelling through the fluid. Their hydrodynamical theory was created in the 19th century by Helmholtz and Kelvin

and has been developing ever since, finding numerous practical applications, as for example in the aircraft engineering. We do not intend to discuss this vast subject here and simply refer to the standard monograph on vortices [148]. We also give the classical formulas of Kelvin relating the vortex ring velocity V and its energy E and momentum P to the ring radius, R, and the vortex core radius, a,

$$E = \frac{1}{2}\eta^2\Gamma^2\left(\ln\frac{8R}{a} - \frac{7}{4}\right), \quad P = \pi\eta\Gamma R^2, \quad V = \frac{\Gamma}{4\pi R}\left(\ln\frac{8R}{a} - \frac{1}{4}\right), \tag{7.190}$$

which are valid in the thin ring limit, $R \gg a$. Here η is the fluid mass density and Γ is the circulation of the fluid velocity around the vortex. These formulas show that large rings have large energy and momentum but move slowly. Very large and slowly moving rings, which could perhaps be described by some version of hydrodynamics of magnetized plasma, are observed in Sun's atmosphere.

7.3.1. Moving vortex rings in the superfluid helium

Moving vortex rings exist also in the superfluid helium, where they are created by moving impurities [140] (see [170] for a survey of defects in helium). It turns out that large rings in helium can be well described by the classical hydrodynamics. However, in the generic case their adequate description should be quantum. The superfluid helium can be approximately modeled by a weakly interacting Bose–Einstein condensate (although in reality the interactions in helium are not weak, see e.g. [23]), in which case vortices can be described by solutions of the Gross–Pitaevskii equation (7.174). In the simplest case one can consider the one-component version of this equation, which, upon setting $V(\mathbf{x}) = 0$, $\kappa_{11} = \kappa$ and $\Psi_1 \equiv \mathrm{e}^{-\mathrm{i}\frac{\kappa}{2}t}\Psi$ reduces to

$$2\mathrm{i}\frac{\partial\Psi}{\partial t} = \left(-\Delta + \kappa(|\Psi|^2 - 1)\right)\Psi. \tag{7.191}$$

Rescaling coordinates and time one can set $\kappa = 1$, if it is positive. Choosing $\Psi = \mathrm{e}^{\mathrm{i}n\varphi}f(\rho)$ gives

$$f'' + \frac{1}{\rho}f' - \frac{n^2}{\rho^2}f = (f^2 - 1)f, \tag{7.192}$$

whose solution with the boundary conditions $f(0) = 0$ and $f(\infty) = 1$ describes a global vortex with n quanta of circulation [78].

Solutions of the GP equation (7.191) describing moving vortex rings and their various properties have been comprehensively analyzed by P.H. Roberts and collaborators in a series of articles written over the last 25 years, of which we only mention Refs. [81,97,24,22,21]. The fundamental vortex ring solutions have been numerically obtained by Jones and Roberts [97] by setting

$$\Psi = \Psi(\rho, z - Vt), \tag{7.193}$$

such that $\Psi(\rho, z)$ satisfies the equation

$$-\mathrm{i}2V\partial_z\Psi = \left(-\Delta + (|\Psi|^2 - 1)\right)\Psi. \tag{7.194}$$

They imposed the reflection condition $\Psi(\rho, z) = \Psi(\rho, -z)^*$ and also the asymptotic conditions for large r,

$$\Re(\Psi) = 1 + O(r^{-3}), \qquad \Im(\Psi) = O(r^{-2}). \tag{7.195}$$

Numerically integrating Eq. (7.194), they obtained a family of solutions labeled by $V \in (0, V_{\max})$, where $V_{\max} = 1/\sqrt{2}$ is the speed of sound in the dimensionless units chosen. For small V the solutions have ring profiles: the function Ψ vanishes at a point $(R, 0)$ in the (ρ, z) plane while its phase increases by 2π after one revolution around this point, so that Ψ has the 'vorton topology' (see Fig. 22). When V is small, the radius of the ring, R, as well as its energy and momentum,

$$E = \frac{1}{2}\int\left(|\nabla\Psi|^2 + \frac{1}{2}(|\Psi|^2 - 1)^2\right)\mathrm{d}^3\mathbf{x},$$
$$P_3 = \Im\int(\Psi^* - 1)\partial_z\Psi\,\mathrm{d}^3\mathbf{x}, \tag{7.196}$$

are large, and in the leading order they agree with the classical Kelvin formulas (7.190) [81]. As V increases, E, P_3 and R all decrease, and the following relation holds,

$$V = \frac{\partial E}{\partial P_3}. \tag{7.197}$$

The ring radius R vanishes for $V = V_0 \approx 0.62$ and for $V_0 < V < V_{\max}$ solutions change their character and describe acoustic excitations in helium, called in [97] rarefaction pulses, in which case Ψ no longer has zeros. The energy and momentum diverge when V approaches 0, $V_{\max}$, and they both assume their minimal values for some $V = V_{\mathrm{crit}} \approx 0.657$. The functions

$E(V)$ and $P_3(V)$ exhibit therefore qualitatively the same behavior as $E(\omega)$ and $Q(\omega)$ for the Q-balls (see Fig. 14). The function $E(P_3)$ shows the two-branch structure with a cusp, similarly to $E(Q)$ in Fig. 14. The moving rings belong to the lower branch, which suggests that they could be stable. Their perturbative stability has been demonstrated by Berloff and Roberts [24], who also studied the ring creation by solving the GP equation for a superfluid flow around a moving solid sphere [22] and showed that rings are created in its wake, provided that its velocity exceeds some critical value.

The moving ring solutions have been generalized for a non-zero trapping potential $V(\mathbf{x})$ in the GP equation (see [110] for a review) and for the two-component condensate case [20]. An interesting solution of the GP equation describing a non-linear superposition of a straight vortex and a vortex ring encircling it and moving along it, somewhat similar to the 'hoop' solution shown in Fig. 19, has been presented by Berloff in [21].

One may also wonder whether the vortex ring solutions could be generalized within a relativistic field theory (as is the case for the vortex solution of Eq. (7.192)). In fact, the answer to this question is affirmative, since taking a solution $\Psi(\rho, z)$ of Eq. (7.194) and setting

$$\phi = \mathrm{e}^{\mathrm{i}V(z\pm t)}\Psi(\rho, z) \tag{7.198}$$

and also $\sigma = 0$ solves Eq. (6.142) of Witten's model for $\lambda_\phi = 2$. However, since $\Psi \to 1$ at infinity, it follows that $\phi \to \mathrm{e}^{\mathrm{i}V(z\pm t)}$ in this limit, which corresponds to a massless Goldstone radiation. The relativistic analogs of the moving vortex rings are therefore radiative solutions and their total energy is infinite.

7.3.2. Moving magnetic rings

An interesting example of moving ring solitons, found by Cooper [41] and studied also by Sutcliffe [159], arises in ferromagnetic systems whose dynamics is described in the continuum limit by the Landau–Lifshitz equation

$$\frac{\partial n^a}{\partial t} = \epsilon_{abc} n^b \Delta n^c. \tag{7.199}$$

Here n^a is a unit three-vector, $n^a n^a = 1$, giving the local orientation of the magnetization. The temporal evolution defined by the Landau–Lifshitz equation preserves the value of the energy

$$E = \frac{1}{4}\int (\partial_k n^a)^2 \mathrm{d}^3\mathbf{x}. \tag{7.200}$$

In addition, it does not change the momentum,

$$P_i = \frac{1}{2}\int \epsilon_{ijk}(x_j \mathcal{B}_k)\mathrm{d}^3\mathbf{x}, \tag{7.201}$$

where $\mathcal{B}_i = \frac{1}{2}\epsilon_{ijk}\mathcal{F}_{jk}$ and $\mathcal{F}_{jk}$ is defined as in the Faddeev–Skyrme model by Eq. (2.2). The number of spin flips,

$$\mathcal{N} = \frac{1}{2}\int (1 - n^3)\mathrm{d}^3\mathbf{x}, \tag{7.202}$$

is also preserved by the evolution; for this number to be finite one should have $n^3 = 1$ at infinity. Since the theory contains a unit vector field, it can be characterized by the topological index of Hopf defined by the same Eq. (2.9) as in the Faddeev–Skyrme model. An axially symmetric field configuration with a non-zero Hopf charge can be parametrized exactly as in Eq. (2.10) (with $n = 1$),

$$n^1 + \mathrm{i}n^2 = \sin\Theta(\rho, z)\exp\{\mathrm{i}[m\varphi - \psi(\rho, z)]\}, \quad n^3 = \cos\Theta(\rho, z). \tag{7.203}$$

The energy density then has a ring structure and the Hopf charge is $N = m$. Using this to calculate the momentum (7.201) shows that its z-component does not vanish,

$$P_z = \frac{1}{4}\int \rho(\partial_z\Theta\partial_\rho\psi - \partial_\rho\Theta\partial_z\psi)\mathrm{d}^3\mathbf{x}. \tag{7.204}$$

This means that if one uses (7.203) as the initial data for the Landau–Lifshitz equation, then this data set will have a non-zero initial momentum. To verify this assertion, Sutcliffe [159] directly integrates the Landau–Lifshitz equation to reconstruct the temporal dynamics of the ring. For largely arbitrary functions $\Theta(\rho, z)$, $\psi(\rho, z)$ in (7.203) he then sees the whole ring configuration drift with an almost constant velocity along the z-axis. He also observes that the phase of $n^1 + \mathrm{i}n^2$ increases as a linear function of the distance travelled by the ring, so that there are internal rotations in the ring as it moves.

These empirical features can be understood by making the following ansatz for the dynamical fields [41],

$$n^1 + \mathrm{i}n^2 = \sin\Theta(\rho, z - Vt)\exp\{\mathrm{i}[m\varphi + \omega t - \psi(\rho, z - Vt)]\}, \quad n^3 = \cos\Theta(\rho, z - Vt), \tag{7.205}$$

with constant V, ω. Inserting this ansatz to the Landau–Lifshitz equation (7.199), the t, φ variables separate and the problem reduces to the 2D elliptic problem for $\Theta(\rho, z)$, $\psi(\rho, z)$,

$$\Delta\Theta = (\omega + V\partial_z\psi)\sin\Theta + \left[((\partial_\rho\psi)^2 + (\partial_z\psi)^2) + \frac{m^2}{\rho^2}\right]\sin\Theta\cos\Theta,$$
$$\sin\Theta\,\Delta\psi = -V\partial_z\Theta - 2\cos\Theta[\partial_\rho\Theta\partial_\rho\psi + \partial_z\Theta\partial_z\psi]. \tag{7.206}$$

This problem is in fact very much similar to that in the vorton case. This can be seen by applying the same change of variables which was used to rewrite the Faddeev–Skyrme model (2.1) in the CP^1 form (2.29), $n^a = \Phi^\dagger\tau^a\Phi$, with $\Phi^\dagger\Phi = 1$. This parametrization of the system allows one to write down a simple Lagrangian for the Landau–Lifshitz equation (7.199),

$$\mathcal{L} = \mathrm{i}\Phi^\dagger\partial_t\Phi - \frac{1}{4}(\partial_k n^a)^2 + \mu(\Phi^\dagger\Phi - 1), \tag{7.207}$$

where μ is the Lagrange multiplier. One can parametrize Φ exactly in the same way as in the vorton case,

$$\Phi = \begin{pmatrix} X + \mathrm{i}Y \\ Z\mathrm{e}^{\mathrm{i}\omega t + \mathrm{i}m\varphi} \end{pmatrix}.$$

Inserting this to the Lagrangian (7.207) and varying with respect to X, Y, Z, μ gives equations similar to Eqs. (6.170) for vortons in the sigma model limit. These equations can be solved with the same boundary conditions (6.162)–(6.165) for X, Y, Z as for vortons. On the other hand, setting $X + \mathrm{i}Y = \cos(\Theta/2)\mathrm{e}^{\mathrm{i}\psi}$ and $Z = \sin(\Theta/2)$, as in Eq. (7.180), gives again Eqs. (7.206).

Fixing m one can solve the equations for suitable input values of ω, V. Having obtained the solutions, one can calculate $E(\omega, V)$, $\mathcal{N}(\omega, V)$ and $P_3(\omega, V)$. Alternatively, instead of solving the equations, one can minimize the energy E with fixed $\mathcal{N}$, P_3. Having found the minimal value $E(\mathcal{N}, P_3)$, one can reconstruct ω, V as [41,159]

$$\omega = \frac{\partial E}{\partial\mathcal{N}}, \quad V = \frac{\partial E}{\partial P_3}. \tag{7.208}$$

Cooper [41] and Sutcliffe [159] choose the latter approach: they minimize the energy with fixed $\mathcal{N}$, P_3 for several values of $m = N$. Their numerics converge to non-trivial configurations $\Theta(\rho, z)$, $\psi(\rho, z)$, inserting which to (7.205) gives dynamical rings travelling with a constant velocity. Fixing all other parameters, the ring velocity decreases with growing m.

In fact, these rings also have an angular momentum, $J = m\mathcal{N}$, but apparently this feature is not so essential for their stabilization as it is for vortons, since solutions with $m = N = J = 0$ also exist and do not exhibit any particular features as compared to the solutions with $m \neq 0$ [159]. Similarly to the other moving ring solitons discussed above, magnetic rings are stabilized by a Magnus-type force produced by the phase circulation *around* the vortex core and directed outwards, orthogonally to the velocity (see Fig. 31). The magnetic rings are stable not only against shrinking but also with respect to all other deformations — since they can be obtained via the 3D energy minimization [159].

8. Concluding remarks

We have reviewed the known field theory solutions describing stationary vortex loops. From the physical point of view, loops of magnetic flux would perhaps be the most interesting. However, as we have seen, almost all explicit solutions describe vortex loops in global field theories, which are effective theories with a relatively limited range of applicability. Perspectives for generalizing these solutions in the context of gauge field theory do not look very promising at the moment, at least as far as knot solitons are concerned. The best known static knot solitons, Faddeev–Skyrme knots, do not seem to admit immediate gauge field theory generalizations, unless one makes additional physical assumptions to fix the charges in the Protogenov–Verbus formula. Such assumptions can be made, as shows the example of Schmid and Shaposhnikov. However this requires a rather exotic physical environment.

The non-Abelian monopole and sphaleron rings are very interesting theoretically, however, they are presumably unstable. It is therefore unclear whether they can find important physical applications. Summarizing, the existence of knots – magnetic vortex loops stabilized against shrinking by internal stresses – does not seem to be very plausible in the context of physically interesting relativistic gauge field theories.

Perhaps gauged vortons have more chances to exist. As we have seen, their global counterparts do exist as stationary, non-radiating field theory objects. Already for these global vortons an additional analysis to study the structure of the parameter space is needed. A natural problem to address would be their analysis in the thin ring limit, for large values of the azimuthal winding number m, when the ring radius is much larger than the vortex core thickness. One can expect that the field theory solutions in this limit should agree with the effective macroscopic description. This limit, however, is difficult to explore numerically, since the vorton fields are then almost everywhere constant, except for a narrow ring region containing all the field gradients. It is difficult to properly adjust the grid in this case, so that some other numerical methods are necessary, as perhaps the multidomain spectral method [80]. Is seems also that some other methods are necessary to study solutions with $n > 1$.

Yet another interesting related problem would be to find vortons with *three* winding numbers. We know that the phase of ϕ winds around the vortex core, while that of σ winds along the ring, the corresponding winding numbers being n and m. However, nothing forbids the phase of σ to wind *both* around the core and along the ring, as does the phase of the twisted Q-balls, in which case one would need a third integer, k, counting the windings of σ around the vortex core. Constructing vortons with $k \neq 0$ remains a challenge.

A very important open problem related to all vortons is their dynamical stability analysis. This problem can be handled either by studying the spectrum of small field fluctuations around the vorton background, or by looking for vorton negative modes within the energy minimization method, or by reconstructing the full temporal evolution of the perturbed vorton configuration. Stable vortons definitely exist, at least in the sigma model limit, but for the generic parameter values vorton stability should be studied.

Generalizing global vortons within gauge field theory does not seem to be impossible. In theories where all the internal symmetries are gauged, as in Witten's model (6.136), all spinning phases of the fields can be gauged away, so that if the fields are stationary and axisymmetric, these symmetries are manifest. In this case the surface integral formula (4.66) for the angular momentum applies, providing higher chances for J to vanish due to the fast asymptotic falloff of the fields. Although the example of spinning gauged Q-balls shows that spinning is possible in local theories, it seems that vortons have better chances to exist in models with both local and global internal symmetries. Such models contain gauge fields, such that one can have magnetic vortices, but the gauge freedom is not enough to gauge away all the phases of the scalars. The symmetries of the fields are therefore not manifest and the surface integral formula does not apply, in which case the angular momentum should normally be non-zero.

For example, it would be natural to analyze the existence of stationary vortons in a half-gauged version of Witten's modes obtained by coupling the two scalars in Eq. (6.138) to a U(1) gauge field. Such solutions could then perhaps be generalized within the fully gauged $U(1) \times U(1)$ Witten's modes to confirm the existence of stationary loops made of superconducting cosmic strings — the idea first put forward more than 20 years ago.

However, a real challenge would be to construct stationary superconducting loops in Standard Model. There are indications that this might be possible. The electroweak sector of Standard Model contains stationary current carrying vortices — superconducting strings [166]. Their stability has been studied so far only in the semi-local limit, where the SU(2) gauge field decouples and the current becomes global [73,72], and it has been found that sufficiently short pieces of strings are perturbatively stable [76]. This suggests that small loops made of these strings may also be stable. If such loops could be constructed for the physical value of the weak mixing angle, this would give stable solitons in Standard Model.

For the sake of completeness, having in mind possible applications of vortex loops in astrophysics and cosmology, it is also interesting to mention the effects of gravity on these solutions. On general grounds, one expects all known ring solitons to admit self-gravitating generalizations with essentially the same properties as in the zero gravity limit, at least for small enough values of the gravitational coupling constant. However, the soliton structure can change considerably in the strong gravity regime [167]. The solitons can then become gravitationally closed and may also contain a small black hole in their center. The spinning of the latter can endow the whole configuration with an angular momentum, even if the soliton itself cannot spin — as for example the monopole [104]. However, if the soliton can spin on its own, as for example a vorton, it would be interesting to put a spinning black hole in its center. Since there are no asymptotically flat toroidal black holes in four dimensions [96], the resulting configuration is expected to be a black hole with spherical horizon topology, surrounded by a vortex ring.

Acknowledgements

The work of E.R. was supported by the ANR grant NT05-1_42856 'Knots and Vortons'. We would like to thank Richard Battye, Brandon Carter, Maxim Chernodub, Ludwig Faddeev, Peter Forgacs, Philippe Grandclement, Betti Hartmann, Xavier Martin, Antti Niemi, Mikhail Shaposhnikov, Matthias Schmid, Paul Shellard, Paul Sutcliffe and Tigran Tchrakian for discussions during various stages of this work.

References

[1] A.A. Abrikosov, On the magnetic properties of superconductors of the second group, Sov. Phys. JETP 5 (1957) 1174–1182.
[2] A. Achucarro, T. Vachaspati, Semilocal and electroweak strings, Phys. Rep. 327 (2000) 347–426.
[3] C. Adam, J. Sanchez-Guillen, R.A. Vazquez, A. Wereszczynski, Investigation of the Nicole model, J. Math. Phys. 47 (2006) 052302.
[4] G. Adkins, C.R. Nappi, The Skyrme model with pion masses, Nuclear Phys. B233 (1984) 109–115.
[5] G. Adkins, C.R. Nappi, W. Witten, Static properties of nucleons in the Skyrme model, Nuclear Phys. B228 (1983) 552–566.
[6] N.N. Akhmediev, A. Ankiewicz, Solitons, Nonlinear Pulses and Beams, Chapman and Hall, London, 1997, p. 299.
[7] P. Amsterdamski, P. Laguna-Castillo, Internal structure and the spacetime of superconducting bosonic strings, Phys. Rev. D37 (1988) 877–884.
[8] H. Aratyn, L.A. Ferreira, A.H. Zimerman, Exact static soliton solutions of 3 + 1 dimensional integrable theory with nonzero Hopf numbers, Phys. Rev. Lett. 83 (1999) 1723–1726.
[9] H. Aratyn, L.A. Ferreira, A.H. Zimerman, Toroidal solitons in 3 + 1 dimensional integrable theories, Phys. Lett. B456 (1999) 162–170.
[10] M. Axenides, E. Floratos, S. Komineas, L. Perivolaropoulos, Q-rings, Phys. Rev. Lett. 86 (2001) 4459–4462.
[11] E. Babaev, Knotted solitons in triplet superconductors, Phys. Rev. Lett. 88 (2002) 177002.
[12] E. Babaev, L.D. Faddeev, A.J. Niemi, Hidden symmetry and duality in a charged two-condensate Bose system, Phys. Rev. B65 (2002) 100512.
[13] A. Babul, T. Piran, D.M. Spergel, Bosonic superconducting cosmic strings. I. Classical field theory solutions, Phys. Lett. B202 (1988) 307–314.
[14] R. Battye, P. Sutcliffe, Knots as stable soliton solutions in a three-dimensional classical field theory, Phys. Rev. Lett. 81 (1998) 4798–4801.

[15] R. Battye, P. Sutcliffe, Solitons, links and knots, Proc. Roy. Soc. Lond. A455 (1999) 4305–4331.
[16] R. Battye, P. Sutcliffe, Q-ball dynamics, Nuclear Phys. B590 (2000) 329–363.
[17] R.A. Battye, N.R. Cooper, P.M. Sutcliffe, Stable Skyrmions in two-component Bose–Einstein condensates, Phys. Rev. Lett. 88 (2002) 080401.
[18] R.A. Battye, S. Krusch, P.M. Sutcliffe, Spinning Skyrmions and the Skyrme parameters, Phys. Lett. B626 (2005) 120–126.
[19] R.A. Battye, P. Sutcliffe, Kinky vortons, 2008. e-Print: arXiv:0806.2212[hep-th].
[20] N.G. Berloff, Nucleation of solitary wave complexes in two-component mixture Bose–Einstein condensates, 2005. arXiv:cond-mat/0412743.
[21] N.G. Berloff, Solitary waves on vortex lines in Ginzburg–Landau models for the example of Bose–Einstein condensates, Phys. Rev. Lett. 94 (2005) 010403.
[22] N.G. Berloff, P.H. Roberts, Motion in a Bose condensate: VII. Boundary-layer separation, J. Phys. A33 (2000) 4025–4038.
[23] N.G. Berloff, P.H. Roberts, Nonlinear Schrödinger equation as a model of superfluid helium, in: C.F. Barenghi, R.J. Donnelly, W.F. Vinen. (Eds.), Quantized Vortex Dynamics and Superfluid Turbulence, in: Lecture Notes in Physics, vol. 571, Springer-Verlag, 2001.
[24] N.G. Berloff, P.H. Roberts, Motion in a Bose condensate: X. New results on stability of axisymmetric solitary waves of the Gross–Pitaevskii equation, J. Phys. A37 (2004) 11333–11351.
[25] M. Betz, H.B. Rodrigues, T. Kodama, Rotating skyrmion in $(2+1)$-dimensions, Phys. Rev. D54 (1996) 1010–1019.
[26] N. Bevis, M. Hindmarsh, M. Kunz, J. Urrestilla, CMB power spectrum contribution from cosmic strings using field-evolution simulations of the Abelian Higgs model, Phys. Rev. D75 (2007) 065015.
[27] E.B. Bogomol'nyi, Stability of classical solutions, Sov. J. Nucl. Phys. 24 (1976) 449–454.
[28] A.H. Boozer, Physics of magnetically confined plasmas, Rev. Modern Phys. 76 (2004) 1071–1141.
[29] R.H. Brandenberger, B. Carter, A.C. Davis, M. Trodden, Cosmic vortons and particle physics constraints, Phys. Rev. D54 (1996) 6059–6071.
[30] Y. Brihaye, B. Hartmann, Interacting Q-balls, 2007. arXiv:0711.1969[hep-th].
[31] C.G. Callan, E. Witten, Monopole catalysis of skyrmion decay, Nuclear Phys. B239 (1984) 161–176.
[32] B. Carter, Duality relation between charged elastic strings and superconducting cosmic strings, Phys. Lett. B224 (1989) 61–66.
[33] B. Carter, Stability and characteristic propagation speeds in superconducting cosmic and other string models, Phys. Lett. B228 (1989) 466–470.
[34] B. Carter, Mechanics of cosmic rings, Phys. Lett. B238 (1990) 166–171.
[35] B. Carter, P. Peter, Supersonic string model for Witten vortices, Phys. Rev. D52 (1995) 1744–1748.
[36] Y.M. Cho, Knot solitons in Weinberg-Salam model, 2001. arXiv:hep-th/0110076.
[37] Y.M. Cho, Monopoles and knots in Skyrme theory, Phys. Rev. Lett. 87 (2001) 252001.
[38] S.R. Coleman, The magnetic monopole fifty years later, in: Lectures given at Int. Sch. of Subnuclear Phys., Erice, Italy, Jul 31–Aug 11, 1981, at 6th Brazilian Symp. on Theor. Phys., Jan 7–18, 1980, at Summer School in Theoretical Physics, Les Houches, France, and at Banff Summer Inst. on Particles & Fields, Aug 16–28, 1981.
[39] S.R. Coleman, Q balls, Nuclear Phys. B262 (1985) 263–283.
[40] S.R. Coleman, S. Parke, A. Neveu, C.M. Sommerfield, Can one dent a dyon? Phys. Rev. D15 (1977) 544–545.
[41] N.R. Cooper, Propagating magnetic vortex rings in ferromagnets, Phys. Rev. Lett. 82 (2001) 1554–1557.
[42] E.J. Copeland, D. Haws, M. Hindmarsh, N. Turok, Dynamics of and radiation from superconducting strings and springs, Nuclear Phys. B306 (1988) 908–930.
[43] E.J. Copeland, M. Hindmarsh, N. Turok, Dynamics of superconducting cosmic strings, Phys. Rev. Lett. 58 (1987) 1910–1913.
[44] F. Paccetti Correia, M.G. Schmidt, Q balls: Some analytical results, Eur. Phys. J. C21 (2001) 181–191.
[45] R.L. Davis, Semitopological solitons, Phys. Rev. D38 (1988) 3722–3730.
[46] R.L. Davis, E.P.S. Shellard, The physics of vortex superconductivity, Phys. Lett. B207 (1988) 404–410.
[47] R.L. Davis, E.P.S. Shellard, The physics of vortex superconductivity. 2, Phys. Lett. B209 (1988) 485–490.
[48] R.L. Davis, E.P.S. Shellard, Cosmic vortons, Nuclear Phys. B323 (1989) 209–224.
[49] H.J. de Vega, Closed vortices and the Hopf index in classical field theory, Phys. Rev. D18 (1978) 2945–2951.
[50] J.J. Van der Bij, E. Radu, On rotating regular nonabelian solutions, Int. J. Mod. Phys. A17 (2002) 1477–1490.
[51] J.J. Van der Bij, E. Radu, Magnetic charge, angular momentum and negative cosmological constant, Int. J. Mod. Phys. A18 (2003) 2379–2393.
[52] G.H. Derrick, Comments on nonlinear wave equations as models for elementary particles, J. Math. Phys. 5 (1964) 1252–1254.
[53] L. Dittmann, T. Heinzl, A. Wipf, A lattice study of the Faddeev–Niemi action, Nucl. Phys. Proc. Suppl. B106 (2002) 649–651.
[54] R.J. Donnelly, Quantized Vortices in Helium II, Cambridge University Press, 1991, p. 346.
[55] C.G. Doudoulakis, On vortices and rings in extended Abelian models, Physica D234 (2007) 1–10.
[56] C.G. Doudoulakis, On vortices and solitons in Goldstone and Abelian-Higgs models, 2007. arXiv:0709.3709[hep-ph].
[57] C.G. Doudoulakis, Search of axially symmetric solitons, Physica D228 (2007) 159–165.
[58] R. Emparan, H.S. Reall, Black rings, Class. Quant. Grav. 23 (2006) R169.
[59] J. Hietarinta, et al. http://users.utu.fi/hietarin/knots/.
[60] W.M. Yao, et al., The review of particle physics, J. Phys. G33 (2006) 1–1232.
[61] L.D. Faddeev, Quantization of solitons, 1975. Princeton preprint IAS-75-QS70; also Einstein and several contemporary tendencies in the theory of elementary particles in Relativity, quanta, and cosmology, vol. 1, M. Pantaleo and F. De Finis (Eds.), pp. 247–266 (1979), reprinted in L. Faddeev, 40 years in mathematical physics, pp. 441–461 (World Scientific, 1995).
[62] L.D. Faddeev, Some comments on the many-dimensional solitons, Lett. Math. Phys. 1 (1976) 289–293.
[63] L.D. Faddeev, L. Freyhult, A.J. Niemi, P. Rajan, Shafranov's virial theorem and magnetic plasma confinement, J. Phys. A35 (2002) L133–L140.
[64] L.D. Faddeev, A.J. Niemi, Knots and particles, Nature 387 (1997) 58–61.
[65] L.D. Faddeev, A.J. Niemi, Toroidal configurations as stable solitons, 1997. hep-th/9705176.
[66] L.D. Faddeev, A.J. Niemi, Partially dual variables in SU(2) Yang–Mills theory, Phys. Rev. Lett. 82 (1999) 1624–1627.
[67] L.D. Faddeev, A.J. Niemi, Magnetic geometry and the confinement of electrically conducting plasmas, Phys. Rev. Lett. 85 (2000) 3416–3419.
[68] L.D. Faddeev, A.J. Niemi, Spin-charge separation, conformal covariance and the SU(2) Yang–Mills theory, Nuclear Phys. B776 (2007) 38–65.
[69] L.D. Faddeev, A.J. Niemi, U. Wiedner, Glueballs, closed fluxtubes and eta(1440), Phys. Rev. D70 (2004) 114033.
[70] B.A. Fayzullaev, M.M. Musakhanov, D.G. Pak, M. Siddikov, Knot soliton in Weinberg-Salam model, Phys. Lett. B609 (2005) 442–448.
[71] P. Forgacs, N. Manton, Space–time symmetries in gauge theories, Commun. Math. Phys. 72 (1980) 15–35.
[72] P. Forgacs, S. Reuillon, M.S. Volkov, Superconducting vortices in semilocal models, Phys. Rev. Lett. 96 (2006) 041601.
[73] P. Forgacs, S. Reuillon, M.S. Volkov, Twisted superconducting semilocal strings, Nuclear Phys. B751 (2006) 390–418.
[74] P. Forgacs, M.S. Volkov, On the existence of knot solitons in gauge field theory, 2002, unpublished.
[75] R. Friedberg, T.D. Lee, A. Sirlin, A class of scalar-field soliton solutions in three space dimensions, Phys. Rev. D13 (1976) 2739–2761.
[76] J. Garaud, M.S. Volkov, Stability analysis of the twisted superconducting electroweak strings, Nuclear Phys. B799 (2008) 430–455.
[77] V.L. Ginzburg, L.D. Landau, On the theory of superconductivity, Zh. Eksp. Teor. Fiz. 20 (1950) 1064.
[78] V.L. Ginzburg, L.P. Pitaevskii, On the theory of superfluidity, Sov. Phys. JETP 34 (1958) 858–861.
[79] J. Gladikowski, M. Hellmund, Static solitons with non-zero Hopf number, Phys. Rev. D56 (1997) 5194–5199.
[80] P. Grandclement, J. Novak, Spectral methods for numerical relativity, 2007. arXiv:0706.2286[gr-qc].
[81] J. Grant, P.H. Roberts, Motion in a Bose condensate III. The structure and effective masses of charged and uncharged impurities, J. Phys. A7 (1974) 260–279.
[82] B. Greenwood, Ball lightning bibliography. www.project1947.com/shg/bl_db.html.
[83] E.P. Gross, Structure of quantized vortex, Nuovo Cimento 20 (1961) 454–477.
[84] B. Hartmann, B. Carter, The logarithmic equation of state for superconducting cosmic strings, 2008. arXiv:0803.0266[hep-th].
[85] B. Hartmann, B. Kleihaus, J. Kunz, Dyons with axial symmetry, Mod. Phys. Lett. A15 (2000) 1003–1012.

[86] D. Haws, M. Hindmarsh, N. Turok, Superconducting strings or springs? Phys. Lett. B209 (1988) 255–261.
[87] I. Hen, M. Karliner, Spontaneous breaking of rotational symmetry in rotating solitons: A toy model of excited nucleons with high angular momentum, Phys. Rev. D77 (2008) 116002.
[88] M. Heusler, N. Straumann, M. Volkov, On rotational excitations and axial deformations of BPS monopoles and Julia–Zee dyons, Phys. Rev. D58 (1998) 105021.
[89] J. Hietarinta, P. Salo, Faddeev–Hopf knots: Dynamics of linked un-knots, Phys. Lett. B451 (1999) 60–67.
[90] J. Hietarinta, P. Salo, Ground state in the Faddeev–Skyrme model, Phys. Rev. D62 (2000) 081701.
[91] C.T Hill, H.M. Hodges, M.S. Turner, Bosonic superconducting cosmic strings, Phys. Rev. D37 (1988) 263–282.
[92] R.H. Hobart, On the instability of a class of unitary field model, Proc. Phys. Soc. 82 (1963) 201–203.
[93] K. Huang, R. Tipton, Vortex excitations in the Weinberg-Salam theory, Phys. Rev. D23 (1981) 3050–3057.
[94] T. Ioannidou, B. Kleihaus, J. Kunz, Spinning gravitating skyrmions, Phys. Lett. B643 (2006) 213–220.
[95] J. Jaykka, J. Hietarinta, P. Salo, Investigation of the stability of Hopfions in the two-component Ginzburg–Landau model, Phys. Rev. B77 (2008) 094509.
[96] J.L. Friedman, K. Schliech, D.M. Witt, Topological censorship, Phys. Rev. Lett. 71 (1993) 1486–1489.
[97] C.A. Jones, P.H. Roberts, Motion in a Bose condensate: IV. Axisymmetric solitary waves, J. Phys. A15 (1982) 2599–2619.
[98] B. Julia, A. Zee, Poles with both magnetic and electric charges in nonabelian gauge theory, Phys. Rev. D11 (1975) 2227–2232.
[99] Y. Kawaguchi, M. Nitta, M. Ueda, Knots in a spinor Bose–Einstein condensate, 2008. arXiv:0802.1968[cond-mat.other].
[100] B. Kleihaus, J. Kunz, A monopole antimonopole solution of the SU(2) Yang–Mills–Higgs model, Phys. Rev. D61 (2000) 025003.
[101] B. Kleihaus, J. Kunz, M. Leissner, Sphalerons, antisphalerons and vortex rings, 2008. arXiv:0802.3275[hep-th].
[102] B. Kleihaus, J. Kunz, M. List, Rotating boson stars and Q-balls, Phys. Rev. D72 (2005) 064002.
[103] B. Kleihaus, J. Kunz, M. List, I. Schaffer, Rotating boson stars and Q-balls II: Negative parity and ergoregions, 2007. arXiv:0712.3742[gr-qc].
[104] B. Kleihaus, J. Kunz, F. Navarro-Lerida, Rotating black holes with monopole hair, Phys. Lett. B599 (2004) 294–300.
[105] B. Kleihaus, J. Kunz, U. Neemann, Gravitating stationary dyons and rotating vortex rings, Phys. Lett. B623 (2005) 171–178.
[106] B. Kleihaus, J. Kunz, Y. Shnir, Monopoles, antimonopoles and vortex rings, Phys. Rev. D68 (2003) 101701.
[107] B. Kleihaus, J. Kunz, Y. Shnir, Monopole–antimonopole chains and vortex rings, Phys. Rev. D70 (2004) 065010.
[108] F.R. Klinkhamer, N.S. Manton, A saddle point solution in the Weinberg-Salam theory, Phys. Rev. D30 (1984) 2212–2220.
[109] Y. Koma, H. Suganuma, H. Toki, Flux-tube ring and glueball properties in the dual Ginzburg–Landau theory, Phys. Rev. D60 (1999) 074024.
[110] S. Komineas, Vortex rings and solitary waves in trapped Bose–Einstein condensates, Eur. Phys. J. Special Topics 147 (2007) 133–152.
[111] A. Kundu, Yu.P. Rybakov, Closed-vortex-type solitons with Hopf index, J. Phys. A15 (1982) 269–275.
[112] A. Kusenko, Small Q-balls, Phys. Lett. B404 (1997) 285–290.
[113] A. Kusenko, Solitons in the supersymmetric extensions of the standard model, Phys. Lett. B405 (1997) 108–113.
[114] A. Kusenko, M. Shaposhnikov, Supersymmetric Q-balls as dark matter, Phys. Lett. B418 (1998) 46–54.
[115] K. Lee, J.A. Stein-Schabes, R. Watkins, L.M. Widrow, Gauged Q-balls, Phys. Rev. D39 (1989) 1665–1673.
[116] T. D. Lee, Y. Pang, Nontopological solitons, Phys. Rept. 221 (1992) 251–350.
[117] A.J. Leggett, Bose–Einstein condensation in the alkali gazes: Some fundamental concepts, Rev. Modern Phys. 73 (2001) 307–356.
[118] Y. Lemperiere, E.P.S. Shellard, Vorton existence and stability, Phys. Rev. Lett. 91 (2003) 141601.
[119] F. Lin, Y. Yang, Existence of energy minimizers as stable knotted solitons in the Faddeev model, Comm. Math. Phys. 249 (2004) 273–303.
[120] V.G. Makhankov, Y.P. Rybakov, V.I. Sanyuk, The Skyrme model, Fundamentals, Methods, Applications, Springer-Verlag, Berlin, 1993.
[121] N. Manton, P. Sutcliffe, Topological Solitons, Cambridge University Press, 2004, p. 493.
[122] C.J.A.P. Martins, E.P.S. Shellard, Vorton formation, Phys. Rev. D57 (1998) 7155–7176.
[123] U.G. Meissner, Toroidal solitons with unit Hopf charge, Phys. Lett. B154 (1985) 190–192.
[124] M. Metlitski, A.R. Zhitnitsky, Vortex rings in two component Bose–Einstein condensates, JHEP 06 (2004) 017.
[125] D. Mihalache, D. Mazilu, L.C. Crasovan, I. Towers, A.V. Buryak, B.A. Malomed, L. Torner, J.P. Torres, F. Lederer, Stable spinning optical solitons in three dimensions, Phys. Rev. Lett. 88 (2002) 073902.
[126] D. Mihalache, D. Mazilu, L.C. Crasovan, I. Towers, B.A. Malomed, A.V. Buryak, L. Torner, F. Lederer, Stable three-dimensional spinning optical solitons supported by competing quadratic and cubic nonlinearities, Phys. Rev. E66 (2002) 016613.
[127] D. Mihalache, D. Mazilu, I. Towers, B.A. Malomed, F. Lederer, Stable spatiotemporal spinning solitons in a bimodal cubic-quintic medium, Phys. Rev. E67 (2003) 056608.
[128] A.D. Nicole, Solitons with non-vanishing Hopf index, J. Phys. 4 (1978) 1363–1369.
[129] H.B. Nielsen, P. Olesen, Vortex line models for dual strings, Nuclear Phys. B61 (1973) 45–61.
[130] A.J. Niemi, K. Palo, S. Virtanen, (Meta)stable closed vortices in $(3+1)$+dimensional gauge theories with an extended Higgs sector, Phys. Rev. D61 (2000) 085020.
[131] V. Paturyan, E. Radu, D.H. Tchrakian, Rotating regular solutions in Einstein–Yang–Mills–Higgs theory, Phys. Lett. B609 (2005) 360–366.
[132] P. Peter, Superconducting cosmic string: Equation of state for spacelike and timelike current in the neutral limit, Phys. Rev. D45 (1992) 1091–1102.
[133] B.M.A.G. Piette, B.J. Schroers, W. Zakrzewski, Dynamics of baby skyrmions, Nuclear Phys. B439 (1995) 205–238.
[134] B.M.A.G. Piette, D.H. Tchrakian, Static solutions in the U(1) gauged Skyrme model, Phys. Rev. D62 (2000) 025020.
[135] L.P. Pitaevskii, Vortex lines in an imperfect Bose gas, Sov. Phys. JETP 13 (1961) 451–454.
[136] A.M. Polyakov, Particle spectrum in quantum field theory, JETP Lett. 20 (1974) 194–195.
[137] A.P. Protogenov, V.A. Verbus, Energy bounds of linked vortex states, JETP Lett. 76 (2002) 53–55.
[138] E. Radu, D.H. Tchrakian, Spinning U(1) gauged skyrmions, Phys. Lett. B632 (2006) 109–113.
[139] R. Rajaraman, Solitons and Instantons, North Holland, Amsterdam, 1982, p. 418.
[140] G.W. Rayfield, F. Reif, Quantized vortex rings in superfluid helium, Phys. Rev. A136 (1964) 1194–1208.
[141] J. Ren, R. Li, Y. Duan, Inner topological structure of Hopf invariant, J. Math. Phys. 48 (2007) 073502.
[142] V.A. Rubakov, On the electroweak theory at high fermion density, Prog. Theor. Phys. 75 (1986) 366–385.
[143] V.A. Rubakov, A.N. Tavkhelidze, Stable anomalous states of superdense matter in gauge theories, Phys. Lett. B165 (1985) 109–112.
[144] J. Ruostekoski, Stable particlelike solitons with multiply-quantized vortex lines in Bose–Einstein condensates, Phys. Rev. A70 (2004) 041601.
[145] J. Ruostekoski, Z. Dutton, Engineering vortex rings and systems for controlled studies of vortex interactions in Bose–Einstein condensates, Phys. Rev. A72 (2005) 063626.
[146] J. Ruostekoski, J. R.J.R. Anglin, Creating vortex rings and three-dimensional skyrmions in Bose–Einstein condensates, Phys. Rev. Lett. 86 (2001) 3934–3937.
[147] J. Ruostekoski, J. R.J.R. Anglin, Monopole core instability and Alice rings in spinor Bose–Einstein condensates, Phys. Rev. Lett. 91 (2003) 190402.
[148] P.G. Saffman, Vortex Dynamics, Cambridge University Press, 1992, p. 311.
[149] C.M. Savage, J. Ruostekoski, Energetically stable particle-like Skyrmions in a trapped Bose–Einstein condensate, Phys. Rev. Lett. 91 (2003) 010403.
[150] M. Schauder, R. Weiß, W. Schönauer, The CADSOL Program Package, Universität Karlsruhe Interner Bericht Nr. 46/92, 1992.
[151] M. Schmid, M. Shaposhnikov, Anomalous Abelian solitons, Nuclear Phys. B775 (2007) 365–389.
[152] W. Schönauer, R. Weiß, The Fidisol blackbox solver, J. Comput. Appl. Math. 27 (1989) 279–297.
[153] S.V. Shabanov, An effective action for monopoles and knot solitons in Yang–Mills theory, Phys. Lett. B458 (1999) 322–330.
[154] S.V. Shabanov, Yang–Mills theory as an Abelian theory without gauge fixing, Phys. Lett. B463 (1999) 263–272.
[155] Y. Shnir, Electromagnetic interaction in the system of multimonopoles and vortex rings, Phys. Rev. D72 (2005) 055016.
[156] Ya.M. Shnir, Magnetic Monopoles, Springer-Verlag, Berlin, Heidelberg, 2005, p. 532.
[157] T.H.R. Skyrme, A nonlinear field theory, Proc. Roy. Soc. Lond. A260 (1961) 127–138.
[158] P. Sutcliffe, Knots in the Skyrme-Faddeev model, 2007. arXiv:0705.1468[hep-th].

[159] P. Sutcliffe, Vortex rings in ferromagnets, 2007. arXiv:0707.1383[cond-mat.mes-hall].
[160] G. t Hooft, Magnetic monopoles in unified gauge theories, Nuclear Phys. B79 (1974) 276–284.
[161] C.H. Taubes, The existence of a non-minimal solution to the SU(2) Yang–Mills–Higgs equations on $\mathbb{R}^3$, Commun. Math. Phys. 86 (1982) 257–298.
[162] W.H. Thomson, On vortex motion, Trans. R. Soc. Edin. 25 (1867) 217–260.
[163] A.F. Vakulenko, L.V. Kapitansky, Stability of solitons in S^2 in the nonlinear σ-model., Sov. Phys. Dokl. 24 (1979) 433–434.
[164] P. van Baal, A. Wipf, Classical gauge vacua as knots, Phys. Lett. B515 (2001) 181–184.
[165] A. Vilenkin, E.P.S. Shellard, Cosmic Strings and Other Topological Defects, Cambridge University Press, 1994, p. 517.
[166] M.S. Volkov, Superconducting electroweak strings, Phys. Lett. B644 (2007) 203–207.
[167] M.S. Volkov, D.V. Gal'tsov, Gravitating non-Abelian solitons and black holes with Yang–Mills fields, Phys. Rep. 319 (1999) 1–83.
[168] M.S. Volkov, E. Wohnert, Spinning Q-balls, Phys. Rev. D66 (2002) 085003.
[169] M.S. Volkov, E. Wohnert, On the existence of spinning solitons in gauge field theory, Phys. Rev. D67 (2003) 105006.
[170] G.E. Volovik, The Universe in a Helium Droplet, Oxford University Press, 2003, p. 507.
[171] R.S. Ward, Hopf solitons on S^3 and R^3, 1998. hep-th/9811176.
[172] R.S. Ward, The interaction of two Hopf solitons, Phys. Lett. B473 (2000) 291–296.
[173] R.S. Ward, Hopf solitons from instanton holonomy, 2001. hep-th/0108082.
[174] R.S. Ward, Stabilizing textures with magnetic fields, Phys. Rev. D66 (2002) 041701.
[175] R.S. Ward, Skyrmions and Faddeev–Hopf solitons, Phys. Rev. D70 (2004) 061701.
[176] R.S. Ward, Hopf solitons on the lattice, J. Phys. A39 (2006) L105–L109.
[177] E. Witten, Superconducting strings, Nuclear Phys. B249 (1985) 557–592.
[178] V.A. Zakharov, E.A. Kuznetsov, Hamiltonian formalism for nonlinear waves, Phys. Usp. 40 (1997) 1087–1116.